THE EFFECT OF LINE CONFIGURATION ON LIGHTNING-INDUCED VOLTAGES ON OVERHEAD CONDUCTING LINES

JOHNSON OLUFEMI ADEPITAN

NOVEMBER, 2012

THE EFFECT OF LINE CONFIGURATION ON LIGHTNING INDUCED VOLTAGES ON OVERHEAD CONDUCTING LINES

BY

JOHNSON OLUFEMI ADEPITAN

B.Sc. (Lagos), M.Sc. (Ibadan), P.G.D.E. (Ago-Iwoye)

A THESIS IN THE DEPARTMENT OF PHYSICS

SUBMITTED TO THE FACULTY OF SCIENCE

FOR THE AWARD OF THE DEGREE OF

DOCTOR OF PHILOSOPHY

OF THE

UNIVERSITY OF IBADAN,

IBADAN, NIGERIA.

NOVEMBER, 2012

ABSTRACT

Lightning-Induced Voltages (LIV) affect all electrical conductors and could damage electronic circuits and gadgets even without applied voltage. Several factors, including electrical power line configuration, can affect the magnitude of the lightning-induced voltages. Previous research paid less attention to the effect of line configuration on lightning-induced voltages on overhead power lines and other lines in the tropical environment. The effect of line configuration of electrical lines (with and without earth-wires) on lightning-induced voltages on overhead power lines in tropical environment was investigated.

Six lightning channel models: transmission line; modified transmission line with linear decay; modified transmission line with exponential decay; Bruce-Golde; traveling current source; and Linearly Rising Current with Constant Tail (LRCCT) were used to reproduce the following lightning parameters: return-stroke peak current, I_p; specific velocity, β and front duration, t_f. The one that duplicated the condition in tropical environment was used to investigate the LIV on power lines of different line configurations: Vertical Profile With Earth-wire (VPWE) above topmost conductor and below lowest; Vertical Profile Without Earth-wire (VPWOE); Horizontal Profile With Two Earth-wires (HPWTE) symmetrically placed above and below conductors; and Horizontal Profile Without Earth-wires (HPWOE). The resulting partial differential equations from the interaction of lightning current with electrical lines were derived from Green's function and solved using the Laplace transform technique. From this, a C-sharp application programme interface was developed with input values of lightning parameters. Output of the programme was induced-voltage as function of time. The Peak Induced-Voltage (PIV) was identified from the plot of induced voltage - time graph. The PIV for HPWOE was validated with available experimental data. For each configuration the Protective Ratios (PR) were determined.

Only the LRCCT model duplicated the condition in tropical environment satisfactorily. The PIV increased linearly with I_p , but decreased exponentially with β and t_f. The PIV on lowest, middle and topmost conductors were 11.6 x 10^3 V, 13.7 x 10^3 V and 15.7 x 10^3 V respectively for VPWOE. The corresponding values for VPWE above topmost conductor were 10.5 x 10^3 V, 12.1 x 10^3 V and 13.0 x 10^3 V; while VPWE below lowest conductor had values 10.0 x 10^3 V, 12.7 x 10^3 V and 15.0 x 10^3 V. The PR for lowest, middle and topmost conductors were 0.91, 0.89 and 0.83 respectively for VPWE above topmost conductor. The PIV values of middle conductor and each of the outer conductors were 9.4 x 10^3 V and 8.7 x 10^3 V respectively for HPWOE; compared with an experimental value of 8.7 x 10^3 V. Above the line conductors, corresponding PIV values were 6.9 x 10^3 V and 7.1 x 10^3 V; while below the line conductors were 7.5 x 10^3 V and 7.2 x 10^3 V for HPWTE. The PR of the middle conductor and each of the outer conductors were 0.73 and 0.8 respectively for HPWTE above conductors. The PIV values dropped by a minimum of 25.0% when the lines carried current for all line configurations.

Line configuration influenced the lightning-induced voltages of which magnitude was reduced by earth-wires. The horizontal profile with two earth-wires symmetrically placed above the conductors may be preferred to the vertical profile with earth-wire above topmost conductor.

Keywords: Lightning-induced voltage, Lightning channel model, Conducting line configuration, Earth-wires.

Word count: 485

ACKNOWLEDGEMENT

God is beautiful for all situations; hence my appreciation goes to HIM first and foremost. I appreciate the contributions of my supervisor, Professor E. O. Oladiran for his guidance, pieces of advice, supply of academic materials and painstakingly going through every stage of the project. My thanks go to Prof. I. P. Farai and the departmental postgraduate committee for their guidance and constructive criticism during the course of the write up of the work.

Thanks to my boy, Johnson, for his involvement in writing out the program of this work. Also I acknowledge the contribution of Dr. Olaiwola Adekoya for sourcing for relevant journals for me. I appreciate the love, prayer and moral supports received from the members of my church- God's Covenant Family Assembly, most especially the Faniyis and the Adeseguns. I cannot but thank my only sister Yewande and her husband Tunde Adenekan , my mother and parents-in-law for their prayer and moral supports.

Finally my acknowledgement goes to The Boys- Oluwadamilola, Mofeyifoluwa, Erioluwa and Oreoluwa- for their understanding and tolerances. BIG THANKS to ABISOLA- my wife and portion in life.

CERTIFICATION

I certify that this work was carried out by Johnson Olufemi ADEPITAN of the Department of Physics, University of Ibadan, Ibadan, Nigeria.

……………………..   ………………….

Supervisor   Date

Professor E. O. Oladiran,
B.Sc., Ph.D. (Ibadan) , M.Sc.(Met.) (Reading)
Department of Physics,
University of Ibadan,
Ibadan, Nigeria.

DEDICATION

This work is dedicated to God, who makes "a way for the lightning of the thunder" (Job 28:26b). He granted me the grace to have some understanding of how the power of lightning influenced the power of electricity and sometimes snuffed it off.

TABLE OF CONTENTS

Title page ………………………………………………. i-ii

Abstract ……………………………………………... iii-iv

Acknowledgement …………………………………... v

Certification vi

Dedication …………………………………………... vii

Table of Contents viii-x

List of Figures ………………………………………. xi-xiii

List of Tables ……………………………………… xiv-xv

Chapter One : Introduction

1.1 Introduction ……………………………………………. 1.

1.2 Statement of problem ……………………………… 4.

1.3 Aim and objectives 4.

Chapter Two : Literature Review And Theoretical Framework

2.1.1 Sources of lightning ………………………………….. 6.

2.1.2 Cloud Classifications and Characteristics …………… 6.

2.1.3 Cloud Charge Structure.. 7.

2.1.4 Process of lightning .... 10.

2.2 Types of lightning …………………………………... 10.

2.3 The lightning current ………………………………... 13.

2.4 Return stroke current ………………………………… 14.

2.5 Typical lightning current wave shape ……………… 15.

2.6 Return stroke model ………………………………… 18.

2.7 Leader model ………………………………………... 24.

2.8 Traveling current source-type model ……………….. 26.

2.8.1 Bruce-Golde model …………………………………. 27.

2.8.2 Traveling current source model ……………………... 28.

2.9 Transmission line type models …………………….... 29.

2.9.1 Transmission line model ……………………………. 30.

2.9.2 The modified transmission line exponential decay …. 31.

2.10 The waveguide model of lightning currents ……….. 32.

2.11 Theoretical framework of lightning induced voltages 36.

2.11.1 Introduction …………………………………………. 36.

2.12 Overvoltages ………………………………………… 37.

2.12.1 Lightning overvoltages ……………………………… 38.

2.13 Past theoretical work on induced voltages on power lines ……… 38.

2.14 Induced electromagnetic field on overhead line and its vicinity 40.

2.15 Striking distance …………………………………….. 45.

2.16 Determination of probable striking points ………….. 46.

2.17 Analysis of lightning induced voltages on overhead lines ……… 49.

2.18 Single-conductor overhead line case ………………... 53.

2.19 Two-conductor overhead line case ………………….. 56.

Chapter Three: Methodology

3.1 Introduction …………………………………………. 70.

3.2 Return stroke models ………………………………... 71.

3.3 Procedure of calculation of lightning induced voltages with MAPLE 13 … 73.

3.4 C-sharp Application Program Interface (API) with Graphical User Interface 74.

CHAPTER FOUR : RESULTS AND DISCUSSIONS

4.1 Introduction ………………………………………… 80.

4.2 Lightning Characteristics …………………………… 80.

4.2.1 Case A- Low heights ……………………………….. 92.

4.2.2 Case B- High heights ……………………………….. 92.

4.3 Influence of lightning parameters on lightning induced voltages 119.

4.4.1 Vertical configuration without earth wire ………….. 120.

4.4.2 Vertical configuration with earth wire ……………. 120.

4.4.3 Horizontal configuration with and without earth wire 121.

4.5 Protective ratio ………………………………………. 123.

CHAPTER FIVE: CONCLUSION AND RECOMMENDATIONS

5.1 Conclusion ………………………………………….. 124.

References …………………………………….............. 126.-133

Appendix I MAPLE 13 program for solving induced voltage, v(x,t) ……… 134-143

Appendix II C-sharp Application Program Interface (API) to determine lightning induced voltages ………………. 144-190

Appendix III Published Articles 191-202.

List of Figures

1. Fig.2.0: Electric dipole nature of charges within the thunderstorm 8.

2. Fig. 2.0a: Double-dipole structure of thunderstorm cloud 9.

3. Fig. 2.1: Wave shape of typical return-stroke current (Adapted from Anderson and Eriksson, 1980) 16.

4. Fig.2.2: Geometry used in deriving the expression is assumed to create an extending channel whose lower end is fixed at ground and whose upper end is associated with the return stroke front that moves from ground ($z' = 0$) upward with a constant speed v. 22.

5. Fig.2.3: Geometry used in deriving the expression is assumed to create an extending downward vertical channel whose charge center at the upper end is associated with the leader front that moves from charge center ($z' = Hm$) downward with a constant speed v. 24.

6. Fig.2.4: Simple model of interaction between cloud and single conductor 31.

7. Fig.2.5: Channel and its image together with a structure in co-ordinate systems 43.

8. Fig.2.6: Critical meeting distances for point P_i 48.

9. Fig.2.7: Coordinate system of line conductors and lightning stroke 51.

10. Fig.2.8: Equivalent circuit for computing lightning-induced voltage on single-conductor over head line 53.

11. Fig.2.9: Equivalent circuit for computing lightning-induced voltage on two-conductor over head line 57.

12. Fig.2.10: 3-phase line with one earth wire (Vertical configuration) 64.

13. Fig.2.11: 3-phase line with two earth wires (Horizontal configuration) 68.

14.	Fig.3.1:	Flow chart for lightning-induced voltage calculation	75.
15.	Fig.3.2:	Window's GUI to interact with API for lightning-induced voltage calculation.	77.
16.	Fig.3.3:	Window's GUI to interact with API to select line configuration for lightning-induced voltage calculation.	79.
17.	Fig.4.1:	Profile of undisturbed base-current, i(0,t),same for TL-type and TCS-type models, using typical parameters in table 3.1.	81.
18.	Fig. 4.2:	Current as a function of time at height, z'=200m (BG and TCS models)	82.
19.	Fig. 4.3:	Current as a function of time at height, z'=2km, cloud height, H=5km. (BG and TCS	83.
20.	Fig. 4.4:	Current as a function of time at height, z'=200m, cloud height, H=5km. (MTLE,TL and MTLL models)	84.
21.	Fig. 4.5:	Current as a function of time at height, z'=500m, cloud height, H=5km. (MTLE,TL and MTLL models	85.
22.	Fig. 4.6:	Current as a function of time for MTLL model	86.
23.	Fig. 4.7:	Current as a function of time at height, z'=2km, cloud height, H=5km. (MTLE,TL and MTLL models	88.
24.	Fig. 4.8:	Current as a function n of time at height, z'=3km, cloud height, H=5km. (MTLE,TL and MTLL models)	89.
25.	Fig. 4.9:	Current as a function of time at height, z'=4000m, cloud height, H=5km. (MTLE,TL and MTLL models	90.
26.	Fig. 4.10:	Relationship between current peak, I_p and channel height,	91.
26.	Fig. 4.11:	Variation of induced voltages with return stroke peak current	102.
27.	Fig. 4.12:	Variation of induced voltages with return stroke specific velocity	103.

28. Fig.4.13: Variation of induced voltages with return stroke front time 104.

29. Fig.4.14: Variation of induced voltages with return stroke peak current 105.

30. Fig.4.15: Variation of peak induced voltages with return stroke specific velocity 106.

31. Fig.4.16: Variation of peak induced voltages with return stroke front time 107.

3. Fig.4.17: Comparing induced voltages for vertical configuration without earth wire with single conductor equivalent 108.

33. Fig.4.18: Induced voltage on lowest conductor for vertical configuration with and without earth wire 109.

34. Fig.4.19: Induced voltage for vertical configuration with earth wires above conductors 110.

35. Fig.4.20: Induced voltage for vertical configuration with earth wire below conductors 111.

36. Fig.4.21: Induced voltage for horizontal configuration with earth wires above conductors 112.

37. Fig.4.22: Induced voltage for horizontal configuration with earth wires below conductors 113.

38. Fig.4.23 Peak induced voltages for vertical configuration 114.

39. Fig.4.24 Peak induced voltages for horizontal configuration 115.

40. Fig.4.25 Variation of peak induced voltage with earth wire height 116.

List of Tables

1.	Table 2.1	Traveling Current Source-Type Models	26.
2.	Table 2.2	Transmission-Line Type Models	29.
3.	Table 2.3	Summary of statistics on the absolute error of the model peak fields	35.
4.	Table 3.1	Typical values of parameters applied to base current.(adapted from Berger,1975)	72.
5.	Table 3.2	Dimension of multi-conductor lines	78.
6.	Table 4.1	Peak values of the currents with different return stroke models at different heights (v=0.5c)	87.
7.	Table 4.2	The variation of induced voltage ,V with peak current, I_p ($h=10m, t_f=5\mu s, \beta=0.3, y_0=100m, x=1000m$)	94.
8.	Table 4.3	The variation of induced voltage ,V with specific velocity ,β (h	95.

		=10m,t_f=5µs, I_p=10kA,y_0=100m,x=1000m)	
9.	Table 4.4	The variation of induced voltage ,V with front time , t_f (h =10m, β=0.3,, I_p=10kA,y_0=100m,x=1000m)	96.
10.	Table 4.5	The variation of Peak Induced Voltage (PIV),V_p with lightning parameters	97.
11.	Table 4.6	Comparison of induced voltages on multiconductors for vertical configuration with single conductor equivalent.	98.
12.	Table 4.7	Peak induced voltages for vertical and horizontal configurations	99.
15.	Table 4.8	Protective ratio values for vertical and horizontal configurations	100.
16.	Table 4.9	Per-Unit Induced Voltages On 3-Conductor Lines	101.

CHAPTER ONE

1.1 INTRODUCTION

Lightning has long been known to man from the earliest existence. The sight of the luminous channels and branches of lightning is awesome, most especially when viewed at night. Though awesome in appearance, the effect of lightning can be terrific, devastating and destructive. Lightning has been of great interest to men; scientist in particular. It is caused by electrical discharge from the atmosphere. The first association of lightning and thunder with electricity was made by Wall (as cited in Ajayi, 1970). He observed cracklings and a flash between amber and his fingers when they were sufficiently close enough. He then drew analogy between these phenomena and lightning and thunder. Over 200 years ago, Franklin (as cited in Uman, 1994), proved that was an electrical discharge and measured the sign of the cloud charge that produced it. Wilson (as cited in Uman, 1994) was the first to infer the charge structure of the thunder cloud and the charge involved in lightning.

According to Uman (1994), lightning research was motivated in the 1930s primarily by the need to reduce the effects of lightning on electric power systems and the desire to understand an important meteorological process. Brook (as cited in Rakov & Uman, 1998), corroborated by Orville and Spencer (as cited in Thurman & Edgar, 1982) calculated that about 100 lightning flashes occur each second around the globe. According to Driscoll et al. (2003), the global lightning flash rate is found to be on the order of 40 flashes per second (fps) as compared to the commonly accepted value of 100 fps, an estimate that dates back to 1925. And that seventy percent of all lightning activity occurs in the tropics. The distinguishing characteristics of the various types of lighting flashes are their rise time. Negative ground flashes have fast rise time, while positive ones have slower rise times (Oladiran et al., 1998).

Electrical power interruptions are one of the most readily apparent effects of lightning on human activity. Others are property damage and deaths caused by direct lightning strikes. According to Christensen et al.,(as cited in Thurman & Edgar,1982), lightning is also a major cause of forest fire. Most of the twenty first century electronics equipments are highly sensitive with low damage threshold level. Thus they are easily damaged by either transient voltage or current. The susceptibility of this equipment to damage, most especially in thunderstorm environment rekindles the interest and understanding of the mechanism of the interaction of lightning generated field with power distribution system. Lightning has always been suspected as one of the reasons of power line outages and damage to equipments in distribution network. For instance, in 2003 United States, Canada and Europe suffered a series of blackouts leaving more than 60 million people without electricity. Some of the reason adduced to the outage was believed to be due to lightning strike (Andersson et al., 2005). According to Power Holding Company of Nigeria (PHCN), a body charged with the responsibility of supplying electricity in Nigeria, a total of 13,324 faults at 33KV and 22,255 faults at 11KV levels were recorded in year 2002 and a bulk of these faults were caused by thunder storms and lightning (NEPA 2002 Annual Report and Accounts). This led to a preliminary work of analyzing the outages experienced on electric power lines in Ijebu-Ode and Sagamu areas in Nigeria for five years (2002-2006). It was discovered that lightning accounted for 10% of the outages in these areas (see appendix v for details).

The reliability of the supply provided by an electric power system is judged by the frequency and duration of supply interruptions to consumers. This depends to a great extent on the surge performance of the system.

Direct strokes to lines (the discharge strikes directly the lines) which are functions of lightning incidence to ground are expected to occur at a rate of approximately one per km per year in area of several lightning electricity (Eriksson and Meal, 1982). Indirect lightning (due to the radiated electric fields by both leader and return stroke) on the other hand is known to give rise to surge voltage of enough amplitude to spark over lightning arresters or even the line insulation, which is generally low in distribution network. The voltage produced by direct lightning is function of the lightning current in the channel and the surge impedance of the line. The over voltage produced by indirect lightning is a function of the way in which the external excitation from the electric field is coupled to the line. The angle of incidence of the electric field with respect to the line plays an important role on the over voltage.

The reliability of an electric power system can also be measured from the knowledge of the efficiency and reliability of lightning protection design of the system. In order to determine these, the need of accurate mathematical models that are capable of reproducing the various aspects of lightning electromagnetic effects, namely, lightning discharge mechanisms, coupling mechanisms between lightning stroke and the system and propagation of lightning transients within the system, are essential. The calculation of lightning induced voltages is essential to the evaluation of the impact of the protective measures and devices utilized to control or minimize them.

The present study advanced knowledge on lightning induced voltages and lightning protection on power lines by examining the influence of some lightning parameters, viz: peak current, I_p; front duration of return stroke current, t_f and specific velocity of return stroke, β, on induced voltages. The effects of line configuration and earth wires were also examined.

1.2 Statement of problem

Lightning induced voltages on overhead conducting lines often result in transient problems such as damage to circuits and gadgets; and outages on lines. Power Holding Company of Nigeria adduced lightning as major cause of interruption of electric power in Nigeria (NEPA 2002 Annual Report and Accounts). Lack of empirical data made it difficult to refute or affirm this. Calculation of lightning induced voltages is important in determination of appropriate protective device or plan against lightning and estimation of outage rates. Previous research paid less attention on the effect of line configuration on lightning induced voltages on overhead conducting lines in the tropical environment.

The present study is focused on determining the effect of line configuration on lightning induced voltages on overhead conducting lines in the tropical environment.

1.3 Aim and objectives

The work aimed at determining the influence of lightning parameters and line configuration on the lightning induced voltages on overhead conducting lines in tropical environment.

The objectives of the work were as follows:

- To identify the return-stroke model that duplicated the condition in tropical environment.
- To determine the relationship between peak-induced-voltages on overhead conducting lines and each of lightning parameters, namely return-stroke peak current, specific velocity and front duration.
- To determine peak-induced-voltages for horizontal configuration of conducting lines (with and without earth wires).

- To determine peak-induced-voltages for vertical configuration of conducting lines (with and without earth wire).
- To determine the protective ratio of each wire for all configurations.
- To assess the configurations and recommend the preferred one.

CHAPTER TWO

LITERATURE REVIEW AND THEORETICAL FRAMEWORK

Lightning is a fast atmospheric transient phenomenon characterized by a discharge along a very long path at very high current rates. Lightning occurs whenever electric charges accumulate sufficiently to initiate a discharge through the air. The most common sources of lightning are thunder clouds.

2.1.1 Sources of lightning

Lightning can occur during thunder storms, sandstorms, snowstorms, volcanic eruptions, and in rare cases during a clear weather (Uman, 1987). During disturbed weather when thunderstorms are experienced, atmospheric electrical currents flow upward; while during fine weather atmospheric electrical currents flow downward. Charges are transferred to earth from thunderstorms by means of rain, lightning and corona discharge. The most common source of lightning is the thundercloud, also referred to as cumulonimbus.

2.1.2 Cloud Classifications and Characteristics

Clouds are classified according to their height above and appearance (texture) from the ground. Clouds can be classified into high-level, prefixed by "cirro" ;mid- level, prefixed by "alto" and low-level .

High-level clouds:

They occur above about 6.1 km . Due to cold tropospheric temperatures at these levels, the clouds primarily are composed of ice crystals, and often appear thin, streaky.

Mid-level clouds:

The bases of clouds in the middle level of the troposphere, appear between 2 and 6.1 km. Depending on the altitude, time of year, and vertical temperature structure of the troposphere, these clouds may be composed of liquid water droplets, ice crystals, or a combination of the two, including supercooled droplets (i.e., liquid droplets whose temperatures are below freezing).

Low-level clouds:

Low-level clouds are not given a prefix, although their names are derived from "strato" or "cumulo," depending on their characteristics. Low clouds occur below 2 km, and normally consist of liquid water droplets or even supercooled droplets, except during cold winter storms when ice crystals (and snow) comprise much of the clouds.

2.1.3 Cloud Charge Structure

Fig. 2.0 shows the classic model for the charge structure of a thundercloud. In this model, a primary positive charge region is found above a primary negative charge region, forming an electric dipole. According to Wilson (as cited lightning in Uman, 1994) , the classical model for charge structure of a thunder cloud was developed in the 1920's and 1930's from ground-based measurements of both thundercloud electric fields and electric field changes that are caused when lightning occurs. By the end of the 1930's, Simpson and co-workers(Simpson and Scarse,1937; Simpson and Robinson,1941) had verified this overall structure from measurements made with sounding balloons inside clouds and has also identified a small localized region of positive charge at the base of the cloud as shown in Fig.2.0a ; thus forming a double-dipole structure.

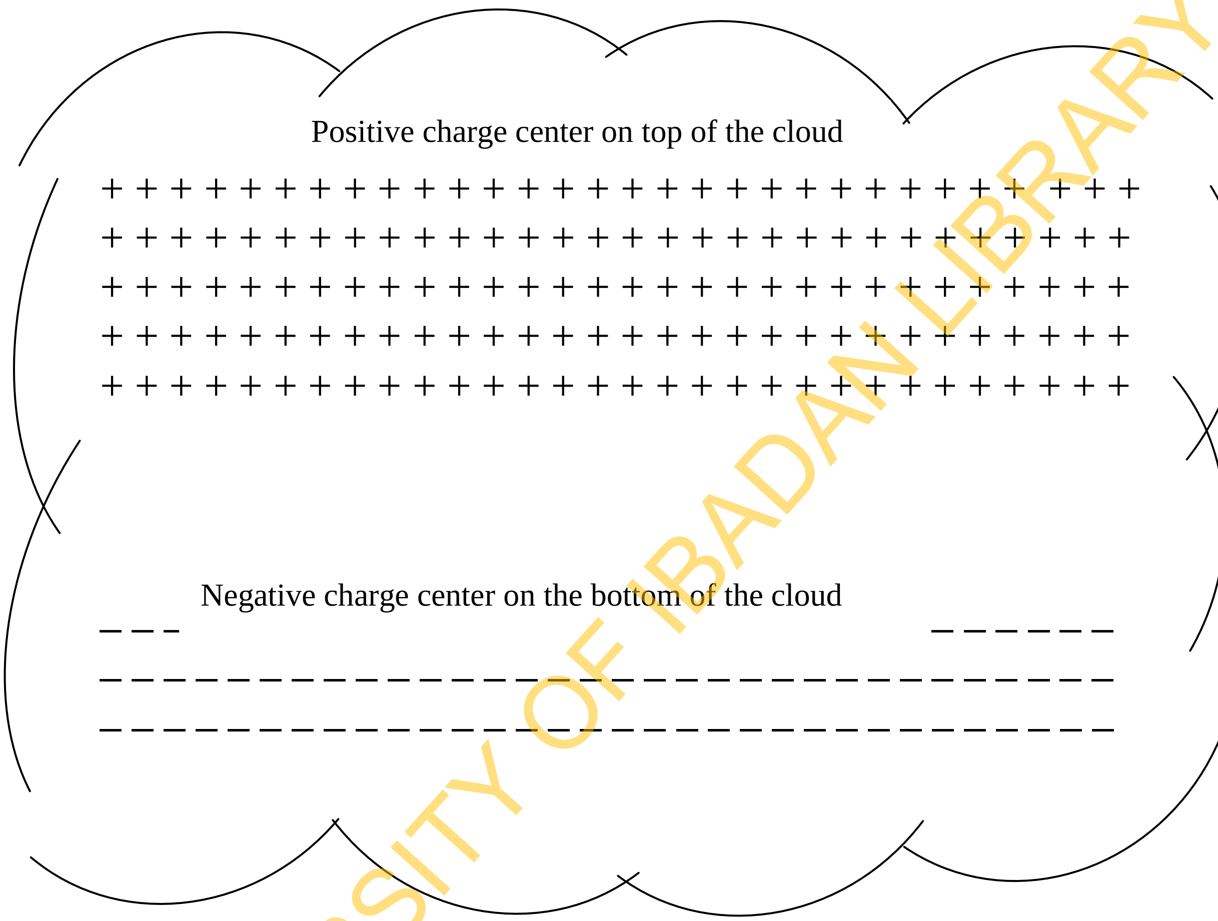

Fig.2.0: Electric dipole nature of charges within the thunderstorm

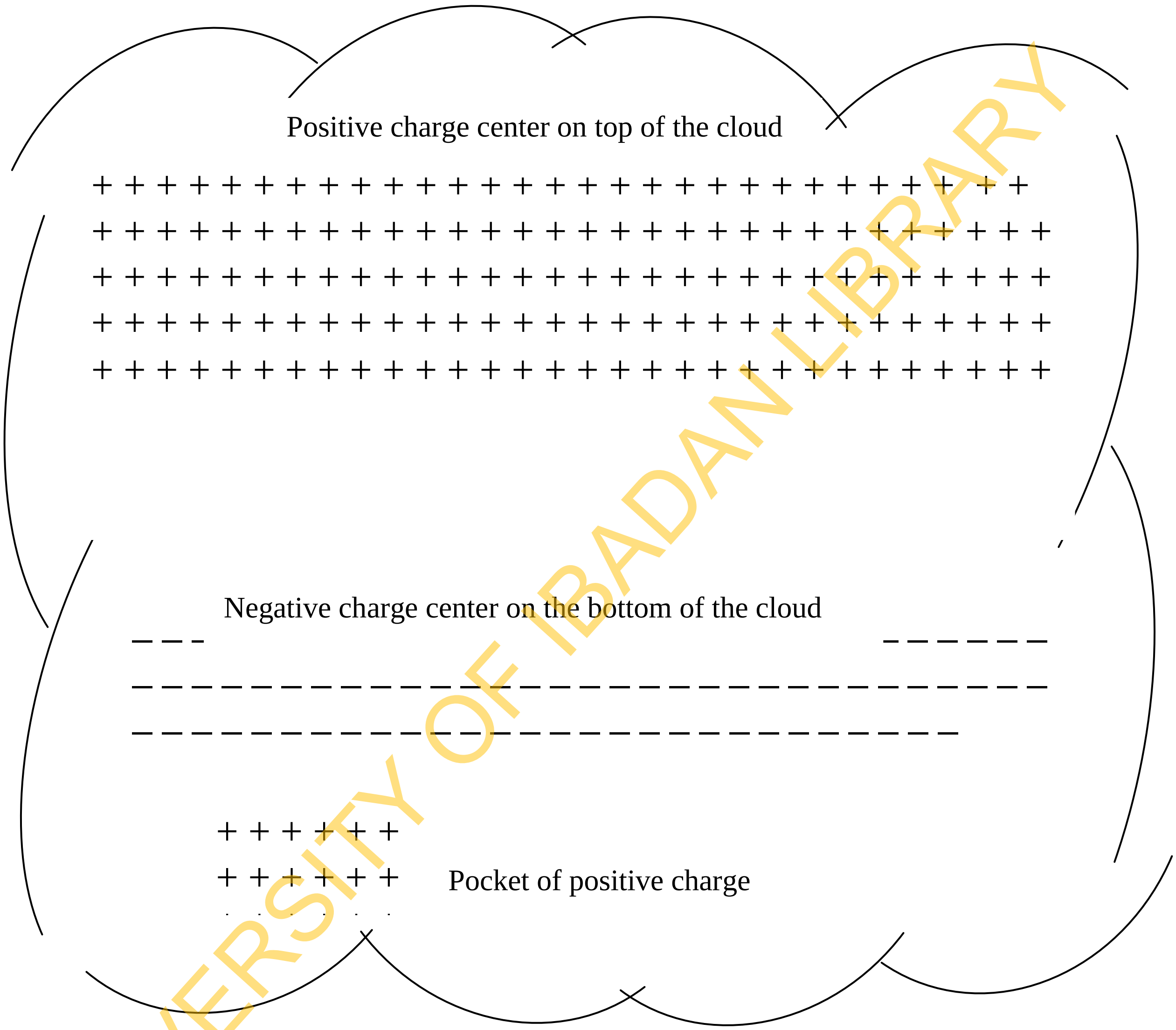

Fig.2.0a: Double-dipole structure of thunderstorm cloud

2.1.4 Process of lightning

The updrafts and downdrafts of the wind in the atmosphere create a charging mechanism that separates electric charges. This results into negative charge at the bottom and positive charge at the top of the cloud. As charge at the bottom of the cloud keeps growing, the potential difference between cloud and ground, which is positively charged, grows as well. This process will continue until air breakdown occurs. The development of a cloud-to-ground flash involves a stepped leader that starts travelling downwards following a preliminary breakdown at the bottom of the cloud. This involves a positive pocket of charge (see Fig.2.0a). The stepped leader travels downwards in steps several tens of meters in length and pulse currents of at least 1 kA in amplitude (Uman, 1969). When this leader is near ground, the potential to ground can reach values as large as 100 MV before the attachment process with one of the upward streamers is completed.

2.2 Types of Lightning

Over half of all flashes occur wholly within the cloud (intra cloud discharges). Four different types of lightning between cloud and earth have been identified.

(a) Cloud-to-ground flashes initiated by downward moving negatively-charged leaders; accounting for 90% of cloud-ground discharges worldwide.

(b) Cloud-to-ground flashes initiated by downward moving positive leaders accounting for less than 10% of cloud-ground discharges.

Ground-to-cloud discharges are also initiated by leaders of either polarity that move upwards from the earth .These upward initiated flashes are relatively rare and usually occur from mountain peaks and tall towers or structures.

Cloud-to-ground lightning has been studied more extensively because of its practical importance of causing electrical power interruption, disturbances in communication systems and ignition of forest fires (Christensen as cited in Thurman & Edgar, 1982). The number of cloud-to-ground flashes per square kilometer per year has a maximum of 30 to 50, and a typical overland value of 2 to 5. Brooks (as cited in Wood,2004), corroborated by Orville & Spencer as cited in Thurman & Edgar, 1982) calculated that about 100 lightning flashes occur each second around the globe for a worldwide average flash density of 6 $km^{-2}yr^{-1}$.

A typical cloud-to-ground flash lasts about 0.5s. It is usually composed of several intermittent discharges called strokes, each of which has duration of milliseconds. A stroke in turn, is made up of a "leader" phase and a "return stroke" phase. The leader initiates the return stroke by lowering cloud charge [of negative sign for all the lightning observed by Lin et al. (1979)] and cloud potential toward the earth. Stepped leaders are heavily branched and carry charges of between 5 to 10C; dart leaders that precede subsequent strokes carry less charge and follow the main channels of previous strokes. The magnitude of charge per unit length of a leader is likely to be greater near the ground than near the cloud owing to the greater capacitance between the lower channel and the ground. The relatively high inferred values of the leader charge per unit length necessitate storage of that charge over a radial distance of the order of 1meter or more. Hence the leader charge is stored in a corona envelope while the average leader current that supplies the charge of the order 100A for the leader and 1000A for dart leaders, flows in an arc channel of radius smaller than 1cm. The leader arc channel is a relatively good conductor and hence is maintained at a high negative potential with respect to the earth. When a step leader is within a few tens of meters to the ground, electrical breakdown takes place between the leader tip and the ground or elevated object on the ground. Part of the breakdown is an upward propagating discharge of earth potential. When the junction is complete, the first return stroke is initiated. Dart leaders probably draw small, if any upward propagating discharges from the earth. Both first and subsequent return strokes are upward traveling waves of the earth potential that have a speed near that of light and that serve to discharge to earth the negative charge on the leader channel.

First return strokes have upward velocities that decrease markedly as each major branch is passed, subsequent stroke velocities tend to be relatively constant with height. The physics of the leader channel is discharged is largely not understood and it is subject of the return stoke model to be discussed. Qualitatively, however each earth potential propagates up the leader channel as it would in the case of a discharged transmission line that was grounded at one end. At any given time a relative large electric field exists in a leader return stoke channel between the region of ground and high negative potential that is at the return stroke wave front. This large field produces ionization resulting in a current of order of 10KA.The power input renders the channel very luminous and causes its rapid expansion, thus producing thunder. As successively higher portions of the upward propagating return stroke, the corona charge surrounding those portions of the leader collapse into the channel and flows to ground (Uman, 1969).

During the discharge, the most energetic and the most dangerous phase is the return stroke. At the short distances from the discharge channel, the ratio between the field radiated by the leader and the return stroke approaches unity (Uman, 1987), Most cloud to ground lightning in temperate regions lower negative charges to earth. Flashes that lower positive charges are generally called positive lightning. In spite of the low percentage (ranging from 10 to about 30% in temperate zones), positive lightning is of particular interest for two reasons: (i) It is responsible for the largest of the recorded lightning current those in the range of 200 to 300kA

(Uman, 1987); and for charges transferred to earth that are considered larger than those of negative flashes. (ii) In some tropical zones the positive lightning percentage seems to be about 80% (Uman, 1987).

2.3 The Lightning Current

Determination of lightning current (the most important single parameter of the lightning discharge) is one of the main problems facing lightning research. Knowledge of the wave shape and current amplitude help in solving the electrical problems of protection against lightning. Lightning current was initially assumed to be oscillatory in nature. This misconception might have arisen from the flickering appearance of a multiple lightning discharge. Lodge (as cited in Golde, 1997a) carried out experiments with Leyden jars to support the oscillatory nature of lightning with a frequency of about 1MHz (p. 310). Creighton (as cited in Golde, 1977a) and Biermanns (as cited in Golde, 1977a) supported the oscillatory nature of lightning current. Humphrey (as cited in Golde, 1977a) argued that lightning current was more likely to be of aperiodic than oscillatory and this was explained by the suggestion that the internal resistance of the lightning current exceeded the critical value for damping. Today, the current flowing to earth in a lightning stroke is known to be unidirectional.

Most lightning current measurements have been made on strokes to tall buildings or towers and represent the current flowing at the lightning channel base (Uman, 1969). In order to determine the properties of lightning strokes not influenced by tall structures, Norinder and Dahle (as cited in Uman and McLain,1969), measured the magnetic fields from distant strokes to earth and from theory derived lightning currents .Uman and McLain, (1969) showed that the theory used by Norinder and team is erroneous. Uman and McLain,(1970 b) derived expression that allowed the calculation of the current in a lightning strike from the measurement of either the magnetic flux density or the radiation field of the discharge.

2.4 Return-stroke current

The lightning return-stroke current and the charge delivered by the stroke are the most important parameters to assess the severity of lightning strokes to power lines and apparatus. The magnitude and the shape of the return stroke current wave play a significant role in the calculation of induced voltages on power lines. According to Anderson and Eriksson (1980) , the return-stroke current is characterized by a rapid rise to the peak, I_p, within a few microseconds and then a relatively slow decay, reaching half of the peak value in tens of microseconds . The return-stroke current is specified by its peak value and its waveshape. The waveshape, in turn, is specified by the time from zero to the peak value (t_f , front time) and by the time to its subsequent decay to its half value (t_h , tail time). The tail time being several orders of magnitude longer than the front time, its statistical variation is of lesser importance in the computation of the generated voltage. The return-stroke current is therefore identified by three parameters: peak value I_p, front time t_f and time to half value t_h .The difficulty with the exponential function representing a return-stroke current is that it is not easy to select the parameters of these analytical expressions to fit the three parameters (I_p, t_f and t_h,). However, this problem does not arise if the return-stroke current is represented as linearly rising and linearly falling functions.

$$I(t) = \alpha_1 t u(t) - \alpha_2 (t - t_f) u(t - t_f) \qquad \text{……….. (2.0a)}$$

where $\alpha_1 = I_p / t_f$ and $\alpha_2 = (2t_h - t_f) I_p / 2t_f (t_h - t_f)$. For short t_f in the order of a few microseconds, equation 2.0a seems to work very well. With equation 2.0a, the three parameters of the return-stroke current can be varied very easily.

The generated voltage is a function of the peak current for both the direct and indirect strokes. For back-flashes in direct strokes and for indirect strokes the generated voltage is higher the shorter the front time of the return-stroke current (Chowdhuri, 1996).The front time (and the tail time, to a lesser extent), influence the withstand capability (volt-time characteristics) of the power apparatus. The charge in a stroke signifies the energy transferred to the struck object. The auxiliary equipment (e.g., surge protectors) connected near the struck point will be damaged if the charge content of the stroke exceeds the withstand capability of the equipment. The return-stroke velocity will affect the component of the voltage which is generated by the induction field of the lightning stroke (Chowdhuri, 1996). Compilation of lightning parameters is best accomplished by direct measurements on actual lightning. The peak of the return-stroke current has been estimated by measuring the radiated magnetic field of the lightning stroke. The relationship between the peak current, I_{peak} , and the radiated electric field, E_{peak} ,was derived from the transmission-line model of the lightning stroke for a lossless earth(EPRI,1997)

$$I_{peak} = \frac{2\pi\varepsilon_0 c^2 D}{v} E_{peak} \quad \text{and} \quad E_{peak} = cB_{peak} \qquad \text{..........(2.0b)}$$

where c = velocity of light in free space, D=distance of the stroke from the antenna, *v*= velocity of the return-stroke, and B_{peak} =peak magnetic induction.

2.5 Typical lightning current waveshapes

More than 90 percent of the cloud-to-ground strokes are of negative polarity, except for seasonal and regional variations. According to Berger et al., 1975, the positive-polarity stroke currents do not have enough common features to produce an acceptable mean waveshape. This could also be partly due to the small number of positive strokes recorded. The waveshape of the mean negative first stroke current is shown in Fig. 2.1.

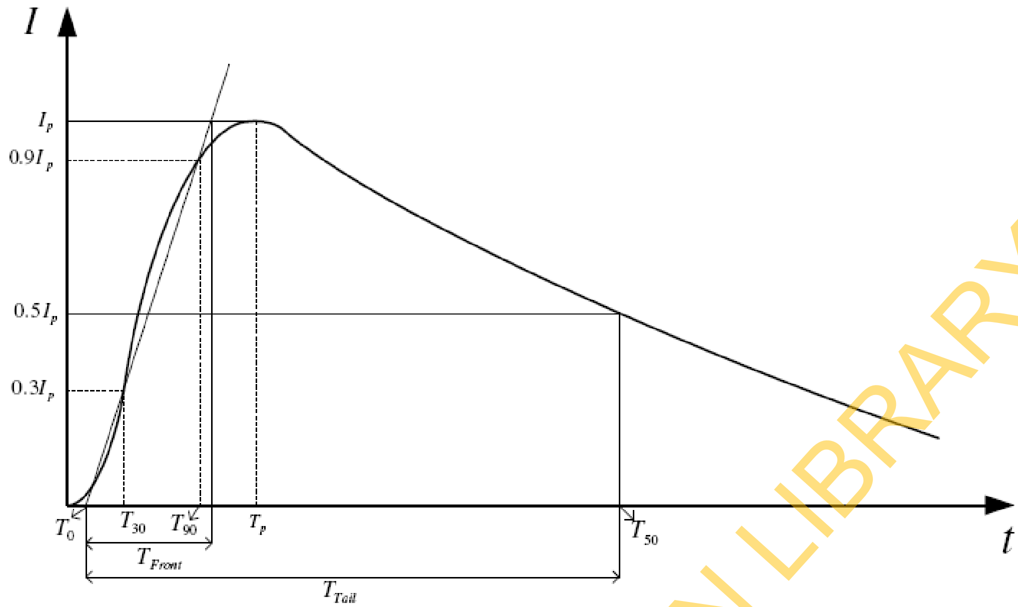

Fig. 2.1: Wave shape of typical return-stroke current

This waveshape has distinctly a concave wavefront with the greatest rate of change near the peak. The return-stroke current rises to its peak in a few microseconds and slowly decays after reaching the peak. The peak current, I_p , is the maximum current of the stroke. Front time, t_f, or virtual time to crest is the interval between the incidence of a line which connects the point 30-90% peak, to zero level and peak level of the stroke shape. Tail time, t_h , or virtual time to half value is the interval between intersection point of mentioned 30-90% line to zero level and time when stroke curve passes level 50% of peak. The current waveshape is called a t_f /t_h wave. The time to half value, t_h, being many times longer than t_f does not play a significant role in the severity of lightning-caused transient overvoltages. However, the influence of the peak of the current wave, I_p, and t_f is very significant.

2.6 Return stroke model

Return stroke models can be broadly classified into four thus:

(i) Gas dynamic or "physical" models, which are primarily concerned with the radial evolution of a short segment of the lightning channel and its associated shock wave.

(ii) Electromagnetic models that are usually based on a lossy, thin-wire antenna approximation to the lightning channel. These models involve a numerical solution of Maxwell's equations to find the current distribution along the channel from which the remote electric and magnetic fields can be computed.

(iii) Distributed-circuit models that can be viewed as an approximation to the electromagnetic models described above and that represent the lightning discharge as a transient process on a vertical transmission line characterized by resistance (R), inductance (L), and capacitance(C), all per unit length.

(iv) “Engineering” models in which a spatial and temporal distribution of the channel current (or the channel-charge density) is specified based on such observed lightning return-stroke characteristics as current at the channel base, the speed of the upward-propagating front, and the channel luminosity profile.

Electromagnetic, distributed-circuit, and “engineering” models can be directly used for the computation of electromagnetic fields, a primary electromagnetic compatibility (EMC) application of such models, while the gas dynamic models can be used for finding as a function of time, which is one of the parameters of the electromagnetic and distributed -circuit models (Rakov and Uman, 1998; Raul Montano, 2006). The most commonly adopted “engineering” models used to calculate lightning-induced voltages nowadays are:

- the Transmission Line (TL) model [*Uman and McLain*, 1969];
- the Traveling Current Source (TCS) model [*Heidler*, 1985];
- the Modified Transmission Line Exponential (MTLE) model [*Nucci et al*., 1988; *Rachidi and Nucci*, 1990];
- the Diendorfer-Uman (DU) model [*Diendorfer and Uman*, 1990].

All the above models allow the reproduction of overall fields that are reasonable approximations of measured fields from natural and triggered lightning (*Rakov and Uman*, 1998; and *Gomes and Cooray*, 2000)

A number of frequently used ‘‘engineering’’ return stroke models have been classified into two categories, transmission-line-type models and traveling current-source-type models, with the implied location of the current source and the direction of the current wave as the distinguishing factors(Rakov and Uman ,1998) . The current source in the transmission- line-type models is often visualized to be at the lightning channel base where it injects an upward-traveling current wave that propagates behind and at the same speed as the upward-propagating return stroke front. The current source in the traveling-current-source-type models is often visualized as located at the front of the upward-moving return stroke from which point the current injected into the channel propagates downward to ground at the speed of light. Traveling-current-source-type models can also be viewed as involving current sources distributed along the lightning channel that are progressively activated by the upward-moving return stroke front, releasing the charge deposited by the preceding leader [e.g., Rachidi et al., 2002].

Any adequate return stroke model must be capable of discussing in a consistent way the following three independent measurable parameters:

(a) Lightning current wave forms at the ground.

(b) Remote electric and magnetic fields

(c) Return stroke velocity

The differential vertical electric field dE_z and the azimuthal magnetic field dB_z at ground level due to a vertical current-carrying channel element of differential length dZ' at height "Z'" above a perfectly conducting earth and horizontal distance r from the observation point can be expressed in terms of current as:

$$dE_z = \frac{dz'}{2\pi\varepsilon_0}\left[\frac{2z'^2 - r^2}{R^5}\int i\left(z', \tau - \frac{R}{c}\right)d\tau + \frac{2z'^2 - r^2}{cR^4}\, i\left(z', t - \frac{R}{c}\right) - \frac{r^2}{c^2R^3}\frac{\partial i\left(z', t - \frac{R}{c}\right)}{\partial t}\right] \quad \ldots\ldots (2.1)$$

[illegible] …… (2.2)

wbere $$\sin\theta = \frac{r}{R(z')} = \frac{r}{\sqrt{z'^2 + r^2}}$$

$$dB_\phi(r,t) = \frac{dz'}{2\pi\varepsilon_0 c^2}\left[\frac{r}{R^3(z')}\, i\left(z', t - \frac{R(z')}{c}\right) + \frac{r}{c R^2(z')}\, \frac{\partial i\left(z', t - \frac{R(z')}{c}\right)}{\partial t}\right] \quad \ldots\ldots\ldots\ldots (2.3)$$

$$dB_\phi(r,t) = \frac{dz'}{2\pi\varepsilon_0 c^2}\left[\frac{\sin\theta}{R^2(z')}\, i\left(z', t - \frac{R(z')}{c}\right) + \frac{\sin\theta}{c R(z')}\, \frac{\partial i\left(z', t - \frac{R(z')}{c}\right)}{\partial t}\right] \quad \ldots\ldots\ldots\ldots (2.4)$$

Where $t_b(z')$ is the time at which the current is seen by an observer at p to begin in the channel section at height z' see fig. 2.2

"c" is the speed of light in vacuum and $R(z') = \{z'^2 + r^2\}^{1/2}$

The total fields are found by integrating either (2.1) and (2.3) or (2.2) and (2.4) over the contributing channel length. Two particularly scientific applications of the general fields (2.1) and (2.3) or (2.2) and (2.4) are to the case of the return stroke propagating upward from ground level and the case of a leader process propagating downwards from a spherically symmetrical cloud charge centre.

The return stroke is assumed to create an extending channel whose lower end is fixed at ground and whose upper end is associated with the return stroke front that moves from ground ($z'=0$) upward with a constant speed v. The observer at P "sees" the return stroke front passing a height Z at time $t_b(z') = Z'/_v + R(z')/_c$ (see fig 2.2).

Thus the "radiating" length H(t) of the channel, that is, the depth traversed by the upward moving front as "seen" by the observer at time t, is given by the solution of

$$t = \frac{H(t)}{v} + \frac{\sqrt{H^2(t)+r^2}}{c} \qquad \text{……… (2.5)}$$

For the case where there is no current discontinuity at the return stroke front, the total electric and magnetic fields are obtained by integrating the differential electric and magnetic fields along the channel from 0 to H(t).

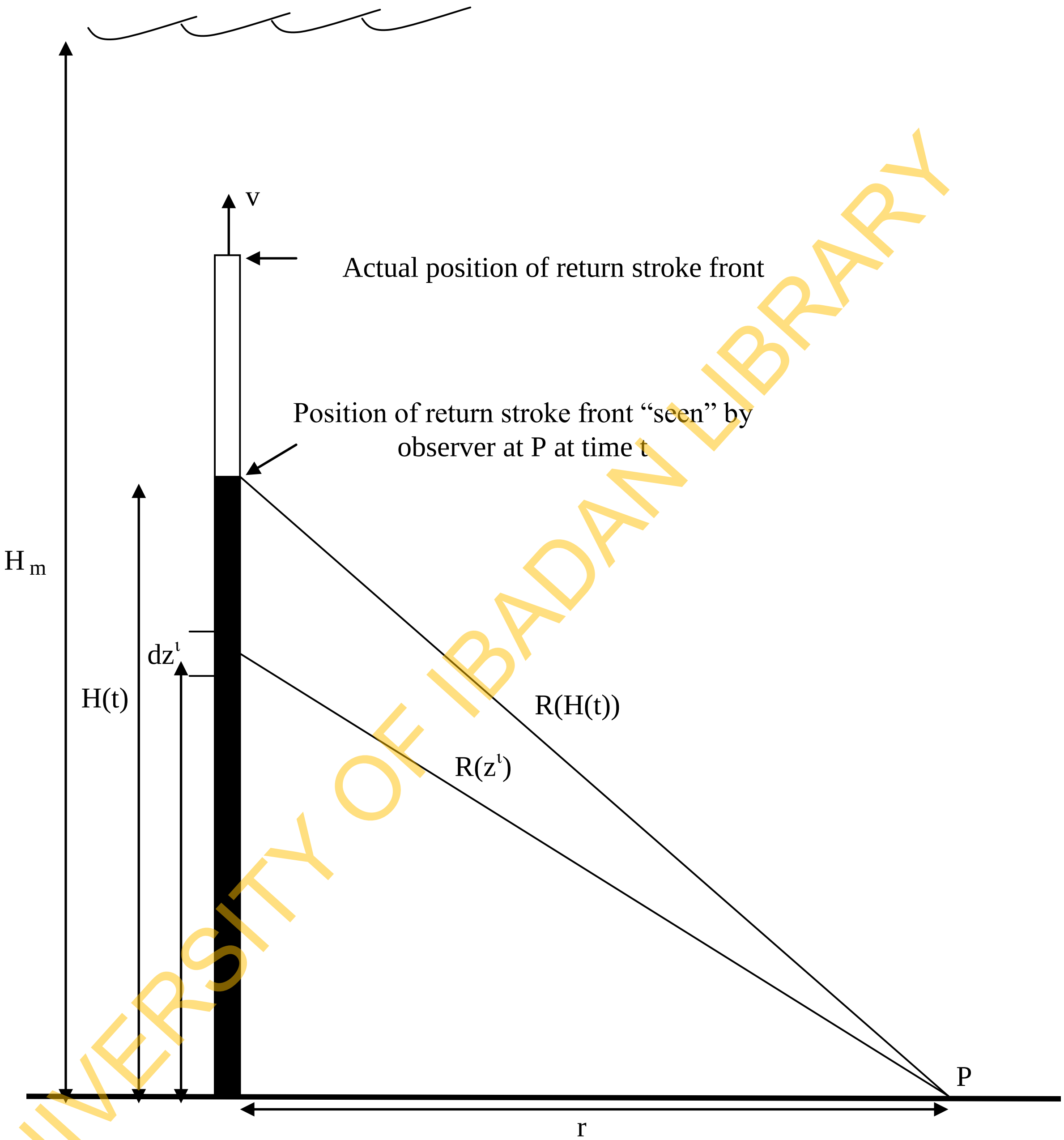

Fig.2.2. Geometry used in deriving the expression is assumed to create an extending channel whose lower end is fixed at ground and whose upper end is associated with the return stroke front that moves from ground ($z' = 0$) upward with a constant speed v . (Adapted from Thottappillil, 1997)

Integrating (2.1) gives

$$E_z(r,t)=\frac{1}{2\pi\varepsilon_0}\left[\int_0^{H(t)}\frac{2z'^2-r^2}{R^5(z')}\int i\left(z',\tau-\frac{R(z')}{c}\right)d\tau\,dz'+\int_0^{H(t)}\frac{2z'^2-r^2}{cR^4(z')}i\left(z',t-\frac{R(z')}{c}\right)dz'-\int_0^{H(t)}\frac{r^2}{c^2R^3(z')}\frac{\partial i\left(z',t-\frac{R(z')}{c}\right)}{\partial t}dz'\right] \quad \text{.... (2.6)}$$

$$E_z(r,t)=\frac{1}{2\pi\varepsilon_0}\int_0^{H(t)}\left[\frac{2-3\sin^2\theta}{R^3(z')}\int i\left(z',\tau-\frac{R(z')}{c}\right)d\tau+\frac{2-3\sin^2\theta}{cR^2(z')}i\left(z',t-\frac{R(z')}{c}\right)-\frac{\sin^2\theta}{c^2R(z')}\frac{\partial i\left(z',t-\frac{R(z')}{c}\right)}{\partial t}\right]dz' \quad \text{... (2.7)}$$

$$B_\varphi(r,t)=\frac{1}{2\pi\varepsilon_0c^2}\int_0^{H(t)}\left[\frac{r}{R^3(z')}i\left(z',t-\frac{R(z')}{c}\right)+\frac{r}{cR^2(z')}\frac{\partial i\left(z',t-\frac{R(z')}{c}\right)}{\partial t}\right]dz' \quad \text{....... (2.8)}$$

$$B_\varphi(r,t)=\frac{1}{2\pi\varepsilon_0c^2}\int_0^{H(t)}\left[\frac{\sin\theta}{R^2(z')}i\left(z',t-\frac{R(z')}{c}\right)+\frac{\sin\theta}{cR(z')}\frac{\partial i\left(z',t-\frac{R(z')}{c}\right)}{\partial t}\right]dz' \quad \text{... (2.9)}$$

where ε_o is the permittivity of free space and c is the speed of light. The first term on the right hand side of (2.1) is called the electrostatic field; the second, the electric induction or intermediate field, and the third, the radiation field. The first term on the right hand side of (2.3) is the magnetic induction field; the second term, the magnetic radiation field.

While the primary channel currents are associated with return stroke of length H (t) and velocity V; a current associated with the leader may exist for Z > H. If the model for the channel current $i(z', t)$ is specified in terms of relatively small number of unknown parameters (2.7) and (2.9) can be used to derive the current parameters from measured values of E and B.

2.7 Leader Model

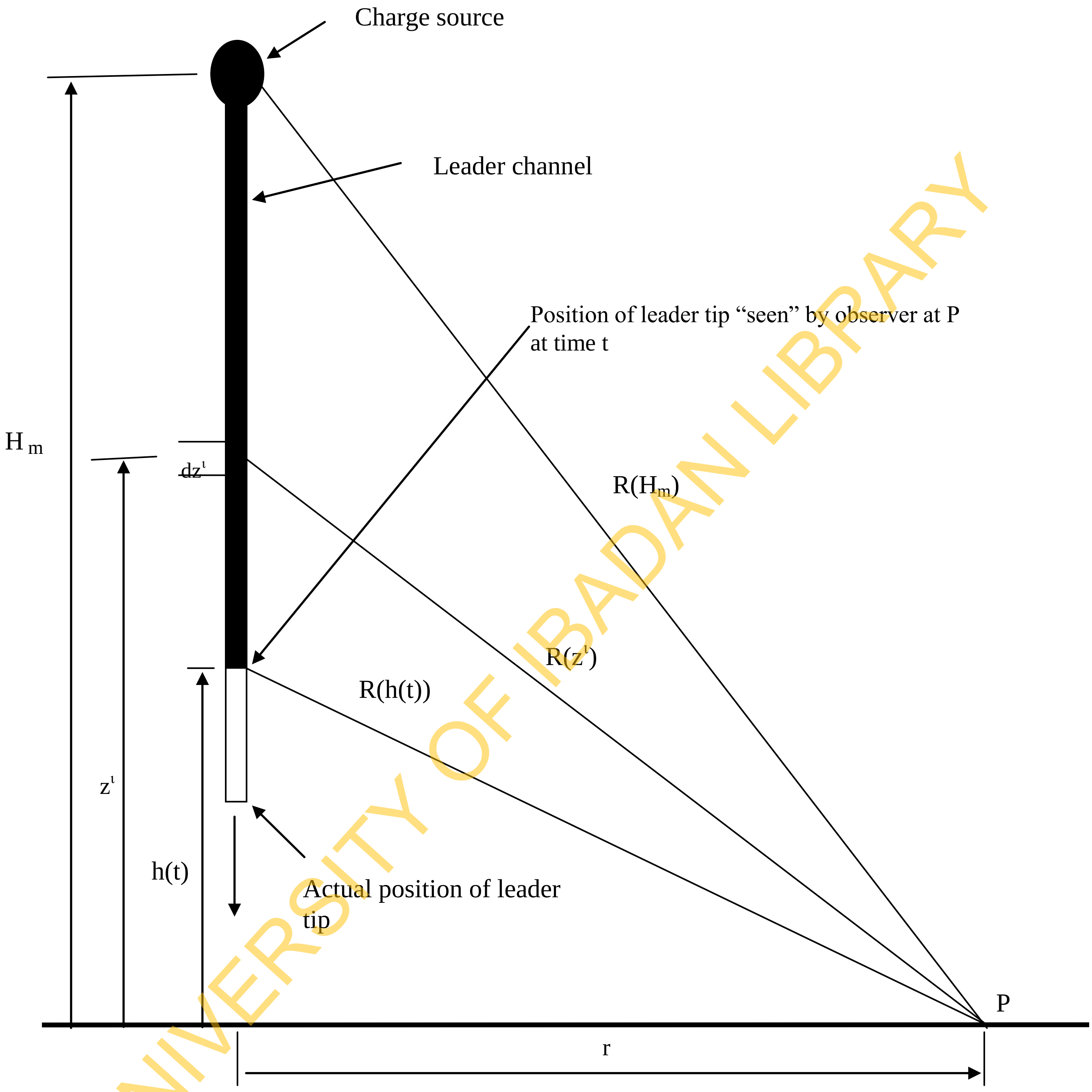

Fig.2.3. Geometry used in deriving the expression is assumed to create an extending downward vertical channel whose charge center at the upper end is associated with the leader front that moves from charge center ($z' = H_m$) downward with a constant speed v. (Adapted from Thottappillil, 1997)

The leader is assumed to propagate vertically downward from a stationary and spherically symmetrical charge center at a height H_m with a constant speed v (fig.2.3). At time t, the observer 'sees' the lower end of the leader channel at a height h(t) given by the solution of

$$t = \frac{H_m - h(t)}{v} + \frac{\sqrt{h^2(t) + r^2}}{c} \qquad \text{…………. (2.10)}$$

The total electric and magnetic fields can be found by respectively integrating equations (2.1) and (2.3) from h(t) to H_m including those in the charge source at H_m.

$$E_z(r,t) = \int_{h(t)}^{H_m} dE_z(r,t) \qquad \text{…………….. (2.11)}$$

$$E_z(r,t) = \frac{1}{2\pi\varepsilon_0}\int_{h(t)}^{H_m}\left[\frac{2z'^2 - r^2}{R^5(z')}\int_0^t i\left(z', \tau - \frac{R(z')}{c}\right)d\tau + \frac{2z'^2 - r^2}{cR^4(z')}\, i\left(z', t - \frac{R(z')}{c}\right) - \frac{r^2}{c^2R^3(z')}\frac{\partial i\left(z', t - \frac{R(z')}{c}\right)}{\partial t}\right]dz' \qquad \text{…(2.12)}$$

$$B_\phi(r,t) = \int_{h(t)}^{H_m} dB_\phi(r,t) \qquad \text{…………. (2.13)}$$

$$B_\phi(r,t) = \frac{1}{2\pi\varepsilon_0 c^2}\int_{h(t)}^{H_m}\left[\frac{r}{R^3(z')}\, i\left(z', t - \frac{R(z')}{c}\right) + \frac{r}{cR^2(z')}\frac{\partial i\left(z', t - \frac{R(z')}{c}\right)}{\partial t}\right]dz' \qquad \text{… (2.14)}$$

2.8 **Traveling Current Source-Type Models**

Table 2.1 :Traveling Current Source-Type Models for t $\geq \frac{z'}{v_f}$ (Adapted from Ravok, 1997)

Models	$P(z')$	V	Current Equation
Bruce and Golde(BG) *Bruce and Golde(1941)*	1	∞	$I(z',t) = I(0,t)$ for $t \geq \frac{z'}{v_f}$ $I(z',t) = 0$ for $t < \frac{z'}{v_f}$
Traveling Current Source (TCS) *Heidler(1985)*	1	-c	$I(z',t) = I\left(0, t + \frac{z'}{v}\right)$ for $t \geq \frac{z'}{v_f}$ $I(z',t) = 0$ for $t < \frac{z'}{v_f}$

P(z′)is model-dependent attenuation function

2.8.1 Bruce-Golde Model

The Bruce-Golde model is a limiting case of what might be expected to occur in the return stroke channel. For the Bruce-Golde model the return stroke current t any given time is assumed to be uniform with the height below the return stroke wave front and zero above (Bruce and Golde, 1941). The current in the channel below the wave front is identical to the current at the ground level:

$$i(z', t) = i(0, t) \qquad z' \leq H$$

$$i(z', t) = 0 \qquad z' \geq H \qquad \text{.......... (2.15)}$$

Uman and McLain (1970 b) showed that for r >50km (2.15) can be combined with (2.7) and (2.9) to yield

$$i(t) = \frac{2\pi r}{\mu_0 H(t)} \int_0^t B\left(t + \frac{r}{c}\right) dt \qquad \text{............ (2.16)}$$

where $$\mu_0 = \frac{1}{\varepsilon_0 c^2} \qquad \text{..........(2.17)}$$

$$H(t) = \int_0^t v(\tau)\, d\tau \qquad \text{.......... (2.18)}$$

and $$E_\phi\left(t + \frac{r}{c}\right) = c B_\phi\left(t + \frac{r}{c}\right) \qquad \text{..............(2.19)}$$

As the return stroke propagates upward for times after the current peak is reached, the current in the channel decreases. As a result, the Bruce-Golde model return stroke lowers to ground charge from the channel; charge originally stored in the leader's corona envelope. The Bruce-Golde model was originally developed because its simplicity allows easy analytical computations. It is not physically reasonable however for the return current to be uniform with altitude, since one point on the return stroke channel cannot know instantaneously what is happening at another point. Dennis and Pierce (1964) modified the Bruce-Golde model to correct for this deficiency. Fields calculated from assumed Dennis-Pierce currents are very similar to Bruce-Golde fields (Uman and Mc Lain, 1969), but a simple method is not available to calculate Dennis-Pierce currents from measured fields.

2.8.2 Traveling **Current Source Models (TCSM)**

The Traveling Current Source Model (TCSM), proposed by Heidler [1985], is the simplest member of the category of traveling-current-source-type models. In the TCSM the current source is implied to be at the upward propagating (at constant speed v) return stroke front and the current wave propagates downward with the speed of light c to the Earth where it vanishes (which implies that the channel is terminated in its characteristic impedance). The current at a height z' from the base of a straight and vertical channel is given by

$$i(z',t) = i\left(0, t + \frac{z'}{c}\right) \qquad z' \leq H$$

$$i(z',t) = 0 \qquad z' > H$$

The current at a given height z′ is equal to the current at ground at time z′/c later.

2.9 Transmission Line Type Model (TLM)

Table 2.2 : Transmission-Line Type Models (Adapted from Ravok, 1997)

Models	$P(z')$	v	Current Equation
Transmission Line(TL) *Uman and McLain(1969)*	1	v_f	$I(z',t) = I\left(0, t - \frac{z'}{v}\right)$ for $t \geq \frac{z'}{v_f}$ $I(z',t) = 0$ for $t < \frac{z'}{v_f}$
Modified Transmission Line with Linear current decay (MTLL) *Rakov and Dulzon (1967)*	$1 - \frac{z'}{H}$	v_f	$I(z',t) = \left[1 - \frac{z'}{H}\right] I\left(0, t - \frac{z'}{v}\right)$ for $t \geq \frac{z'}{v_f}$ $I(z',t) = 0$ for $t < \frac{z'}{v_f}$
Modified Transmission Line with Exponential(MTLE) current decay *Nucci et.al (1988)*	$exp(\frac{-z'}{\lambda})$	v_f	$I(z',t) = I\left(0, t - \frac{z'}{v}\right) exp(\frac{-z'}{\lambda})$ for $t \geq \frac{z'}{v_f}$ $I(z',t) = 0$ for $t < \frac{z'}{v_f}$

H=total channel height =constant, $v = v_f$ = constant, λ =constant = current decay constant

2.9.1 Transmission Line Model (TLM)

The transmission line model (TLM) is the most widely used model of the lightning return stroke and is the simplest of the models in the transmission-line-type category. The TLM is generally attributed to Uman and McLain (Uman and McLain, 1969, 1970 a), who named and developed it mathematically. Like Bruce-Golde model, transmission line model is also a limiting case to the actual return stroke current. In this model, a given current wave shape propagates up the channel behind the return stroke wave front. In other words, the current at ground level is assumed to propagate up the channel as it would along an ideal transmission line (Uman and Mc Lain, 1969).

The TLM has been primarily employed to estimate return stroke peak currents and peak current derivatives from measurements of the peak electric field and peak electric field derivative, respectively, with an assumed return stroke speed [e.g., Weidman and Krider, 1980; Krider et al., 1996]. These measurements are generally made some tens of kilometers or more from the lightning channel, distances at which the radiation field component of the total electric field dominates the peak value. In the TL model, it is assumed that the current wave at the ground travels undistorted and unattenuated up the lightning channel at a constant speed *v*.

$$i(z',t) = i\left(0, t - \frac{z'}{v}\right) \qquad z' \leq vt$$

$$i(z',t) = 0 \qquad z' > H \qquad \text{............. (2.20)}$$

where the return stroke velocity, v is assumed constant.

The current at a given height z' is equal to the current at ground at time z'/v earlier. The transfer of charge takes place only from the bottom of the leader channel to the top; thus no net charge is removed from the channel, this being an unrealistic situation given the present knowledge of lightning physics [*Uman*, 1987].

The transmission line model requires the same current to propagate across any height of the channel; therefore no leader corona charge can be renewed from the return stroke channel during the return stroke propagation time, charge only being transferred from the top to the bottom of the channel. Uman and McLain (1970 b) showed that for r > 50km (2.9) and (2.15) can be combined to yield

$$i(r,t) = \frac{2\pi r}{\mu_0 v} B\left(t + \frac{r}{c}\right) \qquad H \leq H_m \qquad \text{…….. (2.21)}$$

Interestingly, the transmission line model yields an even simpler analytical link between current and distant fields than does the Bruce-Golde model. For this immediately after the return stroke has reached the idealized top of the leader channel, the transmission line model predicts an exact replica of the initial field peaks but with opposite polarity, a so called mirror image wave form. (Uman and Mc Lain, 1970 b) while the Bruce-Golde model yields a field discontinuity (Uman and Mc Lain, 1969). The TLM works reasonably well in reproducing close measured electric and magnetic fields if return stroke speeds during the first microsecond are chosen to be between $1X10^8$ ms^{-1} and 2 $X10^8$ ms^{-1}, and works well in reproducing field derivatives for return stroke speeds near 2 $X10^8$ ms^{-1} (Schoene et. al.,2003) . For this reason, transmission line model (TLM) is adopted for this work.

2.9.2 The Modified Transmission Line Exponential decay (MTLE) model.

In the MTLE model [*Nucci et al*., 1988] the lightning current intensity is supposed to decrease exponentially while propagating up the channel as expressed by:

$$i(z',t) = i\left(t - \frac{z'}{v}\right)e^{-\frac{z'}{\lambda}} \qquad z' \leq vt$$

$$i(z',t) = 0 \qquad z' > vt$$

where : v is the return-stroke velocity; λ is the decay constant which allows the current to reduce its amplitude with height.

This attenuation is not to be considered as due to losses in the channel or to take into account the already mentioned decay with height of the initial peak luminosity, but has been proposed by *Nucci et al*. [1988] to take into account the effect of the charges stored in the corona sheath of the leader and subsequently discharged during the return stroke phase. Its value has been determined to be about 2 km by *Nucci and Rachidi* [1989], by means of tests with experimental results published by *Lin et al*. [1979, 1980].

The MTLE model represents a modification of the TL model which allows net charge to be removed from the leader channel via the divergence of the return stroke current with height, and thus results in a better agreement with experimental results.

2.10 The wave guide model of lightning currents

Volland (1981) reasoned that unsatisfactory application of transmission line theory in spite of the apparent success of the much simpler lump circuit model may be due to the fact that the existing transmission line theories of the return stroke do not take into account the wave guide characteristics of the conducting channel.

The wave guide model treats the return stroke as a thin moderately conducting vertical cylindrical conducting wire of length l which is electrically connected with the highly conducting earth. The vertical electric current at the top of the wire at Z = l must disappear while at the ground (Z = 0) the horizontal component of the electric field strength must be zero. The wire thus behaves like a resonance cavity in which only standing waves can be excited.

Sommerfield (1952) showed that transversal magnetic (TM) waves and transversal electric (TE) waves exist in a wire. However, only the cylindrical principal TM waves are of significance for the energy transportation. The magnetic induction **B** of such TM waves can be derived from a vector potential **A**.

$$B = \nabla X A \qquad \text{………… (2.22)}$$

Where **A** has only a vertical component of the form

$$A = \frac{E_o}{i\omega} Z_o(Kx)\cos hz\, e^{-i\omega t} \qquad \text{……… (2.23)}$$

Z_0 (x) is a cylindrical function of zero order

ω is the angular frequency of the waveS

E_o is the amplitude with dimension of an electric field. Furthermore,

$$h = \frac{(2n-1)\pi}{2l} \quad \text{with} \quad n = 1,2,3 \qquad \text{………. (2.24)}$$

Vertical wave number chosen such that the boundary conditions at Z = 0 and l are fulfilled.

Moreover,

$$K = \sqrt{(k^2 - h^2)}$$

Is a horizontal wave number with

K = $\omega(\sqrt{\varepsilon\mu})$ and

$$\varepsilon = \begin{cases} \varepsilon + \frac{i\sigma}{\omega} & \text{within the wire } (x < a) \\ \varepsilon_o & \text{outside the wire } (x > a) \end{cases}$$

the complex dielectric constant, r the electric conductivity within the wire, $\mu = \mu_o$ the permittivity of free space, and ε_o the dielectric constant of free space.

With B derived from (2.22) and (2.23) and the electric field E derived from the first Maxwell equation, the following components of **E** and **B** are obtained.

$$B_\phi = -\frac{\partial A}{\partial x} = \frac{E_o K}{i\omega} Z_1(Kx)\cos hz\, e^{-i\omega t} \qquad \text{……………. (2.25a)}$$

$$E_\rho = \frac{1}{i\sigma\mu\omega}\frac{\partial B_\phi}{\partial z} = \frac{ih}{K} A Z_1(K\rho) e^{i(hz-\omega t)}$$ .... (2.25b)

$$E_z = \frac{1}{i\sigma\mu\omega}\frac{1}{\rho}\frac{\partial(\rho B_\phi)}{\partial \rho} = A Z_0(K\rho) e^{i(hz-\omega t)}$$ .... (2.25c)

$$E_\phi = B_\rho = B_z = 0$$

Within the wire, Z_0 is the Bessel function J_0 because it must be finite at $\rho = 0$. Outside the wire Z_0 is a Hankel function of first order H which decays with ρ if Im(K) > 0.

Continuity of the horizontal components B_ϕ/μ and E_z at the surface of the wire at d/2 (d is its diameter) yields the eigenvalue equation

$$\frac{J_1(Kd/2)}{J_0(Kd/2)} = \frac{k^2 K_0 H_1^{(1)}(K_0 d/2)}{k_0^2 K H_0^{(1)}(K_0 d/2)}$$ .... (2.26)

where K; k are the wave numbers within the wire, and K_0, k_0 the numbers outside the wire:

$K^2 = k^2 - h^2$; $K_0^2 = k_0^2 - h^2$

$$k = \sqrt{i\sigma\mu\omega} \quad ; \quad k_0 = \omega\sqrt{\varepsilon_0\mu_0} = \omega/c$$

…..(2.27)

with h from Equation (1.23), and c is the velocity of light.

Considering the fact that for lightning-induced voltage calculation it is the early time region of the field that plays the major role in the coupling mechanism [*Nucci et al.*,1993], it follows that the most adequate models are probably the MTL-type ones (see Tab.2.3). Although the TL model does not allow for any net charge removal from the channel and does not reproduce realistic fields for late time calculations [*Nucci et al.*, 1990], the early time field prediction of the TL model is very similar to that of the more physically reasonable MTLL and MTLE models and thus, it can be considered a useful and relatively simple tool.

Tab. 2.3. – Summary of statistics on the absolute error of the model peak fields Adapted from *Thottappillil and Uman* [1993].

Absolute Error $=\lvert(E_{cal} - E_{meas})/E_{meas}\rvert$				
	TL	MTL	TCS	DU
Mean	0.17	0.16	0.43	0.23
St. Dev.	0.12	0.11	0.22	0.20
Min.	0.00	0.00	0.14	0.00
Max.	0.51	0.45	0.84	0.63

2.11 Theoretical framework of lightning induced voltages

2.11.1 Introduction

Hitherto, attention had been paid on the electromagnetic fields produced by the lightning flashes. These fields illuminate and interact with the overhead powerlines resulting in overvoltages on the lines and at times power outages where insulation of the power system breaks down. Here, field to wire coupling model will be examined in order to determine the induced voltages on overhead powerlines.

In any lightning discharge, the charge on the down coming leader causes the conductors of the line to have a charge induced in them. These charges are bound (held in that portion of the line nearest to the cloud) so long as the cloud remains near without discharging its electricity by a lightning stroke to an object. If however, the cloud is suddenly discharged, as it is when lightning strikes some object nearby, the induced charges are no longer bound, but travel with nearly the velocity of light, along the line to equalise the potential at all points of the line.

The voltage induced on a line by an indirect lightning stroke has four components:

1. The charged cloud above the line induces bound charges on the line while the line itself is held electrostatically at ground potential by the neutrals of connected transformers and by leakage over the insulators. When the cloud is partially or fully discharged, these bound charges are released and travel in both directions on the line giving rise to the travelling voltage and current waves.

2. The charges lowered by the stepped leader further induce charges on the line. When the stepped leader is neutralized by the return stroke, the bound charges on the line are released and thus produce travelling waves similar to that caused by the cloud discharge.

3. The residual charges on the upper part of the return stroke induce an electrostatic field in the vicinity of the line and hence an induced voltage on it.

4. The rate of change of current in the return stroke produces a magnetically induced voltage on the line. If the lightning has subsequent strokes, then the subsequent components of the induced voltage will be similar to one or the other of the four components discussed above. The magnitudes of the voltages induced by the release of the charges bound either by the cloud or by the stepped leader are small compared with the voltages induced by the return stroke. Therefore, only the electrostatic and the magnetic components induced by the return stroke are considered in the following analysis.

2.12 Overvoltages

The reliability of the supply provided by an electric power system is judged by the frequency and duration of supply interruptions to consumers which depends to a great extent on the surge performance of the system. Breakdown in insulation is one of the major and most frequent causes of interruption of electric power supply. If the insulation is subjected only to the normal operating voltages which vary within quite narrow limits, there would be no problem. In reality the insulation has to withstand a variety of overvoltages with a large range of shapes, magnitudes and durations.

Overvoltages impressed upon a power system by atmospheric discharges are called “lightning overvoltages”. Overvoltages can be generated within the power system by the connection or disconnection of circuit elements or the initiation of faults. These are classified as "temporary overvoltages" . When the overvoltages are highly damped and of short duration, they are referred to as "switching overvoltages"

2.12.1 Lightning Overvoltages

Overvoltages due to lightning may occur on any supply line. Majority of lightning overvoltages originate on overhead lines. Transient voltages can appear on an overhead line either by direct hit (direct stroke) or by induction from nearby lightning stroke (induced stroke).

2.13 Past Theoretical Work on Induced Voltages on Power Lines

The first theoretical work on induced lightning surges on transmission lines was carried out by Wagner K.W in the year 1908. He assumed that a charged thundercloud situated above a transmission line will induce charges of opposite polarity in the lines on the assumption that free charges can move to earth via the leakage resistance of the line and through the earth connection of its neutral. During the time when the field is increasing, the induced charge at every point of the line is determined by the fact that the resulting potential of the line should be equal to zero. If the charge of the thundercloud, and with it also the induced field also disappears, the induced charges would be free to move along the line as traveling waves. According to this theory, the induced voltage of the lines is given by the product of the height of the conductor above the ground and the inducing electrical field strength prior to the lightning discharge. The fronts and time to half value of the waves are given by the variation along the line of the inducing field strength which implies long smooth surges.

Wagner's theory was improved by Bewley (as cited in Golde, 1977) by accounting for the fact that induced field cannot disappear instantaneously but must have a limited time derivative (p.757). Thus implying that the traveling waves will be longer and the amplitudes will decrease as compared with Wagner's calculations. Aigner (as cited in Golde, 1977) was the first to take into account the inducing effect of the vertical lightning path of a lightning stroke to the ground (p. 757). Only the magnetic field of the lightning discharge was considered here and the calculations were carried out on a questionary basis, assuming a sinusoidally varying lightning current which limits the value of the work.

Wagner and McCann (as cited in Matsubara and Sekioka, 2009) considered the influence of the charge and current in the lightning channel during the return stroke on investigating the nature of currents over voltages. It was discovered that the field of the lighting current is of a dominating importance in comparison with the field of the thunder cloud. The authors showed that it is only during the return stroke that high voltages can be found. The charge and the current in the lightning channel are approximated in the following way. Just prior to the return stroke, an electric charge is assumed to be uniformly distributed along the lightning channel. It is then instantaneously neutralized as the current in the return stroke is propagated upward along the lightning path with a constant velocity. Consequently current will behave as a step-function. With these assumptions as starting points, Wagner and McCann (as cited in Matsubara and Sekioka, 2009) computed the inducing electric field using Maxwell's equation and retarded potentials. The induced voltage is then calculated by a numerical integration method.

According to Szpor (as cited in Golde, 1977), taking both electrostatic and magnetic induction into consideration calculated the induced voltages caused by a vertical lightning stroke. The problem was treated as a quasi-stationary one, the results being valid only in the vicinity of the lightning strokes. The numerical values of the induced voltages are of the same magnitude as those given by Wagner and McCann. Golde (1954) on investigating the influence of the induced voltages on the fault frequency of distribution lines made assumptions different from Wagner and McCann in calculating the induced voltages. He assumed that the charge distributed along the leader channel decreased exponentially with the height above ground and that the propagation velocity of the return stroke decrease exponentially with time. Both assumptions were probably in better agreement with experience than that of Wagner and McCann. Golde (1954) carried out his calculations using numerical integrations in computing only the scalar potential by assuming the propagation velocity of the return stroke at the ground to be of constant value of 80mus^{-1} which is about 27% of velocity of light. Lundholm (as cited in Golde, 1977), considered the relationship between the velocity of the return stroke and the lightning current in the deduction of the induced voltage. The neglect of the magnetic field in the deduction made the result not quite satisfactory from theoretical point of view.

Rusck (1958) postulated a theory in the calculation of indirect over-voltages, taking into consideration both the scalar and vector potentials of the inducing field in a current way. Chowduri and Gross (1967) developed a theory that Jakubouski (as cited in Golde, 1977) pointed out as not correct because instead of using the inducing scalar potential, they used inducing voltage which is the sum of the inducing scalar potential and the line integral of the vector potential.

2.14 Induced Electromagnetic Field on Overhead Line and its Vicinity

A lightning discharge always causes an electromagnetic field,which propagates out from the discharge with the velocity of light. It is this field which can induce voltages and currents in an overhead line. The sources of the discharges, thunderclouds, have a height above the earth's surface of about 2 km, whereas the height of the power line seldom exceeds some tens of meters. The area of the total field which is of any interest in this connection is consequently small in comparison to the total area and therefore the variation of the field strength with the height above the ground can be neglected with the area occupied by the line. So in principle, it is the field at the surface of the earth which determines the induced voltage.

Brown and Whitehead (1969), Braunstein (1970) and Golde (1973) used physical model for determining lightning strokes to power transmission lines. Izraeli and Braunstein (1983), in developing a model for study of the lightning stroke on an object used an approach which depended on the sequence events of the stroke thus:

(a) the induced electric field at various points on the object and its vicinity.

(b) the criteria for the initiation of up going discharges for various points at the object and its vicinity.

(c) determination of probable striking point

The following assumptions are made in evaluating the induced electromagnetic field during the discharge phenomena.

(i) The main discharge occurs in a single channel. The contributions of the possible secondary branches to the induced electromagnetic field are negligible.

(ii) The leader is a uniform negative electric charge of the form of a traveling step function which moves at constant velocity, *v*, on the channel from the bottom of the cloud to the ground.

(iii) The shape of the line and its vicinity is a small perturbation on the ground plan. This is the first approximation it is ignored.

(iv) The ground is assumed to have infinite conductivity. (Izraeli and Braunstein, 1983)

Using the image method the induced electric field at various points is studied. A single traveling charge can be determined in a two dimensional system (ξ, r)

The coordinates are of the plane including the point P_1 and the straight line representing the channel. The origin is the charge source (the bottom of the cloud).

According to Braunstein (as cited in Chowdhuri et al., 2002), by studying the Maxwell equations and using the retarded potentials, it has been shown that the electric field strength components due to a single traveling charge at a point P(ξ, r) are:

$$E_{\xi}=\frac{q}{4\pi\varepsilon}\left[\frac{\frac{c-v}{c}}{\sqrt{(u^2+R^2)}}-\frac{1}{\sqrt{(\xi^2+r^2)}}\right] \qquad \ldots\ldots\ldots\ldots(2.8)$$

$$E_{r}=\frac{q}{4\pi\varepsilon}\left[\frac{u}{\sqrt{(u^2+R^2)}}+\frac{1}{\sqrt{(\xi^2+r^2)}}\right] \qquad \ldots\ldots\ldots\ldots\ldots\ldots\ldots\ldots(2.29)$$

where $u=\frac{c}{c+v}(vt-\xi)$; $\quad R=\sqrt{\frac{c-v}{c+v}}\,r$ ………………(2.30)

and

v, c = velocities of traveling charge front and light respectively.

T = time

q = charge density, $C m^{-1}$

ε_o = dielectric constant in vacuum , $F\ m^{-1}$.

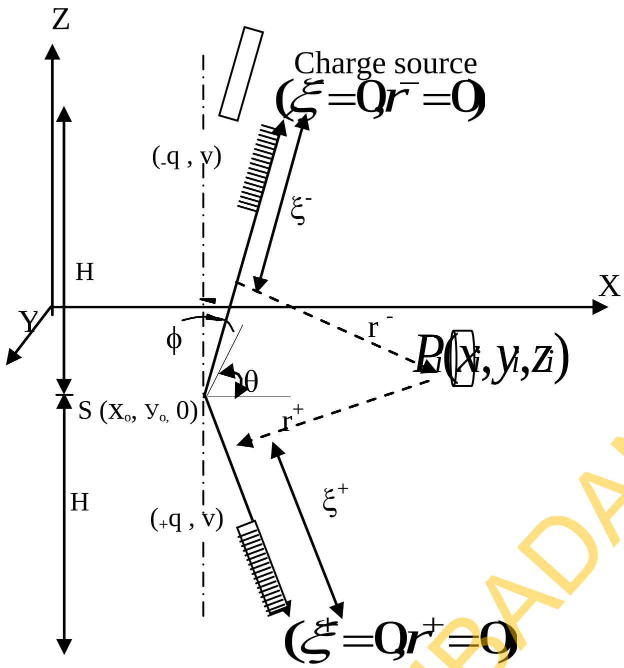

Fig. 2.5: Channel and its image together with a structure in co-ordinate systems (Adapted from Izrael & Braunstein, 1983)

The two traveling charges, the leader and its image have opposite polarity but same shape as each other the field strength components at any point are obtained by the superposition of the contribution by each of the traveling charges involved. As the object in this case the overhead line is always located far away from the charge source. It was contribution of these additional traveling charges to the electric field strength at the object is negligible. Thus these additional traveling charges will be omitted leaving the physical model with the leader and its image.

The electric field at the point P_1 is the sum of the field due to the leader and its image. The transformation of a point P_1 to each relevant coordinate system (ξ^-, r^-) and (ξ^+, r^+) is according to the trigonometrical relations:

$$r^{\pm} = \left\{ (x - x_{Ni})^2 + (y - y_{Ni})^2 + (z \mp z_{Ni})^2 \right\}^{1/2} \qquad \ldots\ldots\ldots\ldots\ldots(2.31)$$

$$\xi^{\pm} = \frac{(H \mp z_N)}{C\varsigma}$$

where

$$z_{ni} = \frac{1}{2}\left[\cdots \right] \qquad \ldots\ldots\ldots\ldots(2.32)$$

$$x_{ni} = z_{ni} \tan\phi \cos\theta + x_o$$

$$y_{Ni} = z_{ni} \tan\phi \sin\theta + y_o$$

The point (x_{Ni}, y_{Ni}, z_{Ni}) is the intersection point of the normal passing with the P_1 traveling charge–channel axis. The point can be determined by simple vector analysis procedures. H is the height of the charge source above the ground. (the bottom of the cloud). (x_o , y_o) is the intersection point of the charge-channel axis and the ground plane. ϕ is the inclination angle of the channel axis measured to the normal at the point $s(x_o, y_o, 0)$ thus $0 \leq \theta \leq 360^o$. - or +

is used where necessary to distinguish between quantities concerned with the leader and its image respectively.

Once the electric field vectors $E_p^-(E_\xi^-, E_\eta^-)$ and $E_p^+(E_\xi^+, E_\eta^+)$ have been calculated, the total electric field strength at the point P_i is

$$E_p = \sqrt{(E_x^2 + E_y^2 + E_z^2)} \quad \text{…………….(2.33)}$$

where

$$[illegible]$$

$$[illegible] \quad \text{……………. (2.34)}$$

$$[illegible]$$

With the above measured parameters of the stroke, the general expression for the electric field at the point P_i takes the form

$$[illegible] \quad \text{……………(2.35)}$$

where vt is the distance of the leader from the origin (the bottom of the cloud) at a given time t.

2.15 Striking Distance

The lightning discharge starts at the cloud end for strokes to level ground or to low objects. In the initial slope, the leader stroke proceeds downward without being influenced by grounded objects. As the charge of the cloud is lowered along the leader stroke, the electric field on the surface of ground objects increases. Finally at a certain distance of the tip of the leader stroke from the grounded object, the critical electric field for the breakdown of air at the surface of the grounded object is reached and an upward streamer starts from the object to meet the leader stroke. This distance of the leader tip from the grounded object which produces the upward streamer is caked the striking distance. An intensely illuminated discharge called the return stroke has been estimated to be between 0.1 and 0.5 that of light in free space. Currents of high magnitude are associated with return stroke.

The striking distance is a very significant parameter in the estimating of lightning performance of overhead power lines. The longer the striking distance the higher will be the attractiveness of overhead line to a lightning strike, therefore the possibility of a line outage will be higher. The striking distance r_s is a function of return stroke current. The most widely used relationship is $r_s = 8\ I^{0.65}$. I = return stoke current in KA.

Eriksson (1987) combined the effects of both the structure height, say horizontal shield wire or phase conductor of even head power lines and the return-stroke current on the attractive radius R_a

$$R_a = 0.67\ H^{0.6}\ (I)^{0.74}$$

2.16 Determination of probable striking points

The final stage of the lightning phenomenon occurs when the electric field exceeds the critical value at point P_i and an up-going discharge is initiated. The down-going leader continues towards the ground without any changes. A streamer stars to move at that time , from the leader front location towards the point P_i in the opposite direction ,If the two streamers meet, a channel for the return stroke exists and the point P_i is likely to be struck by that lightning. As there are several points on the structure (the power line) and its vicinity where this process takes place, the4 question is which point will be struck, The two streamers, which will meet first, will determine the striking point.

It is assumed that all streamers travel with the same velocity as the leader. Distance can be measured instead of time. The critical distance from the point P_i is D_{ci} which is the distance of the leader from its origin when the electric field at P_i equals the critical value E_{ci}. At that instant two streamers are initiated. The D_{ci} values are computed for each P_i (i=1,2,….n) for a given lightning current(or charge density) by evaluating vt for which of the following condition is fulfilled:

$$E_{pi}\ (vt = D_{ci}) = E_{ci} \qquad \text{……(2.36)}$$

(from equation 2.7,where all terms of E_{pi} are constants except vt).

The location of the leader front P_{ci} when vt = D_{ci}, is

$$\begin{aligned} z_{ci} &= H - D_{ci}\cos\phi \\ x_{ci} &= z_{ci}\tan\phi\cos\theta + x_0 \\ y_{ci} &= z_{ci}\tan\phi\sin\theta + y_0 \end{aligned} \qquad \text{……………………(2.37)}$$

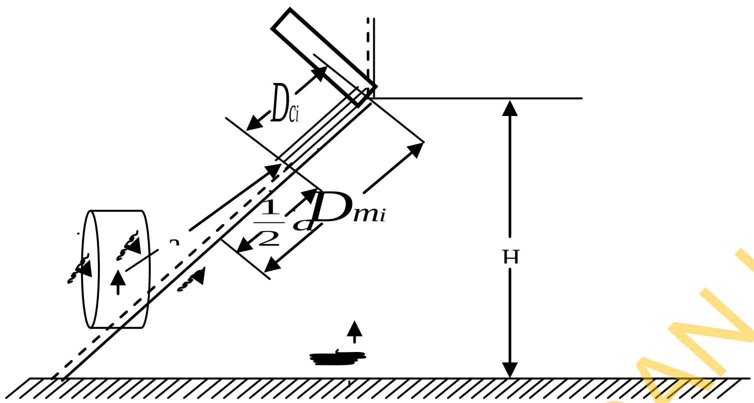

Fig. 2.6: Critical meeting distances for point P_i

The 'meeting' distance D_{mi} ,is the distance of the leader front from its origin, when the streamers of the point P_i and the leader meet. The leader is assumed to continue its down-going movement until one pair of streamers from various points meets. The computation of D_{mi} involves the calculation of geometrical distances. For each P_i, D_{mi} is given by

$$D_{mi} = D_{ci} + \frac{1}{2}\sqrt{(x_i - x_{ci})^2 + (y_i - y_{ci})^2 + (z_i - z_{ci})^2}$$

……………(2.38)

where D_{ci} is the critical distance

$P_c(x_{ci}, y_{ci}, z_{ci})$ is defined in equation (2.37)

$P_i(x_i, y_i, z_i)$ are the points under discussion. Fig.2.6 shows the critical and 'meeting' distances for some points P_i .Once all the D_{mi} values are computed for a given lightning current and channel , the point which involves the smallest D_m value is the one most likely to be struck. The reason is that this is the first one in the time which provides a conductive path for the lightning discharge between the cloud and the ground.

2.17 Analysis of lightning induced voltages on overhead lines

Factors affecting the calculation of lightning induced voltages on overhead lines

• The nature of the electromagnetic field produced by the lightning; which depends on the model of the return stroke and on the model of the ground.

• The coupling process of the electromagnetic field to the overhead line; which is a function of the coupling model.

• The line response to the electromagnetic field produced by the lightning discharge (dependent on the line model and on the ground model).

This implies that the following steps are required in the calculation of lightning induced.

First, selection of return stroke current model that defines the space and time distribution of return stroke current through channel.Then, the computation of time varying electromagnetic sfield along the observing line. Lastly, the computation of the resulting overvoltage on the overhead line due to electromagnetic interaction of the computed field and the observed line.

The basic assumptions of the analysis are:

1. Only the electrostatic and the magnetic components induced by the return strike are considered.
2. Only the charges on the upper part of the return stroke are considered.
3. Charge distribution along the leader stroke is uniform.
4. The return-stroke current is rectangular and it has a finite speed *v*, that is less than the speed of light ($\beta = v/c < 1$,where c is the speed of light). However, the result with the rectangular current wave can be transformed to that with currents of any other waveshape by the convolution integral (Duhamel's theorem).The computations were extended to current waves having linearly rising front, in order to study the effect of wavefront of the current on the induced voltage wave.
5. The stroke channel is vertical, where the upper part consists of a column of residual charge that is neutralized by the rapid upward movement of return-stroke current in the lower part of the channel
6. Overhead lines are loss free and the earth is perfectly conducting.

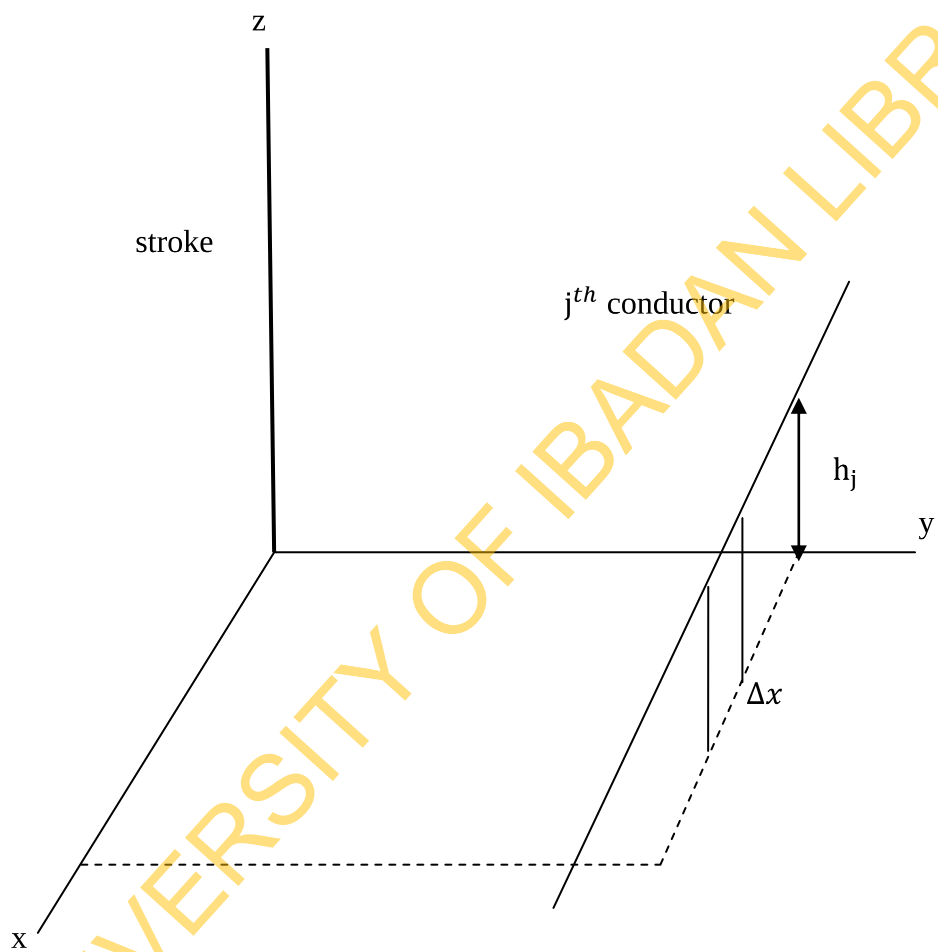

Fig.2.7: Coordinate system of line conductors and lightning stroke.

The geometrical configuration of the stroke and lines is based on the rectangular system of coordinates where the origin of the system is the point where lightning strikes the surface of the earth (Fig.2.7) The line conductor under consideration is located at a distance y_{0j} (m) from the origin, having a mean height of h_j (m) above ground and running along the *x*-direction. The origin of time (t = 0) is assumed to be the instant when the return stroke starts at the earth level.

2.18 Single-**conductor overhead line case**

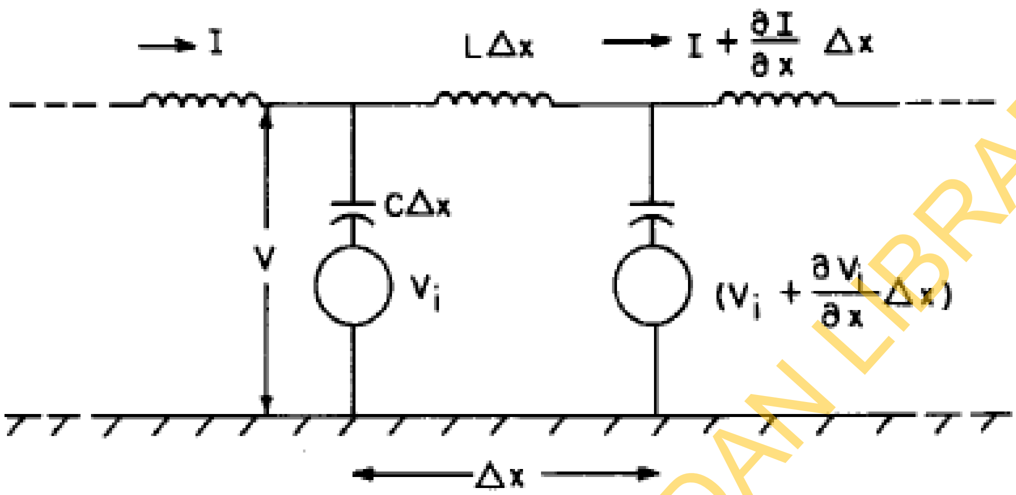

Fig.**2.8** Equivalent circuit for computing lightning-induced voltage on single-conductor over head line

The two transmission-line equations of the equivalent circuit for lightning-induced voltage on single-conductor over head line (Fig.2.8) are given by :

$$-\frac{\partial V}{\partial x} = L\frac{\partial I}{\partial t} \qquad \text{.............(2.39)}$$

$$-\frac{\partial I}{\partial x} = C\frac{\partial}{\partial t}(V - V_i) \qquad \text{............. (2.40)}$$

Differentiating eqn.(2.39) and eliminating current

$$\frac{\partial^2 V}{\partial x^2} - \frac{1}{c^2}\frac{\partial^2 V}{\partial t^2} = \frac{1}{c^2}\frac{\partial^2 V_i}{\partial t^2} = F(x,t) \qquad \text{..........(2.41)}$$

where V (x, t) is the induced voltage at a point x on the overhead line, c is the velocity of light in free space and V_i (x, t) is the inducing voltage – the voltage which would have existed without the presence of the overhead line ; defined as

$$V_i = -\int_0^{h_p} E_i.dz = \int_0^{h_p}\left(\nabla\phi + \frac{\partial A}{\partial t}\right).dz = \int_0^{h_p}(E_{ei} + E_{mi}).dz = V_{ei} + V_{mi} \qquad \text{..........(2.42)}$$

where $\bar{E}_i = \bar{E}_{ei} + \bar{E}_{mi} = -\nabla\phi - \frac{\partial\bar{A}}{\partial t}$, $\bar{E}_{ei} = -\nabla\phi$ and $\bar{E}_{mi} = -\frac{\partial\bar{A}}{\partial t}$

E_i in eqn.(2.42) contains both the electrostatic component ($\nabla\phi$) from the charge above the current column and the magnetic component (∂A/ ∂t) due to the current column of Fig.2.2 Eqn.(2.41) is an inhomogeneous wave equation for the induced voltage along the overhead line. It is valid for any charge distribution along the leader channel and any waveshape of the return-stroke current. Its solution can be obtained by assuming *F(x,t)* to be the superposition of impulses that involves the definition of Green's function.

For a rectangular return-stroke current, the induced voltage at a point x along the line (Fig. 2.7) is given by

$$V(x,t) = \left(V_{11} + V_{12} + V_{21} + V_{22}\right)U(t - t_0)$$ ………………….(2.43)

Chowdhuri (1989), improved on his earlier solution of equation (2.41) after taking Cornfield's correction into consideration and obtained equation (2.43)

where

$$V_{11} = \frac{30 I_0 h\left(1-\beta^2\right)}{\beta^2(ct-x)^2 + {y_0}^2}\left[\beta(ct-x) + \frac{(ct-x)x - {y_0}^2}{\left\{c^2t^2 + \frac{1-\beta^2}{\beta^2}\left(x^2 + {y_0}^2\right)\right\}^{\frac{1}{2}}}\right],$$ ……(2.44)

$$V_{12} = \frac{30 I_0 h}{\beta}\left[\frac{1}{\sqrt{K_1^2+1}} - \beta^2\right]\frac{1}{ct},$$ ………………(2.45)

$$V_{21} = \frac{30 I_0 h\left(1-\beta^2\right)}{\beta^2(ct+x)^2 + {y_0}^2}\left[\beta(ct+x) - \frac{(ct+x)x + {y_0}^2}{\left\{c^2t^2 + \frac{1-\beta^2}{\beta^2}\left(x^2 + {y_0}^2\right)\right\}^{\frac{1}{2}}}\right],$$ …………… (2.46)

$$V_{22} = \frac{30 I_0 h}{\beta}\left[\frac{1}{\sqrt{K_2^2+1}} - \beta^2\right]\frac{1}{ct},$$ ……………..……(2.47)

$$K_1 = \frac{2h_c(ct-x)}{{y_0}^2 + (ct-x)^2},$$ ………..… (2.48)

$$K_2 = \frac{2h_c(ct+x)}{{y_0}^2 + (ct+x)^2},$$ ……………………………(2.49)

$$t_0 = \frac{\sqrt{x^2 + {y_0}^2}}{c}$$

$U(t - t_0)$ = shifted unit step function

I_o = return – stroke current

β = ratio of return-stroke velocity to velocity of electromagnetic wave in free space

h_c = height of cloud

The induced voltage caused by linear-rising return stroke current

$I(t) = \alpha t - \alpha(t-t_f)u(t-t_f) = I_1(t) + I_2(t)$, is $V(t) = V_1(t) + V_2(t)$ where $V_1(t)$ and $V_2(t)$ are the induced voltages caused by $I_1(t)$ and $I_2(t)$, respectively. The expressions for $V_1(t)$ and $V_2(t)$ are given in appendix 1.

2.19 **Two-conductor overhead line case**

Coupling of an electromagnetic field to a transmission line consists of describing the voltages and currents induced in the conductors of the line in terms of the inducing fields. The current *ij(x,t)* at a point along a line conductor "j" is defined, as usual, as the charge flow through the cross section of the conductor at that point; and the induced voltage at that point $V^j(x,t)$ is defined, for a horizontal line, as the integral of the electric field along a vertical trajectory from that point on the conductor to some reference point (usually the ground)

$$V^j(x,t) = \int_{h_j}^{0} \bar{E}.d\bar{l} = -\int_{0}^{h_j} E_z\, dz \qquad \text{……(2.50)}$$

Defining the vector field **A** (*x*, *y*, *z*, *t*), that is called the vector potential, such that,

$$\bar{B} = \nabla \times \bar{A} \qquad \text{……………(2.51)}$$

we can write Faraday's law as:

$$\oint \left(\bar{E} + \frac{\partial \bar{A}}{\partial t}\right).d\bar{l} = 0 \qquad \text{…………….. (2.52)}$$

$$\Rightarrow \bar{E} = -\nabla\phi - \frac{\partial \bar{A}}{\partial t} \qquad \text{………………. (2.53)}$$

where, the scalar field ϕ (*x*, *y*, *z*, *t*) is the scalar potential.

The schematic diagram of the method of analysis applied to study the induction process of the electromagnetic fields of the lightning retum-stroke channel to an overhead line is shown in fig.2.7

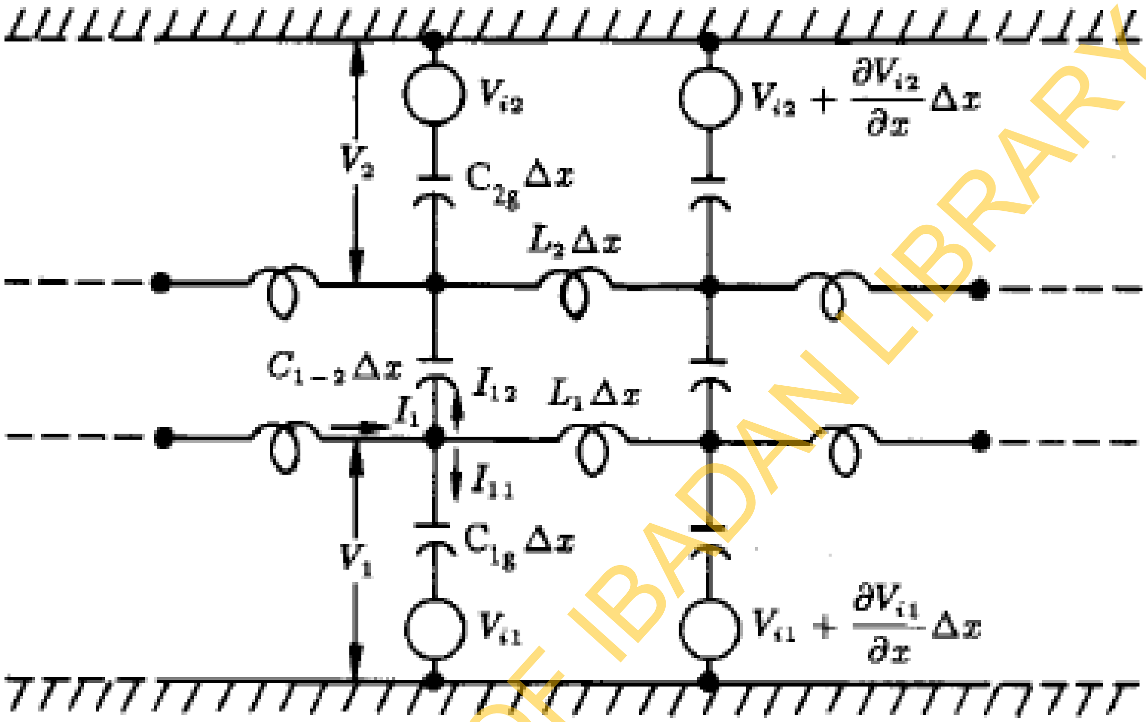

Fig.**2.9** Equivalent circuit for computing lightning-induced voltage on two-conductor over head line

Rusck(1958), assumed that

$$[V] = [Vi] + [p][q], \qquad \text{.............(2.54)}$$

where [V] = matrix of induced voltages,

[Vi] = matrix of inducing voltages,

[p] = matrix of potential coefficients , and

[q] = matrix o f conductor charges.

The inducing voltage Vi is defined as that voltage which would have been caused by the charges on the lightning stroke a t the same points in space now occupied by the conductor, in the absence *of* the conductor.

Following Maxwell's principle of superposition, the potential of the j^{th}conductor in an n-conductor system is given by: :

$$V_j = p_{j\,1}q_1 + \cdots + p_{j\,j}q_j + \ldots . + p_{j\,r}q_r + \cdots . + p_{j\,n}q_n \qquad \text{...............(2.55)}$$

when all conductors are present. In other words, the component of voltage induced on the j^{th}conductor by the charge q_r on the r^{th}conductor is $p_{j\,r}q_r$, irrespective of the presence of the other conductors . This is ***not*** the voltage which would have existed at the location of the j^{th} conductor in its absence. Including the lightning stroke in the conductor system, the voltage induced on the j^{th} conductor should then be given by

$$V_j = p_{j\,1}q_1 + \cdots + p_{j\,n}q_n + V_{j\,s} \qquad \text{...................... (2.56)}$$

where V [s] is the voltage induced by the lightning stroke on the j^{th}conductor. In the absence of all other conductors. Therefore, eq.(3.26) should be rewritten as

$$[V] = [V_s] + [p] + [q] \quad \text{.................. (2.57)}$$

Chowdhuri and Gross extended their single-conductor transmission-line analysis to multi-conductor lines by the equation given by

$$-\frac{\partial I_j}{\partial x} = C_{j\,1}\frac{\partial V_1}{\partial t} + \cdots + C_{j\,j}\frac{\partial}{\partial t}\left(V_j - V_{i\,j}\right) + \cdots + C_{j\,r}\frac{\partial V_r}{\partial t} + \cdots + C_{j\,n}\frac{\partial V_n}{\partial t}: \quad \text{..........(2.58)}$$

where I_j = current in the j^{th}conductor,

V_j= induced voltage on the j^{th} conductor,

V_{ij}= inducing voltage of the j^{th} conductor,

and

C_{jr} (r=l, ... n) = coefficient of capacitance and induction.

$$I_1 = I_{1\,1} + I_{1\,2} \quad \text{................ (2.59)}$$

$$-\frac{\partial I_{1\,1}}{\partial x} = C_{1\,g}\frac{\partial}{\partial t}(V_1 - V_{i\,1}) \quad \text{............. (2.60)}$$

$$-\frac{\partial I_{1\,3}}{\partial x} = C_{1-2}\frac{\partial}{\partial t}(V_1 - V_2) \quad \text{.....................(2.61)}$$

and

$$-\frac{\partial I_1}{\partial x} = -\frac{\partial}{\partial x}(I_{1\,1} + I_{1\,2}) \quad \text{.................. (2.62)}$$

$$= \left(C_{1\,g} + C_{1-2}\right)\frac{\partial V_1}{\partial t} - C_{1\,g}\frac{\partial V_{i\,1}}{\partial t} - C_{1-2}\frac{\partial V_2}{\partial t}$$

However, $C_{1\,1} = C_{1\,G} + C_{1-2}$ ....(2.63)

$$C_{2\,2} = C_{2\,G} + C_{1-2} \quad \text{...............(2.64)}$$

$$C_{1\,2} = -C_{1-2} \quad \text{......(2.65)}$$

Where $C_{1\,1}$, $C_{2\,2}$, $C_{1\,2}$ are the elements of matrix $[C]$

$$[C] = [p]^{-1} \quad \text{...................(2.66)}$$

and $[p]$ is the matrix element of coefficients of potential.

$$-\frac{\partial I_1}{\partial x} = C_{1\,1}\frac{\partial V_1}{\partial t} + C_{1\,2}\frac{\partial V_2}{\partial t} - (C_{1\,1} + C_{1\,2})\frac{\partial V_{i\,1}}{\partial t} \quad \text{.......(2.67)}$$

Extending it to n-conductor system,

$$-\frac{\partial I_1}{\partial x} = C_{1\,1}\frac{\partial V_1}{\partial t} + \cdots + C_{1\,n}\frac{\partial V_n}{\partial t} - (C_{1\,1} + \cdots + C_{1\,n})\frac{\partial V_{i\,1}}{\partial t} \quad \text{..........(2.68)}$$

$$-\frac{\partial I_j}{\partial x} = C_{j\,1}\frac{\partial V_1}{\partial t} + \cdots + C_{j\,j}\frac{\partial V_j}{\partial t} + \cdots + C_{j\,n}\frac{\partial V_n}{\partial t} - \left(C_{j\,1} + \cdots + C_{j\,j} + \cdots + C_{j\,n}\right)\frac{\partial V_{i\,j}}{\partial t} \quad \text{.(2.69)}$$

$$-\frac{\partial I_n}{\partial x} = C_{n\,1}\frac{\partial V_1}{\partial t} + \cdots + C_{n\,n}\frac{\partial V_n}{\partial t} - (C_{n\,1} + \cdots + C_{n\,n})\frac{\partial V_{i\,n}}{\partial t} \quad \text{...... (2.70)}$$

In matrix form ,

$$-\frac{\partial}{\partial x}[I] = [C]\frac{\partial}{\partial t}[V] - [I'] \quad , \quad \text{..........(2.71)}$$

where ,

$$[I] = \begin{bmatrix} I_1 \\ \vdots \\ I_n \end{bmatrix};\ [C] = \begin{bmatrix} C_{11} \cdots C_{1n} \\ \vdots \quad\quad \vdots \\ C_{n1} \cdots C_{nn} \end{bmatrix};\ [V] = \begin{bmatrix} V_1 \\ \vdots \\ V_n \end{bmatrix} \text{ and}$$

$$[I'] = \begin{bmatrix} C_{1\,g}\frac{\partial V_{i\,1}}{\partial t} \\ \vdots \\ C_{j\,g}\frac{\partial V_{i\,j}}{\partial t} \\ \vdots \\ C_{n\,g}\frac{\partial V_{i\,n}}{\partial t} \end{bmatrix} = [C_g]\frac{\partial}{\partial t}[V_i] \quad \text{.........(2.72)}$$

$$C_{j\,g} = C_{j\,1} + C_{j\,2} + \ldots + C_{j\,n} \quad \text{..........(2.73)}$$

and $[C_g]$ is the diagonal matrix of element $C_{j\,g}$ (j=1,…..,n)

The other eq. is the same as before

$$-\frac{\partial}{\partial x}[V] = [L]\frac{\partial}{\partial t}[I] \quad \text{.......(2.74)}$$

Combining eq(2.71)and(2.74)

$$\frac{\partial^2}{\partial x^2}[V] - [L][C]\frac{\partial^2}{\partial t^2}[V] = -[L]\frac{\partial}{\partial t}[I'] = -[F_0] \quad \text{....(2.75)}$$

Or $\frac{\partial^2}{\partial x^2}[V] - \frac{1}{c^2}\frac{\partial^2}{\partial t^2}[V] = -[L]\frac{\partial}{\partial t}[I'] = -[F_0]$ …….(2.76)

Where c is the velocity of light in free space and $[L] = \begin{bmatrix} L_{11} \cdots L_{1n} \\ \vdots \quad\quad \vdots \\ L_{n1} \cdots L_{nn} \end{bmatrix}$.

This is the modified wave equation for a multiconductor system. The elements of the inductance matrix *[L]* are :

$$L_{rr} = \frac{\mu_0}{2\pi} p_{rr} \; ; \; L_{rs} = \frac{\mu_0}{2\pi} p_{rs}$$

$$p_{rr} = \ln\frac{D_{rr}}{r_r} \; ; \; p_{rs} = ln\frac{D_{rs}}{d_{rs}} \quad \text{………. .(2.77)}$$

where

D_{rr} = distance between the conductor *r* and its own image below earth

D_{rs} = distance between the conductor *r* and the image of conductor *s*

r_r = radius of conductor *r*

d_{rs}= distance between the conductors *r* and s

In eqn. (2.72), the magnetic flux inside the conductors has been neglected, which is justified for high-frequency phenomena such as lightning.

For a system with.perfect earth plane (i.e. infinite conductivity), the capacitance matrix [C] is related to the inductance matrix [L] by

$$[L][C] = \frac{[1]}{\mu_0 \varepsilon_0} = \frac{[1]}{c^2} \quad \text{………. .(2.78)}$$

where *c* = velocity of electromagnetic waves in free space

[1] = identity matrix

Taking the Laplace transform of eqn. (2.75) and assuming the initial conditions to be zero,

$$\frac{\partial^2}{\partial x^2}[\bar{v}] - \frac{s^2}{c^2}[1][\bar{v}] = -[\bar{f_0}] \quad \text{……….(2.79)}$$

Because of the identity matrix [1], the component equations are already uncoupled; therefore, they can be solved separately, similarly to the single-conductor case. Thus, for example, the equation for conductor r of a n-conductor system is

$$\frac{\partial^2 \overline{v_r}(x,s)}{\partial x^2} - \frac{s^2}{c^2}\overline{v}_r(x,s) = -\{L_{r1}C_{11}\overline{f_1}(x,s) + L_{r2}C_{22}\overline{f_2}(x,s) + \cdots + L_{rn}C_{nn}\overline{f_n}(x,s)\}. \quad ..(2.80)$$

Knowing Green's function1 of eqn. (2.39), the solution for $\overline{v}_r(x,s)$can be obtained as

$\overline{v}_r(x,s) =$

$$-\int_{-\infty}^{x} G_1(x;x',s)\{L_{r1}C_{11}\overline{f_1}(x',s) + \cdots + L_{rn}C_{nn}\overline{f_n}(x',s)\}dx' -$$

$$\int_{x}^{+\infty} G_2(x;x',s)\{L_{r1}C_{11}\overline{f_1}(x',s) + \cdots + L_{rn}C_{nn}\overline{f_n}(x',s)\}dx' \quad \ldots\ldots\ldots(2.81)$$

$$\overline{v}_r(x,s) = \overline{v}_r(1) + \overline{v}_r(2) \quad \ldots\ldots\ldots(2.82)$$

The induced voltage on conductor r as a function of time is then computed by finding the inverse Laplace transform of eqn. (2.82) using Maple 13 software package.

$$G_1(x;x',s) = \frac{-c}{2s}\,exp\left(-\frac{s(x'-x)}{c}\right) \text{ for } x < x' \quad \ldots\ldots\ldots(2.83)$$

$$G_2(x;x',s) = \frac{-c}{2s}\,exp\left(\frac{s(x'-x)}{c}\right) \text{ for } x > x' \quad \ldots\ldots\ldots(2.84)$$

<u>Horizontal configuration without earth wires</u>

$$[P] = \begin{bmatrix} 13.8 & 3.08 & 1.92 \\ 3.08 & 13.8 & 3.08 \\ 1.92 & 3.08 & 13.8 \end{bmatrix} X\ 10^{10}$$

$$[C] = \begin{bmatrix} C_{11} & C_{12} & C_{13} \\ C_{21} & C_{22} & C_{23} \\ C_{31} & C_{32} & C_{33} \end{bmatrix} \quad \ldots\ldots\ldots(2.85)$$

$$[C] = [P]^{-1}$$

$$[C] = \begin{bmatrix} 7.70 & -1.56 & -0.72 \\ -1.56 & 7.94 & -1.56 \\ -0.72 & -1.56 & 7.70 \end{bmatrix} \text{ X } 10^{-12}$$

$$[L] = \begin{bmatrix} L_{11} & L_{12} & L_{13} \\ L_{21} & L_{22} & L_{23} \\ L_{31} & L_{32} & L_{33} \end{bmatrix} \qquad \text{……...(2.86)}$$

$$[L] = \begin{bmatrix} 1.540 & 0.343 & 0.214 \\ 0.343 & 1.540 & 0.343 \\ 0.214 & 0.343 & 1.540 \end{bmatrix} \text{ X } 10^{-6}$$

$$M_1' = L_{11}C_{11} + L_{12}C_{22} + L_{13}C_{33} \quad = 1.62 \text{ X } 10^{-17} \qquad \text{……...(2.87)}$$

$$M_2' = L_{12}C_{11} + L_{22}C_{22} + L_{23}C_{33} \quad = 1.75 \text{ X } 10^{-17} \qquad \text{……...(2.88)}$$

$$M_3' = L_{13}C_{11} + L_{23}C_{22} + L_{33}C_{33} \quad = 1.62 \text{ X } 10^{-17} \qquad \text{……...(2.89)}$$

Induced voltages on conductors 1, 2 and 3 are $V_1 = V_s M'_1c^2$, $V_2 = V_s M'_2c^2$ and $V_3 = V_s M'_3c^2$ respectively. Where $c = 3 \text{ X } 10^8 \text{ ms}^{-1}$ and V_s is the induced voltage on single wire of same height with the horizontal ly configured conductors.

Hence,

$V_1 = 1.45V_s$

$V_2 = 1.57V_s$ and

$V_3 = 1.45 V_s$

<u>Calculations for vertical configuration without earth wire</u>

$$[P] = \begin{bmatrix} 13.84 & 3.36 & 3.62 \\ 3.36 & 14.40 & 3.84 \\ 3.62 & 3.84 & 14.83 \end{bmatrix} \text{ X } 10^{10} \qquad \text{……...(2.90)}$$

$$[C] = [P]^{-1}$$

$$[C] = \begin{bmatrix} 7.99 & -1.44 & -1.58 \\ -1.44 & 7.72 & -1.64 \\ -1.58 & -1.65 & 7.55 \end{bmatrix} \text{X } 10^{-12} \qquad \text{.........(2.91a)}$$

$$[L] = \begin{bmatrix} 1.540 & 0.373 & 0.402 \\ 0.373 & 1.600 & 0.427 \\ 0.402 & 0.427 & 1.650 \end{bmatrix} \text{X } 10^{-6} \qquad \text{.........(2.91b)}$$

$$M_1 = L_{11}C_{11} + k_{12}L_{12}C_{22} + k_{13}L_{13}C_{33} = 2.15 \text{ X } 10^{-17} \qquad \text{.........(2.91c)}$$

$$M_2 = L_{12}C_{11} + k_{12}L_{22}C_{22} + k_{13}L_{23}C_{33} = 2.54 \text{ X } 10^{-17} \qquad \text{.........(2.92)}$$

$$M_3 = L_{13}C_{11} + k_{12}L_{23}C_{22} + k_{13}L_{33}C_{33} = 2.93 \text{ X } 10^{-17} \qquad \text{.........(2.93)}$$

Where $k_{12} = \frac{h_2}{h_1}$ and $k_{13} = \frac{h_3}{h_1}$, c = 3 X 10^8 ms^{-1} and V_{sn} is the induced voltage on single wire of height, h_n , n =1..3

$$\frac{V_n}{V_{sn}} = \frac{M_n}{k_{1n}} c^2 \qquad n = 1..3$$

$V_1 = 1.94V_{s1}$

$V_2 = 1.67V_{s2}$

$V_3 = 1.52V_{s3}$

Fig. 2.10: Vertical configuration of 3-phase line with one earth wire (4)

Calculations for vertical configuration with earth wire above topmost conductor

$$[L'] \begin{bmatrix} L_{11} - \frac{L_{14}^2}{L_{44}} & L_{12} - \frac{L_{14}L_{24}}{L_{44}} & L_{13} - \frac{L_{14}L_{34}}{L_{44}} \\ L_{12} - \frac{L_{12}L_{24}}{L_{44}} & L_{22} - \frac{L_{24}^2}{L_{44}} & L_{23} - \frac{L_{24}L_{34}}{L_{44}} \\ L_{13} - \frac{L_{14}L_{34}}{L_{44}} & L_{23} - \frac{L_{24}L_{34}S}{L_{44}} & L_{33} - \frac{L_{34}^2}{L_{44}} \end{bmatrix} \quad \text{.........(2.94)}$$

$$[C] = \begin{bmatrix} 7.99 & -1.44 & -1.58 \\ -1.44 & 7.72 & -1.64 \\ -1.58 & -1.65 & 7.55 \end{bmatrix} \text{X } 10^{-12} \quad \text{.........(2.95)}$$

$$[L'] = \begin{bmatrix} 1.509 & 0.326 & 0.320 \\ 0.298 & 1.526 & 0.297 \\ 0.320 & 0.300 & 1.430 \end{bmatrix} \text{X } 10^{-6} \quad \text{.........(2.96)}$$

$$M_1' = L_{11}'C_{11} + k_{12}\, L_{12}'C_{22} + k_{13}\, L_{13}'C_{33} = 1.968 \text{ X } 10^{-17} \quad \text{.........(2.97)}$$

$$M_2' = L_{12}'C_{11} + k_{12}\, L_{22}'C_{22} + k_{13}\, L_{23}'C_{33} = 2.258 \text{ X } 10^{-17} \quad \text{.........(2.98)}$$

$$M_3' = L_{13}'C_{11} + k_{12}\, L_{23}'C_{22} + k_{13}\, L_{33}'C_{33} = 2.438 \text{ X } 10^{-17} \quad \text{.........(2.99)}$$

$$\frac{V_n'}{V_{sn}} = \frac{M_n'}{k_{1n}} c^2 \quad \text{.........(2.100)}$$

n =1..3

$V_1' = 1.77V_{s1}$

$V_2' = 1.49V_{s2}$

$V_3' = 1.26V_{s3}$

Calculations for vertical configuration with earth wire below lowest conductor

_ $[C] = \begin{bmatrix} 7.99 & -1.44 & -1.58 \\ -1.44 & 7.72 & -1.64 \\ -1.58 & -1.65 & 7.55 \end{bmatrix} \text{X } 10^{-12}$ ……...(2.101)

$[L'] = \begin{bmatrix} 1.392 & 0.287 & 0.338 \\ 0.308 & 1.550 & 0.390 \\ 0.338 & 0.390 & 1.623 \end{bmatrix} \text{X } 10^{-6}$ ……...(2.102)

$M_1' = L_{11}'C_{11} + k_{12} L_{12}'C_{22} + k_{13} L_{13}'C_{33} = 1.857 \text{ X } 10^{-17}$ ……...(2.103)

$M_2' = L_{12}'C_{11} + k_{12} L_{22}'C_{22} + k_{13} L_{23}'C_{33} = 2.374 \text{ X } 10^{-17}$ ……...(2.104)

$M_3' = L_{13}'C_{11} + k_{12} L_{23}'C_{22} + k_{13} L_{33}'C_{33} = 2.811 \text{ X } 10^{-17}$ ……...(2.105)

$\frac{V_n'}{V_{sn}} = \frac{M_n'}{k_{1n}} c^2$ n =1..3

$V_1' = 1.67V_{s1}$

$V_2' = 1.56V_{s2}$

$V_3' = 1.46V_{s3}$

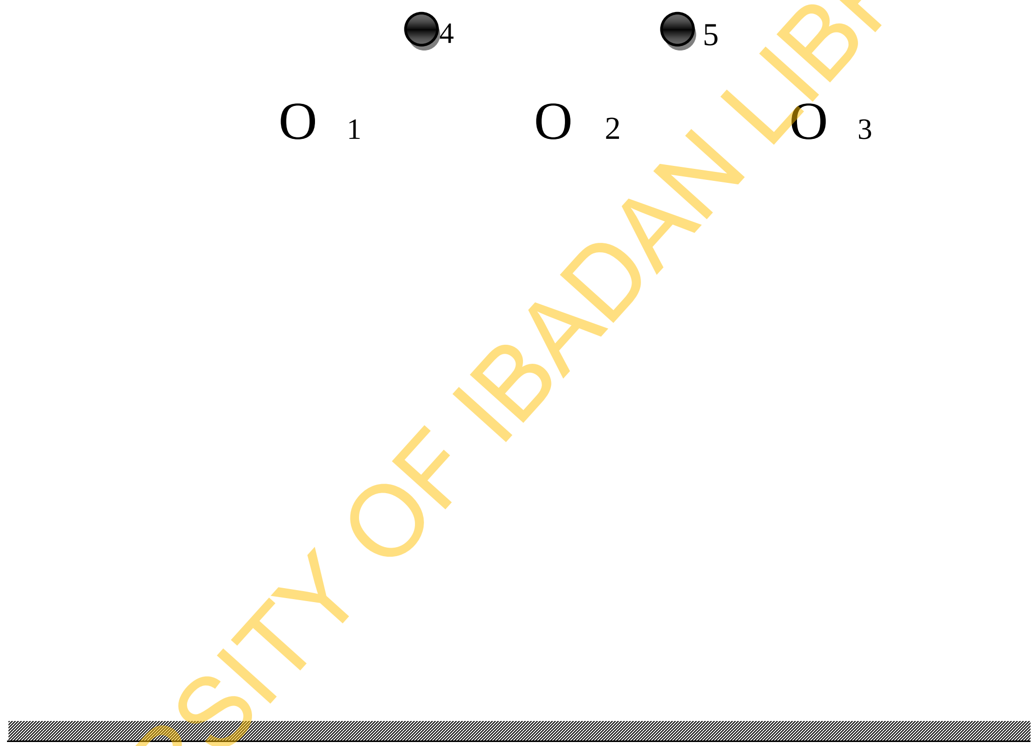

Fig. 2.11: Horizontal configuration of 3-phase line with two earth wires (4 & 5)

Calculations for horizontal configuration with two earth wires placed above conductors

$$L'_{11} = L_{11} - L_{14}\frac{A}{D} - L_{15}\frac{B}{D}$$ ……...(2.106)

$$L'_{12} = L_{12} - L_{14}\frac{E}{D} - L_{15}\frac{E}{D}$$ ……...(2.107)

$$L'_{13} = L_{13} - L_{14}\frac{B}{D} - L_{15}\frac{A}{D}$$ ……...(2.108)

$$L'_{22} = L_{11} - 2\,L_{14}\frac{E}{D}$$ ……...(2.109)

$$L'_{23} = L_{12} - L_{14}\frac{B}{D} - L_{14}\frac{A}{D}$$ ……...(2.110)

$$L'_{33} = L_{11} - L_{14}\frac{A}{B} - L_{15}\frac{B}{D}$$ ……...(2.111)

Where $A = L_{14}\,L_{44} - L_{15}L_{45}$ ……...(2.112)

$B = L_{15}\,L_{44} - L_{14}L_{45}$ ……...(2.113)

$D = L_{44}^2 - L_{45}^2$ ……...(2.114)

$E = L_{14}\,L_{44} - L_{14}L_{45}$

$$[C] = \begin{bmatrix} 7.99 & -1.44 & -1.58 \\ -1.44 & 7.72 & -1.64 \\ -1.58 & -1.65 & 7.55 \end{bmatrix} \text{X } 10^{-12}$$ ……...(2.115)

$$[L'] = \begin{bmatrix} 1.406 & 0.190 & 0.103 \\ 0.190 & 1.350 & 0.190 \\ 0.103 & 0.190 & 1.406 \end{bmatrix} \text{X } 10^{-6}$$

……...(2.116)

$$M'_1 = L'_{11}C_{11} + L'_{12}C_{22} + L'_{13}C_{33} = 1.312 \text{ X } 10^{-17}$$ ……...(2.117)

$$M'_2 = L'_{12}C_{11} + L'_{22}C_{22} + L'_{23}C_{33} = 1.288 \text{ X } 10^{-17} \qquad \text{……...(2.118)}$$

$$M'_3 = L'_{13}C_{11} + L'_{23}C_{22} + L'_{33}C_{33} = 1.313 \text{ X } 10^{-17} \qquad \text{……...(2.119)}$$

$$\frac{V'_n}{V_{sn}} = M'_n c^2 \qquad n = 1..3 \qquad \text{……...(2.120)}$$

$$V'_1 = 1.18V_{s1}$$

$$V'_2 = 1.15V_{s2}$$

$$V'_3 = 1.18V_{s3}$$

CHAPTER THREE

METHODOLOGY

3.1 Introduction

The geometrical configuration of the stroke and the conducting lines is based on rectangular system of coordinate. The assumed vertical lightning channel along the z-axis, strikes the perfectly conducting ground at the origin. The lines, located at distances y_{oj} *m* from the origin with mean height h_j *m* above ground run along x-direction, where j=1,2,3. Six lightning channel return-stroke models were used to simulate the induced voltages in order to investigate the lightning channel characteristics and their interactions with conductors. The summary is shown in tables 3.2 and 3.3. The return stroke modeled as a linearly rising current wave form with constant tail which was in agreement with monitored waves with transient storage oscilloscopes was chosen for few parameters involved. The induced voltages on the line conductors were calculated by adopting Chowdhuri coupling method. The partial differential equations genereated were solved analytically as Green's functions using the Laplace transform technique with MAPLE 13 package. Line configurations considered were (i) vertical profile, with and without earth wire above topmost conductor; and (ii) horizontal profile, with and without two earth wires symmetrically placed above conductors. Placements of earth wires below conductors were also considered. A C-sharp Application Programme Interface (API) was developed. The API was interacted with via a custom-built Window's Graphical User Interface (GUI) upon which the effects of the parameters of the return stroke current and line configurations on induced voltages were examined. Also, for each configuration the Protective Ratios (PR) were determined.

3.2 Return stroke models

For the current at the channel base $i(0,t)$, of ground-initiated lightning return stroke, analytical expression (Heidler,1985) is adopted:

$$i(0,t) = \frac{I_0}{\eta} \frac{\left({t}/{\tau_1}\right)^n}{1+\left({t}/{\tau_1}\right)^n} \exp\left(-{t}/{\tau_2}\right) \qquad \text{............(3.1)}$$

where $$\eta = \exp\left[-\left(\frac{\tau_1}{\tau_2}\right)\left(\frac{n\tau_2}{\tau_1}\right)^{\left({1}/{n}\right)}\right] \qquad \text{.............(3.2)}$$

and

I_0 amplitude of the channel-base current;

τ_1 front time constant;

τ_2 decay time constant;

η amplitude correction factor; and

n exponent (2 .. . 10)

The function allows for the adjustment of the current amplitude by varying I_0.

Sum of two functions given in equation (1) was chosen so as to obtain the overall waveshape of the current as observed in typical experimental results .The parameters listed in table 3.1 were chosen. These values were adapted from Berger *et al (1975)*.The same undisturbed base current was employed in the comparison of the transmission-line type and traveling-current-source-type models.

Adapting MTLE ,TL,MTLL,BG and TCS models (Tables 2.1 and 2.2), the current at various heights (z' =200m,300m,1km,2km,3km and 4km) and a time window frame of between 0 and 15μs were calculated. Most literature relating to propagation of lightning over the ground adopted the value of n=2.The same value is also adopted in this work. Wave speed of 0.5c is assumed The cloud height ,H=5km for tropic was adopted

I_1(kA)	τ_{11}(μs)	τ_{12}(μs)	n_1	I_2(kA)	τ_{21}(μs)	τ_{22}(μs)	n_2
10.7	0.25	2.5	2	6.5	2.1	230	2

Table 3.1 :Typical values of parameters applied to base current.(adapted from Berger,1975)

Linearly rising current wave form with constant tail

To see how the duration of the front of the wave effects the amplitude and the waveshape of the induced voltage, the return-stroke current could be, with sufficient accuracy, modelled with linearly rising wave. The analytic representation of such wave is given by Eq. (3.3)

$$I(t) = \alpha t - \alpha(t - t_f)u(t - t_f) \qquad \text{……………………..(3.3)}$$

Where $\alpha = \frac{I_p}{t_f}$; *Ip*– Amplitude of the return stroke current and *tf* – duration of the wave front,

3.3 Procedure of calculation of lightning induced voltages with MAPLE 13

The procedure for calculation of lightning induced voltages is stated thus:

1. Second order partial differential wave equation was generated in terms of induced voltage, $v(x,t)$ and inducing voltage $v_i(x,t)$

2. The initial conditions $v(x,0)$and $\frac{d}{dt}v(x,0)$ were set at zero

3. The Laplace transform equations of 1. and 2. above were determined in terms of V(x, s)

4. The Wronskian was evaluated in terms of the basic vectors $\varphi_{1(x,s)=e^{-sx}}$ and $\varphi_{2(x,s)=e^{sx}}$

5. Second order Green's function was evaluated

6. Particular solution was determined

7. The general solution of the transformed induced voltage was determined on substituting the boundary conditions

8. The solution is the inverse Laplace of V(x, s)

The details of the program is shown in appendix 1 .

3.4 C-sharp Application Programme Interface (API) with Graphical User Interface (GUI)

In order to easily change the values of both the lightning parameters and line dimensions, a C-sharp Application Programme Interface (API) with Graphical User Interface (GUI) was developed. Table 3.4 showed the dimensions of conductors and eath wires for an experimental case in Mexico. The flow chart of the program is shown in Fig. 3.1. Appendix 2 showed the details of thf program. Figs. 3.2 and 3.3 showed samples of input data; while Fig.3.4 showed the generated output..

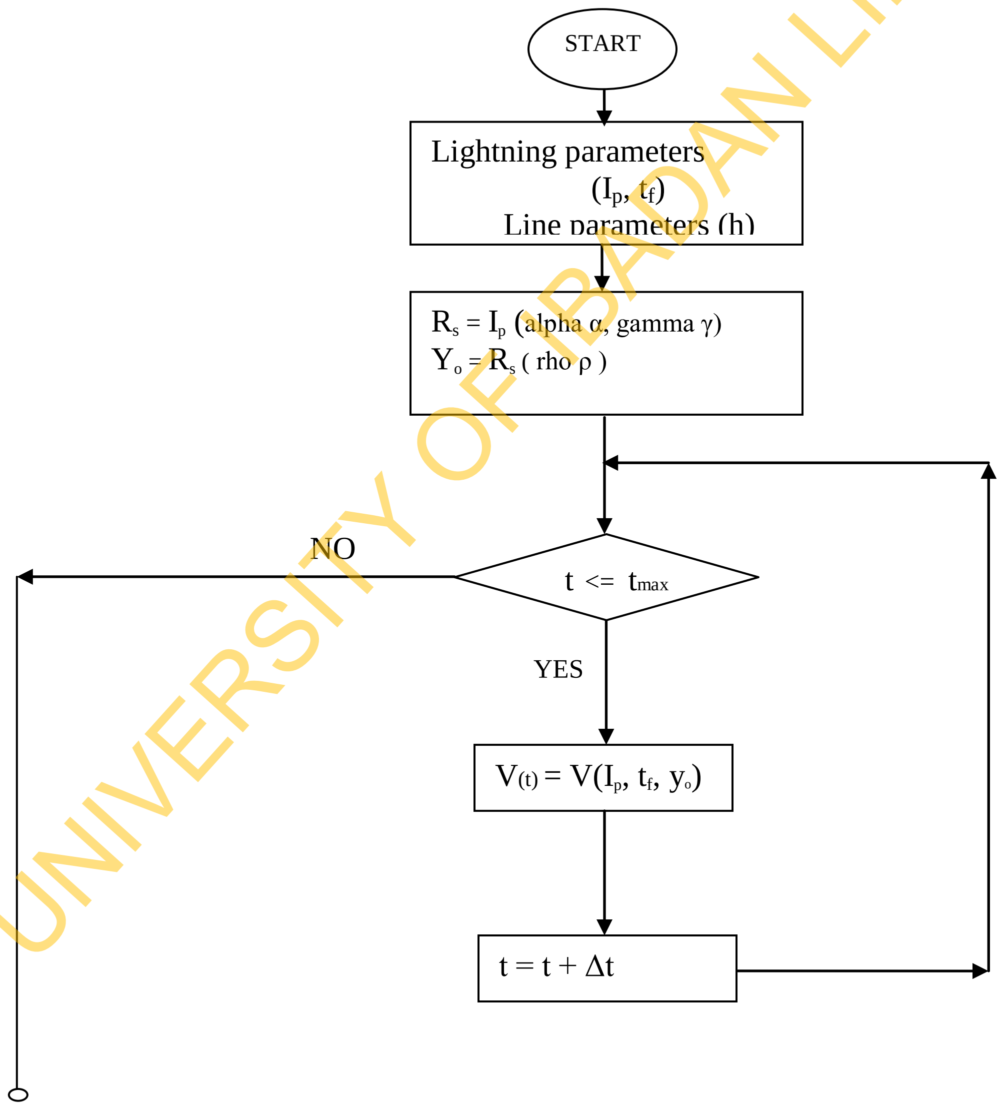

START
Lightning parameters
(I_p, t_f)
Line parameters (h)
$R_s = I_p$ (alpha α, gamma γ)
$Y_o = R_s$ (rho ρ)
NO
$t <= t_{max}$
YES
$V_{(t)} = V(I_p, t_f, y_o)$
$t = t + \Delta t$

Fig.3.1 (a): Flow chart for lightning-induced voltage calculation

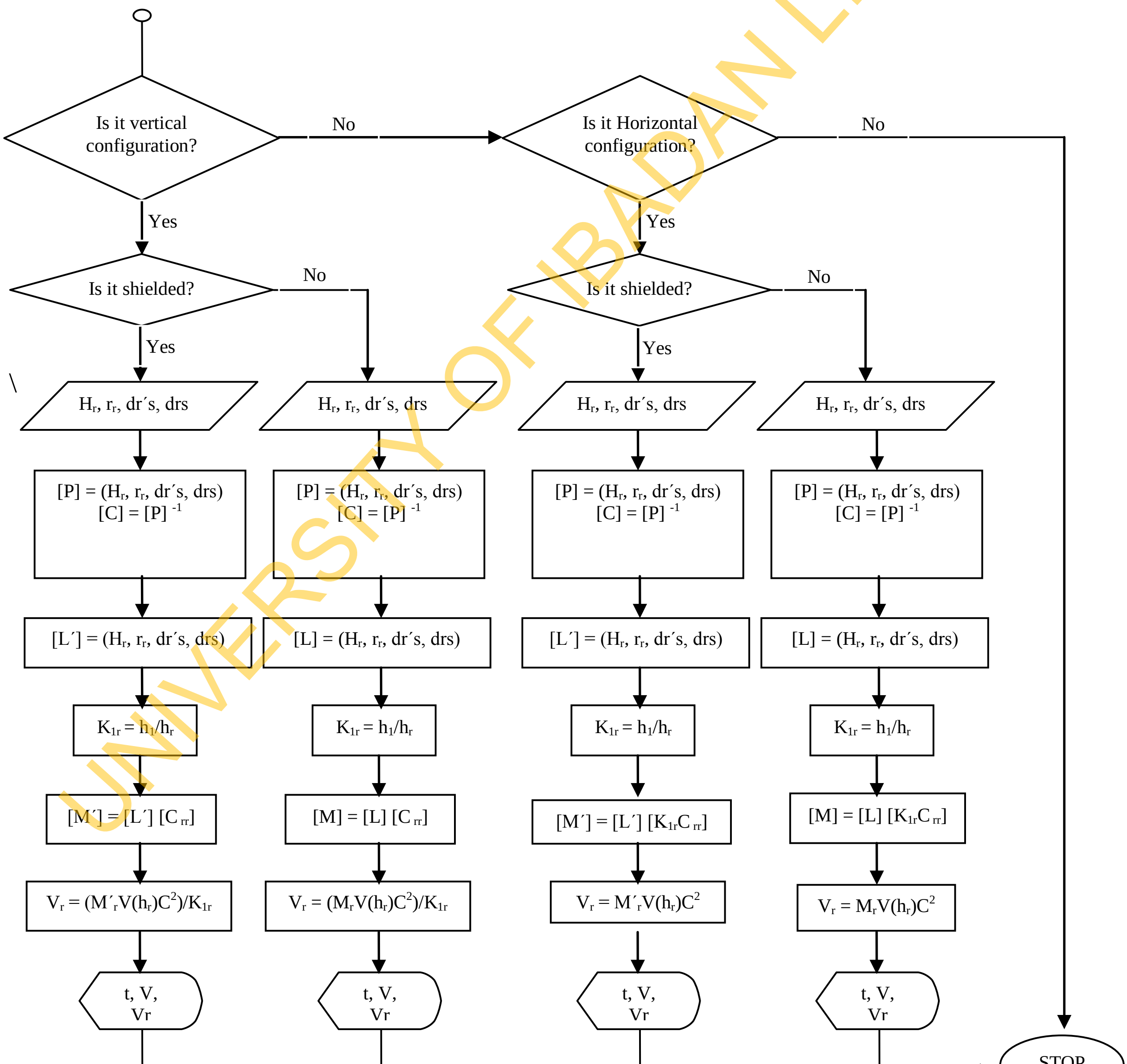

Fig.3.1 (b): Flow chart for lightning-induced voltage calculation (continued)

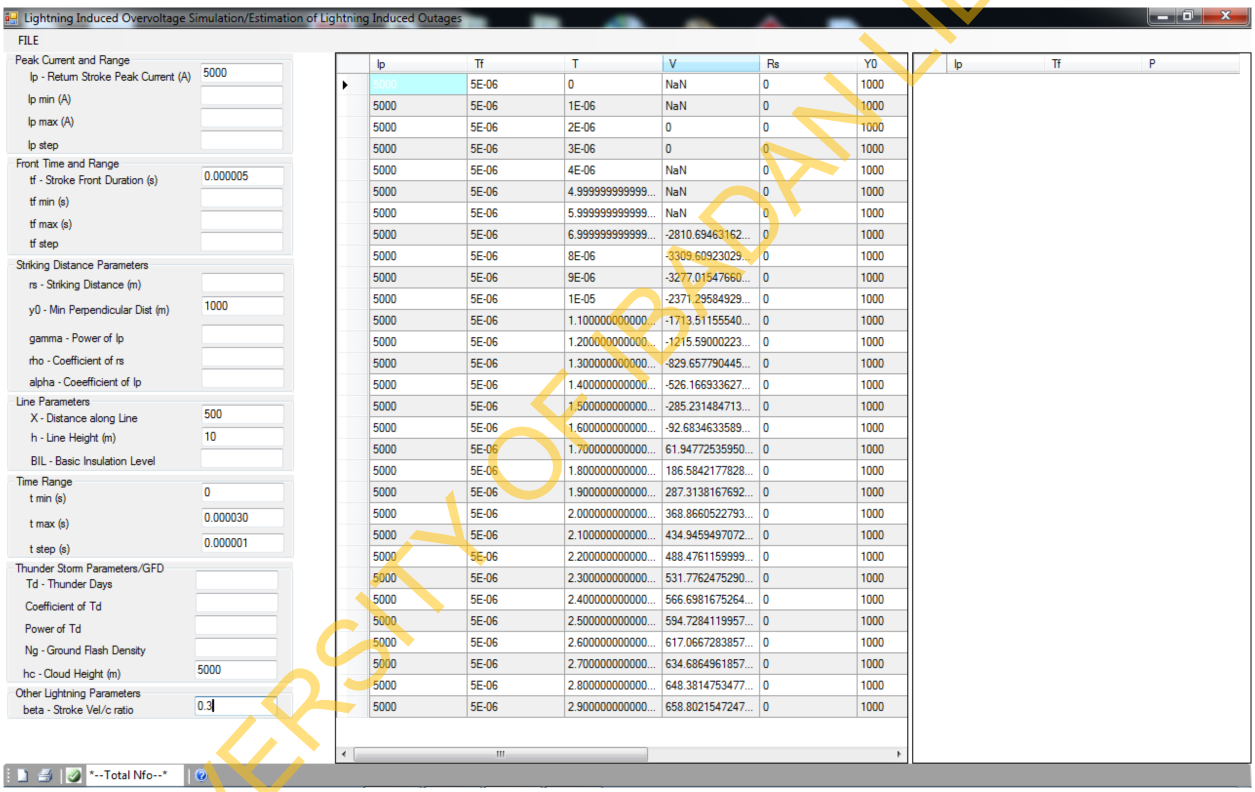

Fig.3.2 : Window’s GUI tointeract with API for lightning-induced voltage calculation

Configuration	Radius of conductor	Radius of earth wire	Height of conductor above ground			Height of earth wire above ground	Sepration between conductors
Vertical	r_c/mm	r_e/mm	H_1/m	H_2/m	H_3/m		
	9.14	3.16	10	13.66	17.32	18.82	3.66
Horizontal	9.14	3.16	10	10	10	11.5	3.66

Table 3.2: Dimension of multi-conductor lines

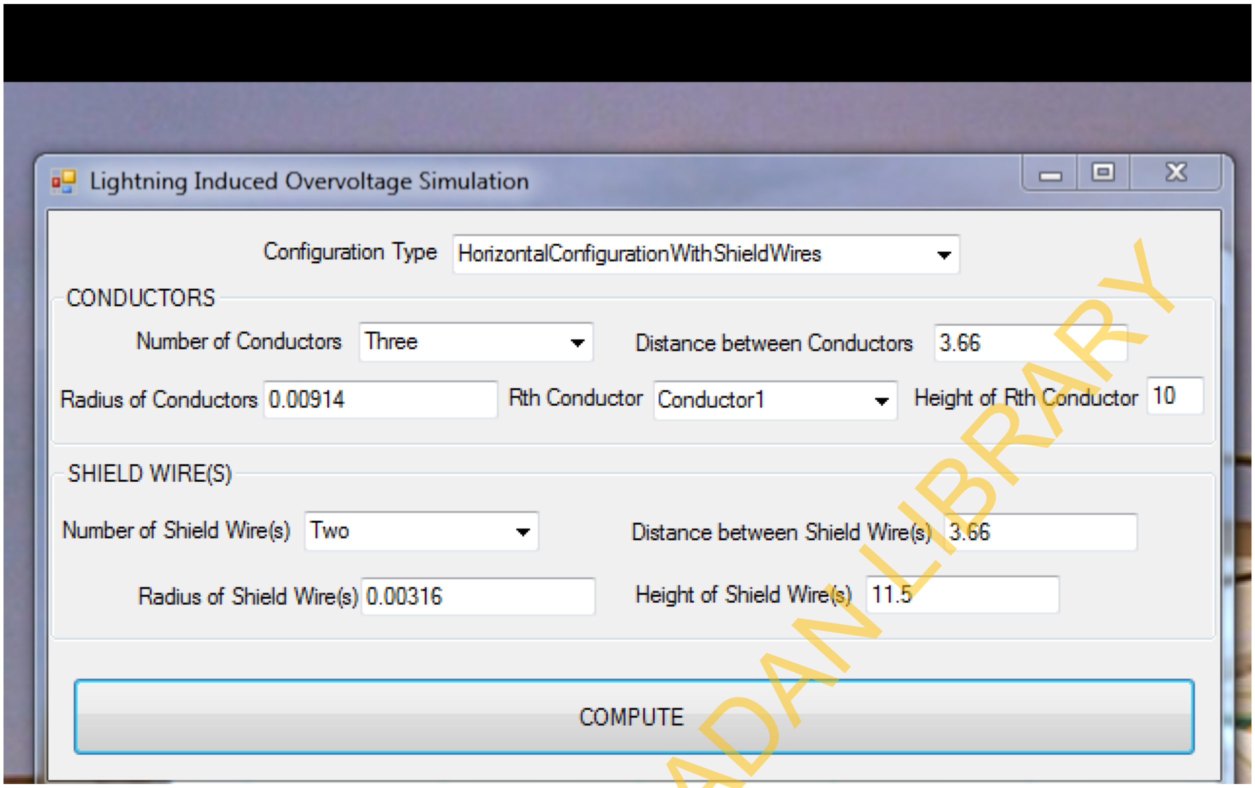

Fig.3.3: Window's GUI to interact with API to select line configuration for lightning-induced voltage calculation

CHAPTER FOUR

RESULTS AND DISCUSSION

4.1 Introduction

The results are presented in tabular and graphical forms. The discussions are in three parts, viz: (a) lightning characteristics, (b) influence of lightning parameters on induced voltages, (c) the configuration and the shielding effect.

4.2 Lightning Characteristics

The profile of the common undisturbed base current is shown in Figure 4.1 using the parameters in table3.1. Figures 4.2 and 4.3 show the profiles of TCS type models at channel heights 200m and 2km respectively. For channel height z'=200m, a time lag of 0.65 μs occurred between the peaks of the current of BG model compare and that of TCS. It was observed that the current almost coincided in both case beyond the time for the peak values of the currents. Figure 3 revealed that at high channel height, say z'=2km, the current of TCS model is almost constant with time, with no peak value.

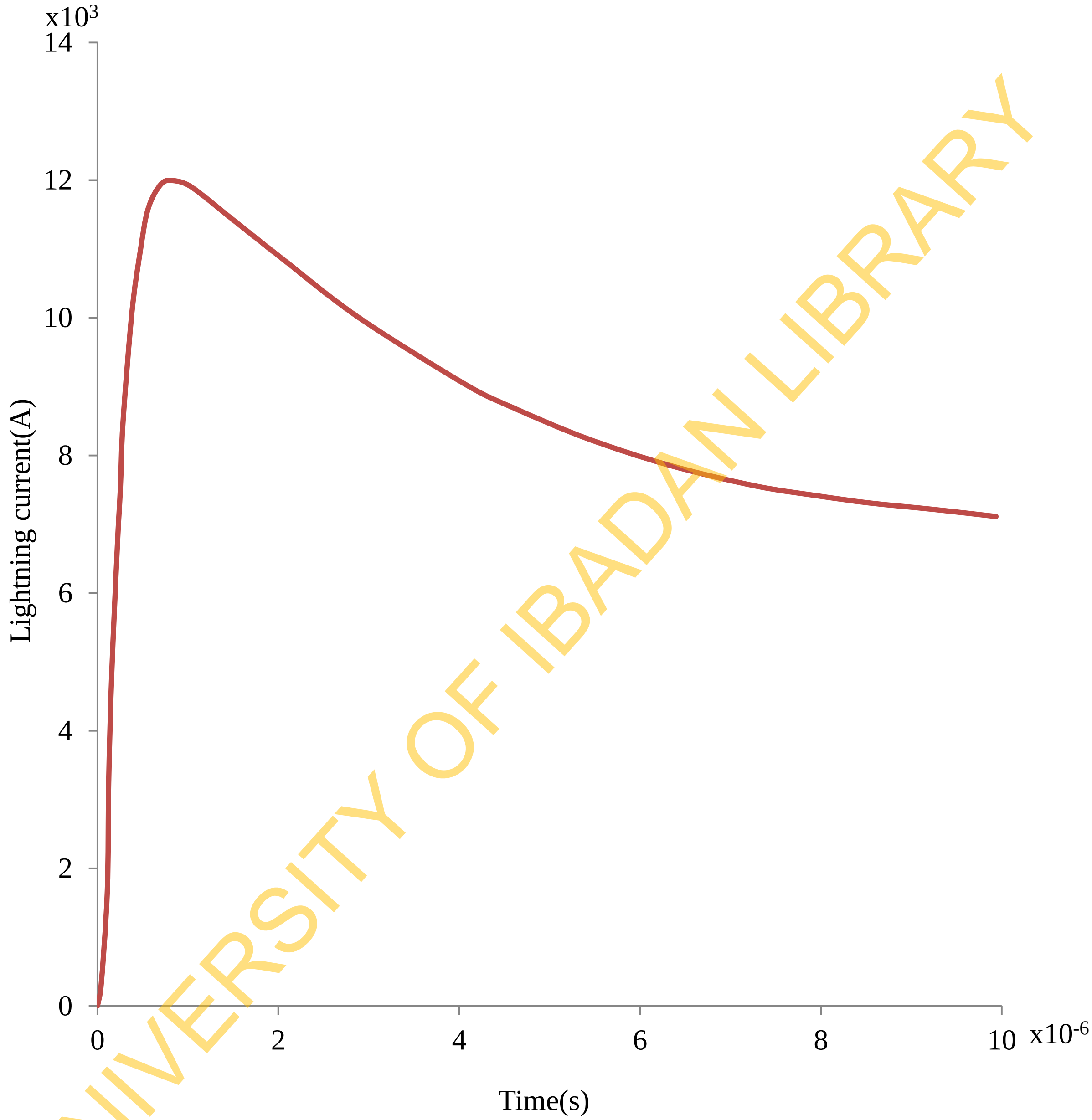

Figure 4.1: Profile of undisturbed base current for TL-typel and TCS-typel models, using typical parameters in table 3.1. The total channel height, H=5km,.Retturn stroke speed, v = 0.5c (m/μs)

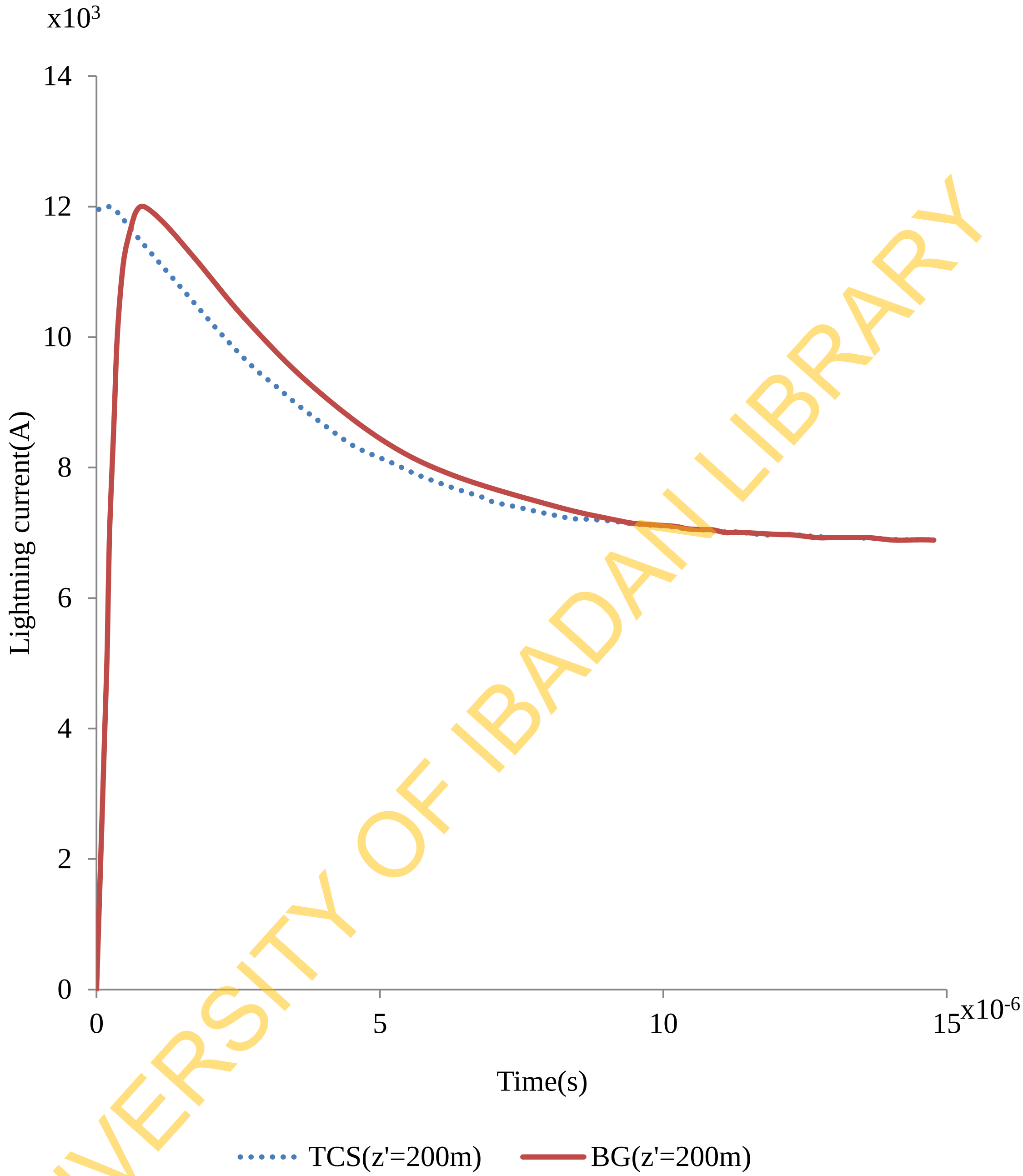

Figure 4.2: Current as a function of time at height, z'=200m (BG and TCS models)

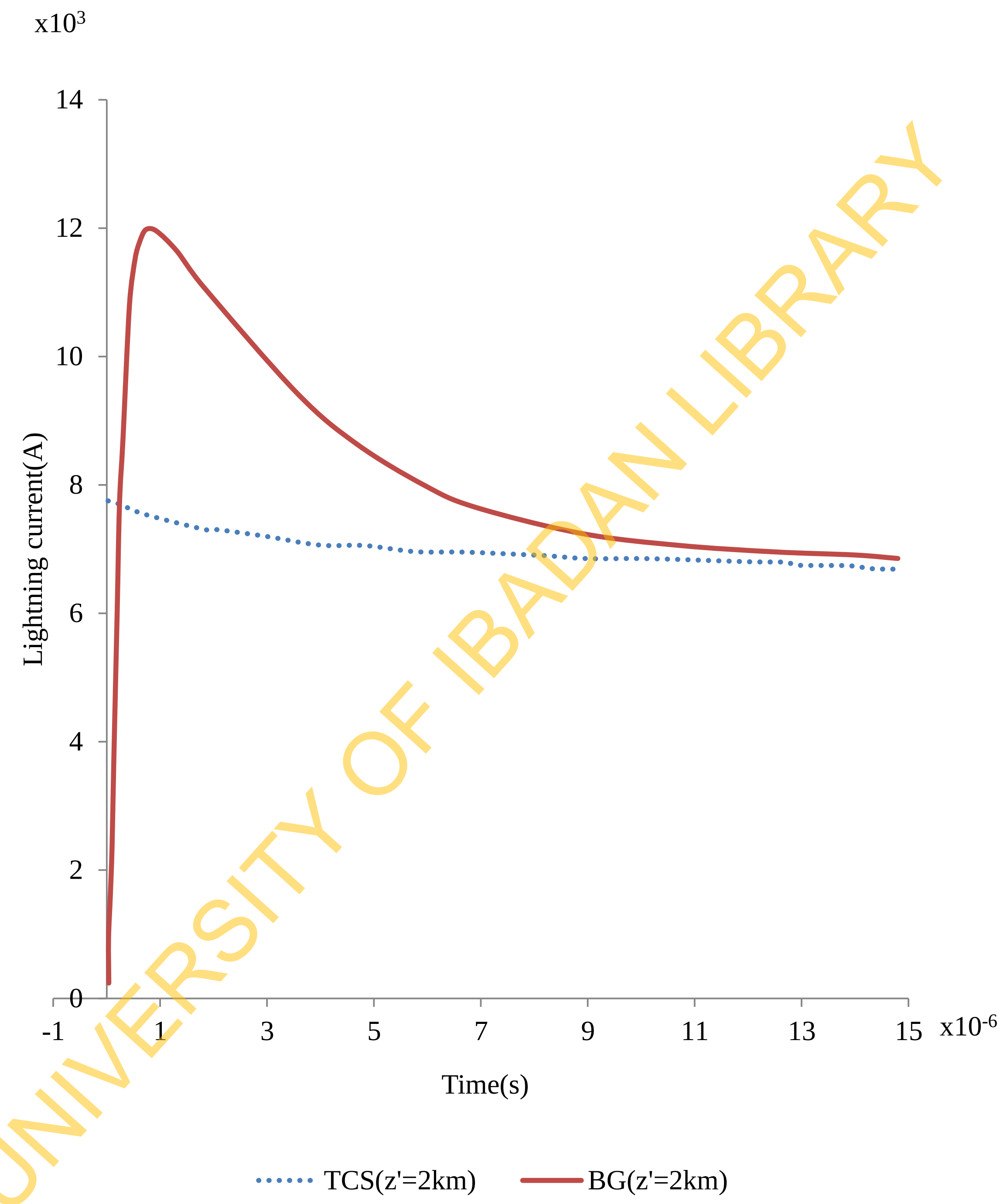

Fig. 4.3: Current as a function of time at height, z'=2km, cloud height, H=5km. (BG and TCS models)

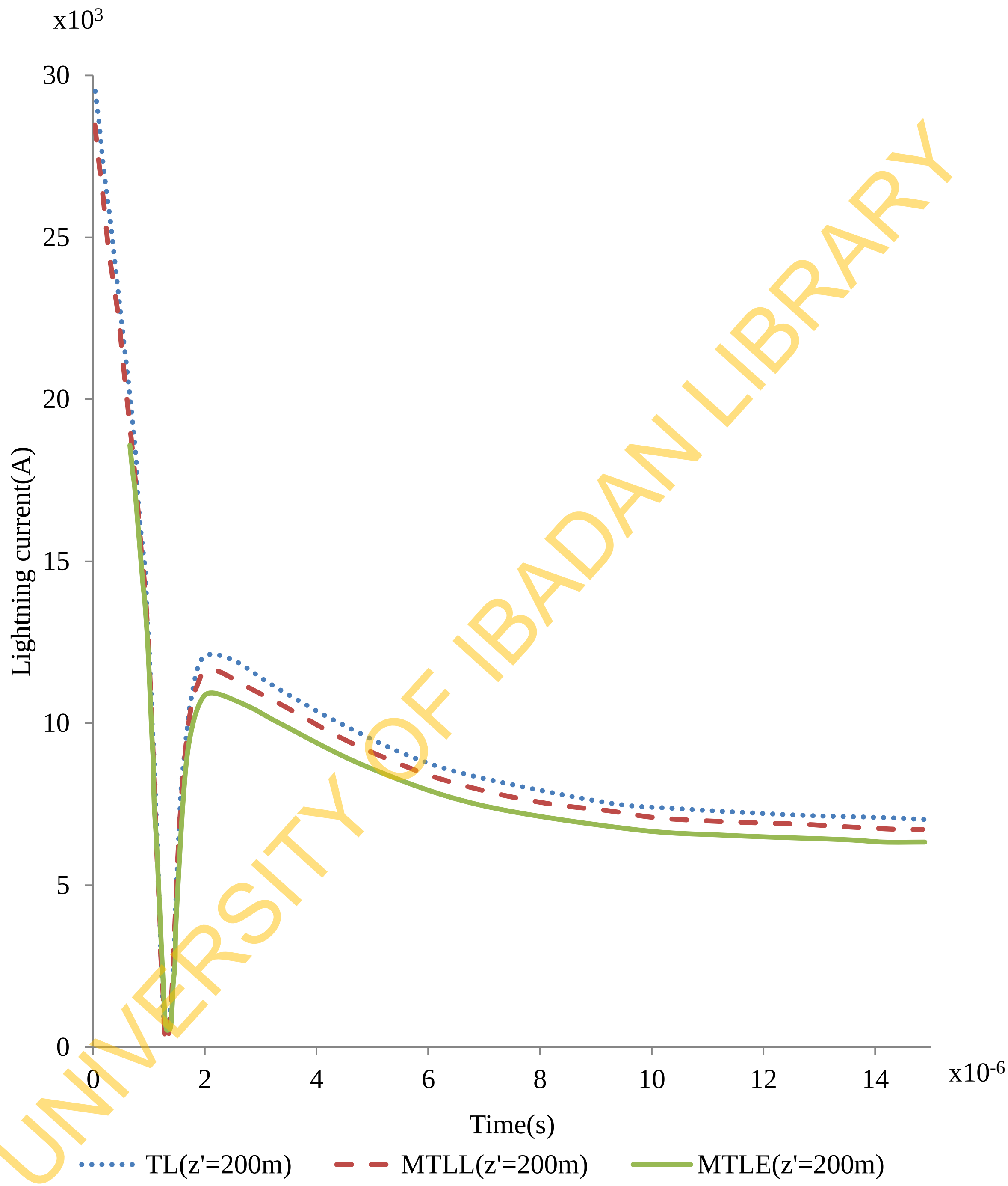

Figure 4.4: Current as a function of time at height, z'=200m, cloud height, H=5km. (MTLE,TL and MTLL models)

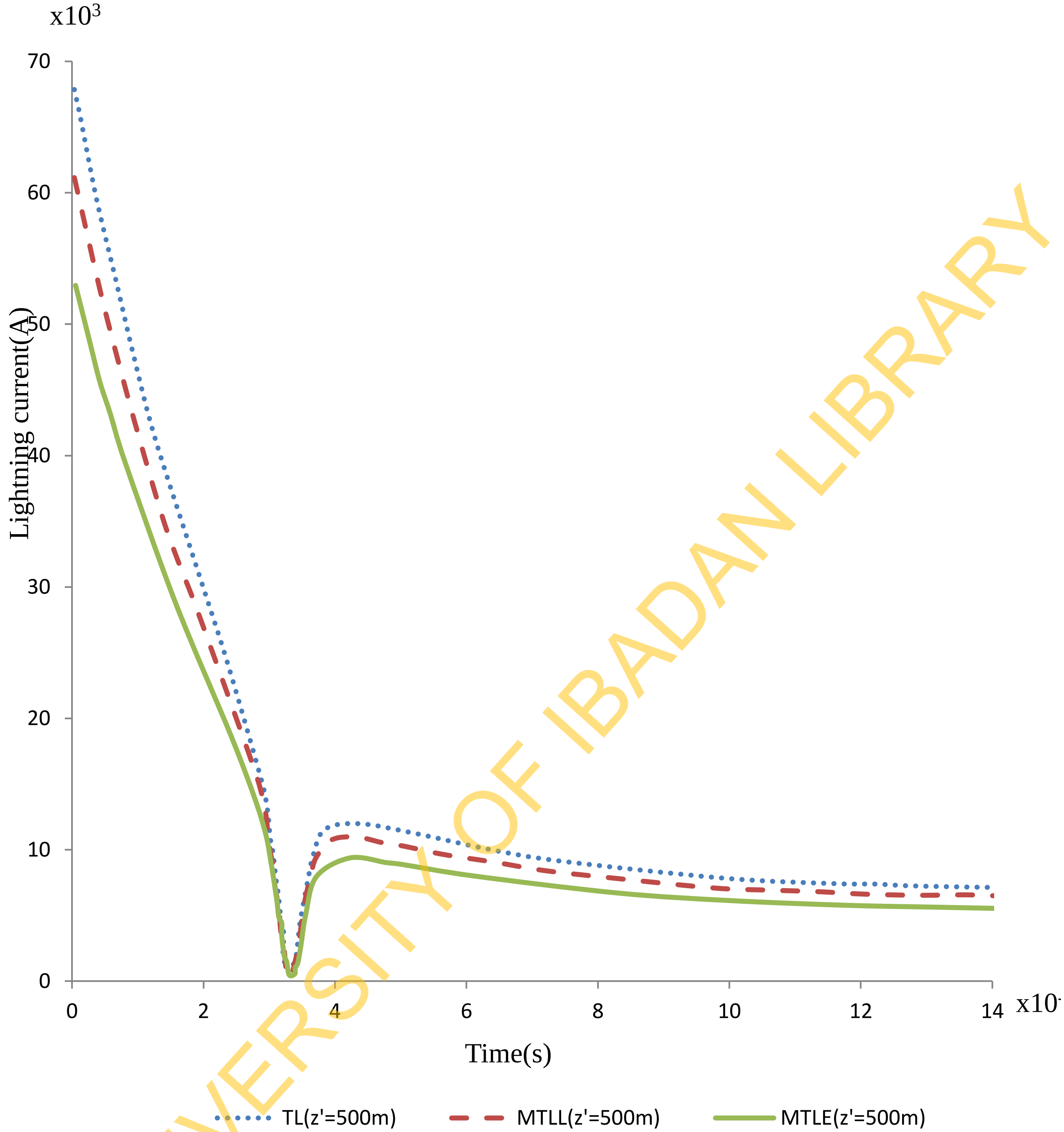

Figure 4.5: Current as a function of time at height, z'=500m, cloud height, H=5km. (MTLE,TL and MTLL models

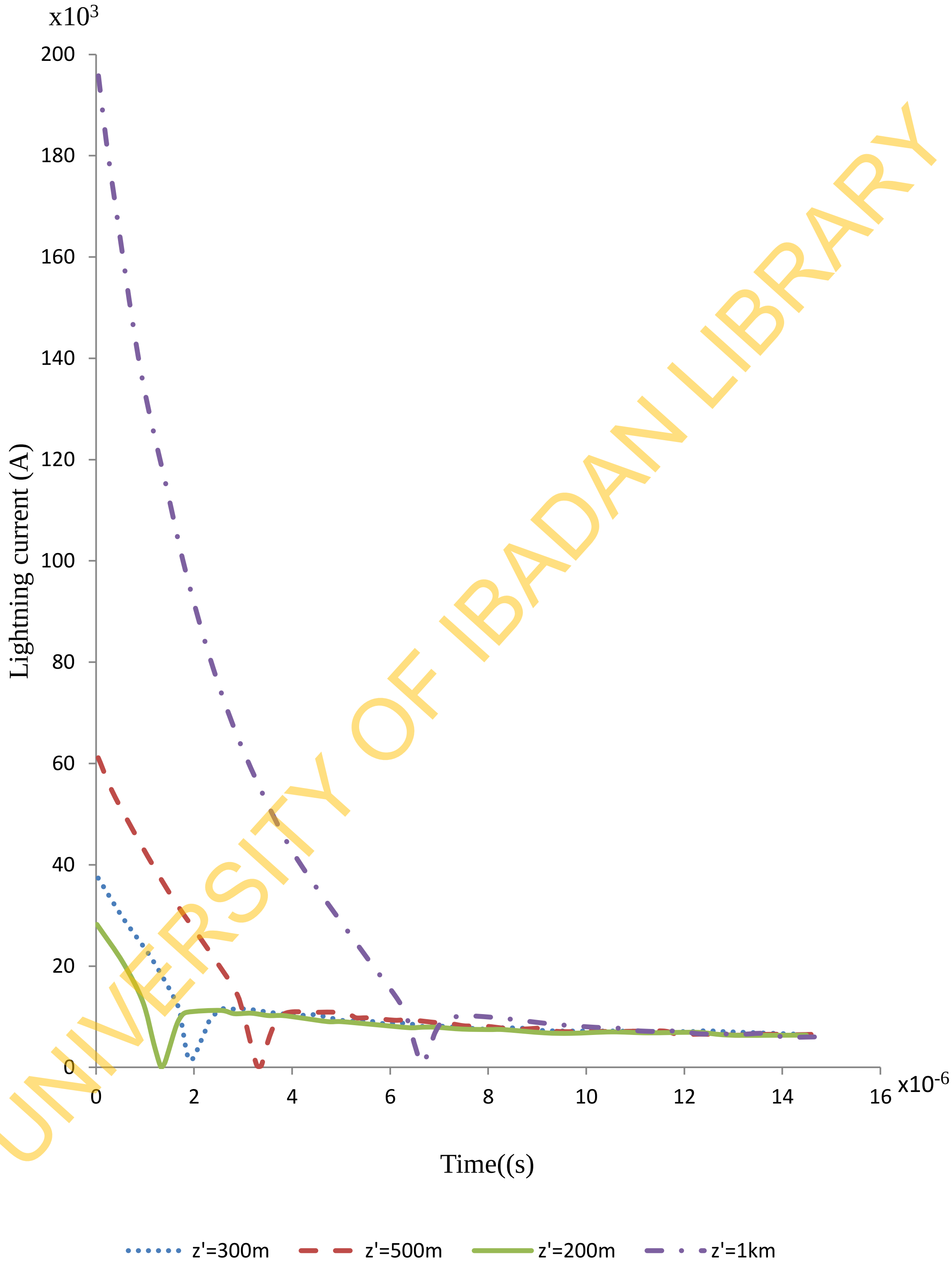

Figure 4.6: Current as a function of time for MTLL model

Model	$z' = 200m$	$z' = 300m$	$z' = 500m$	$z' = 1km$
MTLE	10.9kA	10.9kA	9.7 kA	7.6kA
MTLL	11.6kA	10.9kA	10.9kA	9.9kA
TL	12.1kA	12.1kA	12.1kA	12.1kA

Table 4.1: Peak values of the currents with different return stroke models at different heights (v=0.5c)

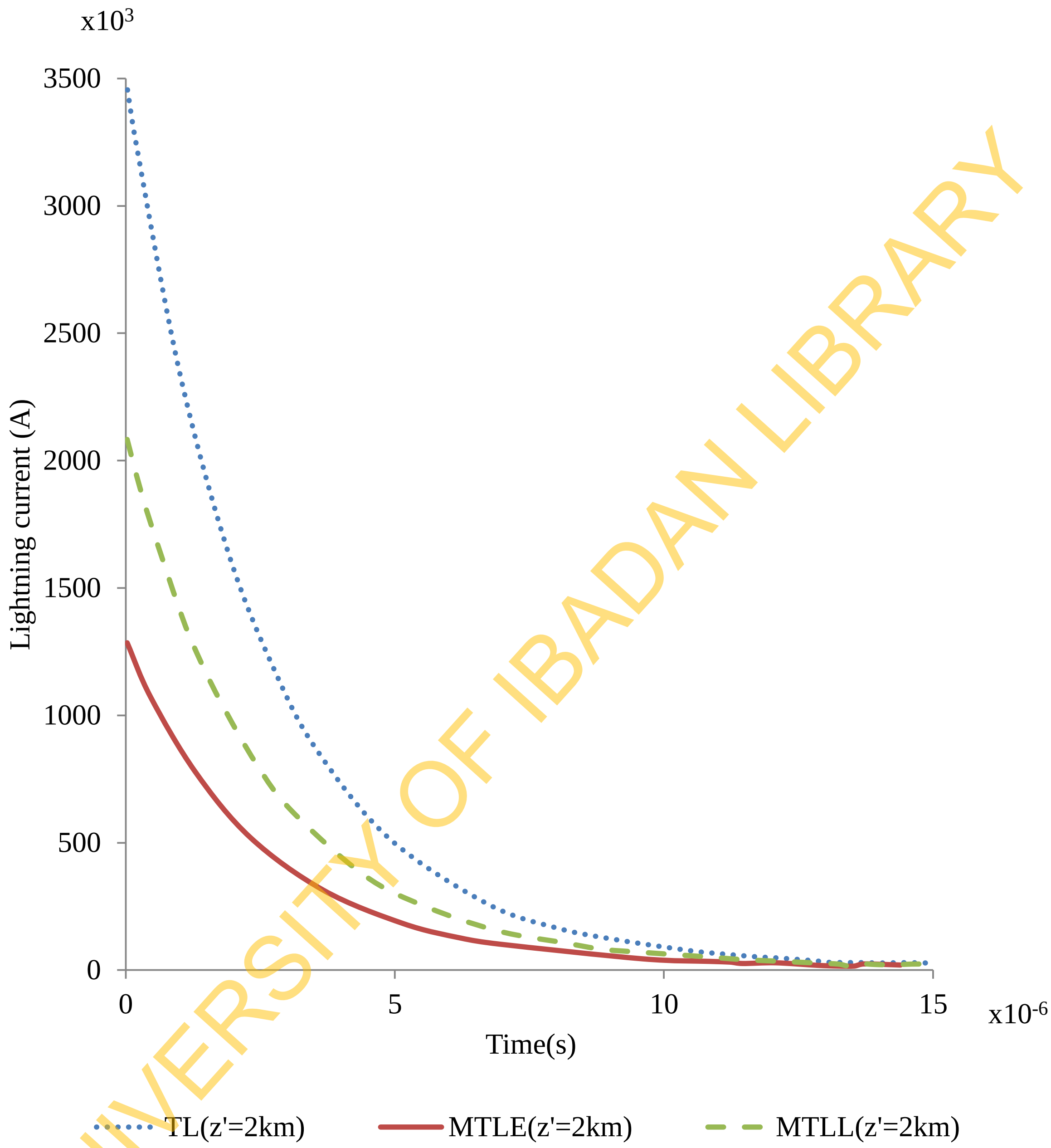

Figure 4.7: Current as a function of time at height,z'=2km, cloud height,H=5km. (MTLE,TL and TLL models

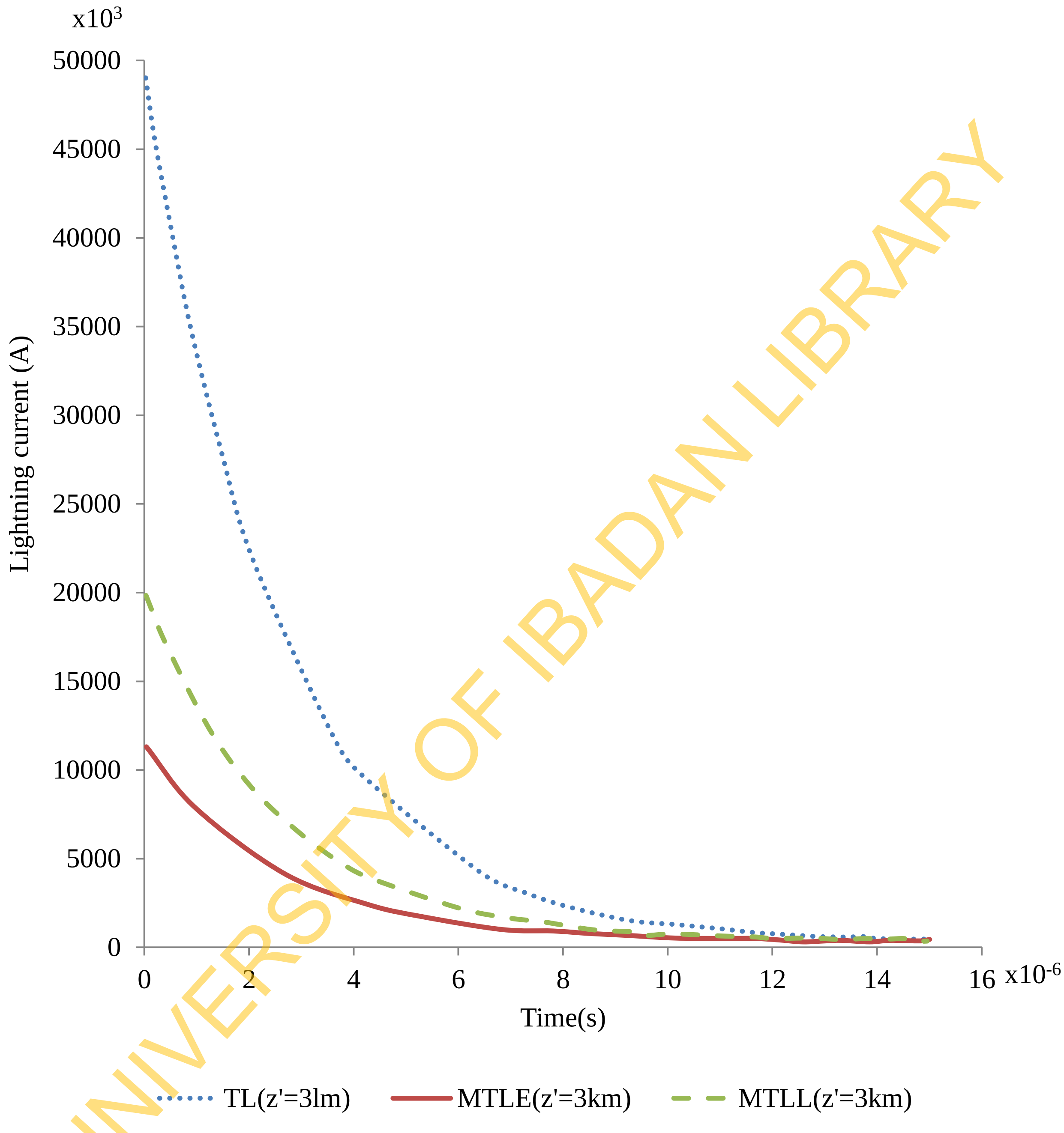

Figure 4.8: Current as a function of time at height,z'=3km, cloud height,H=5km. (MTLE,TL and MTLL models)

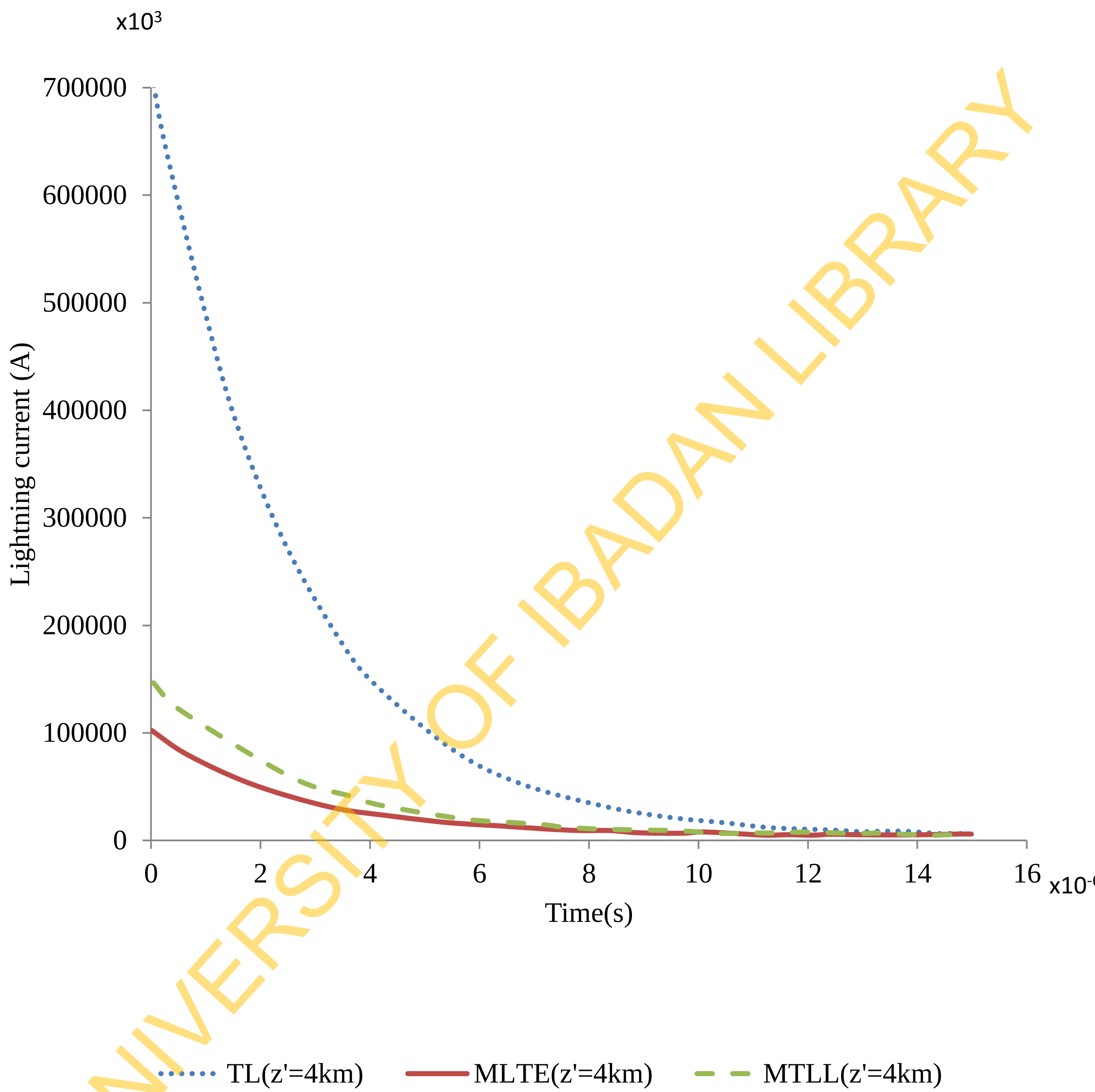

Figure 4.9: Current as a function of time at height,z'=4000m, cloud height,H=5km.

(MTLE, TL and MTLL models)

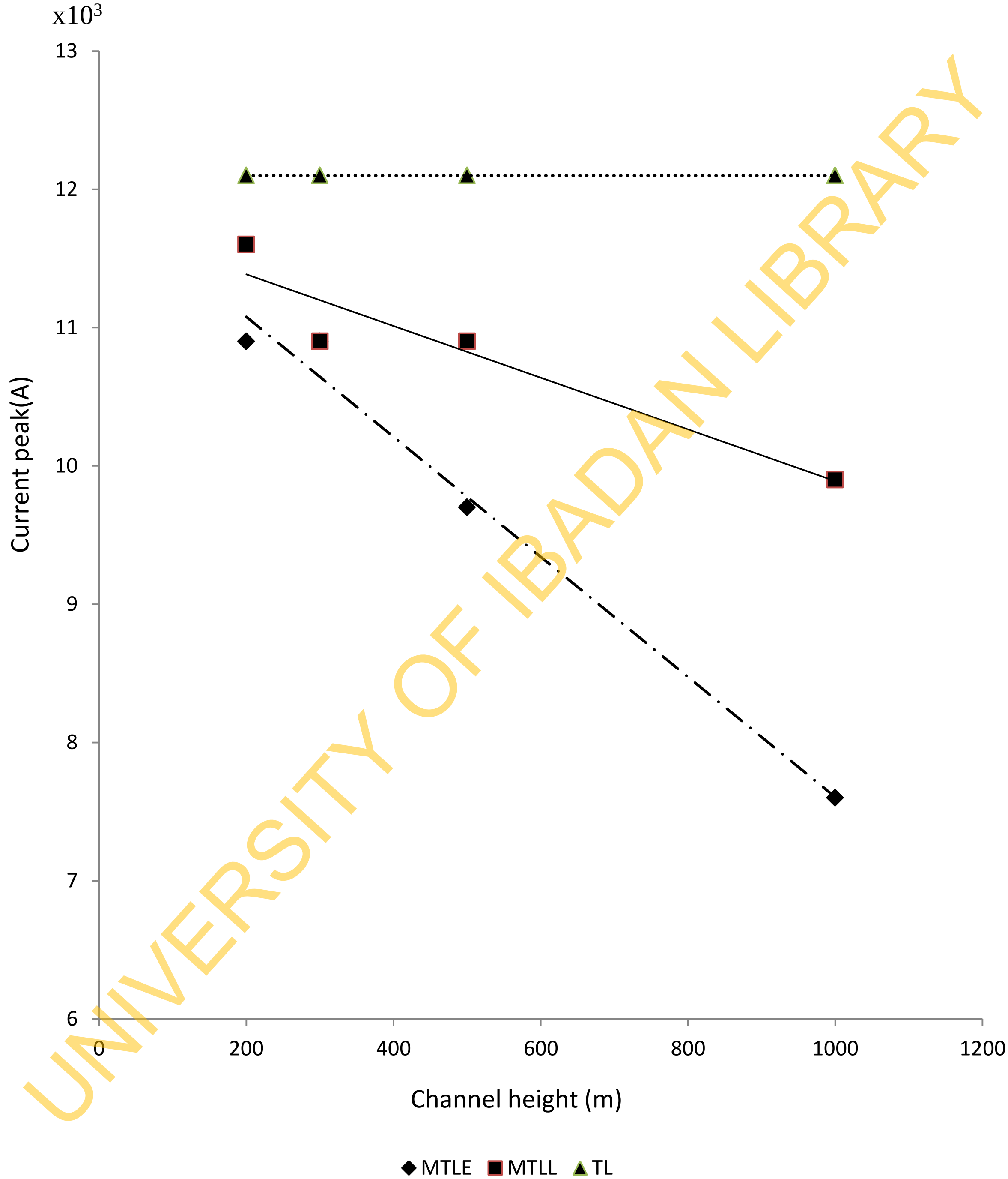

Figure 4.10: Relationship between current peak, I_p and channel height,

4.2.1 Case A- Low heights

Figure 4.4 presents return stroke current profile as a function of time, t, within a window frame of 15μs and channel height ,z' =200m for MTLE,TL and MTLL models. In case of MTLE model, at this height, the current dropped rapidly from 27.1 x 10^3A at time t=0 to a minimum turning point with current i=0 within 1.3 x 10^{-6} s. The current picked up to a maximum turning point with peak current, I_p=10.9 x 10^3 A within the next 0.9 x 10^{-6} s. Thereafter the current decreased gradually with time.

TL and MTLL models followed the same wave form as that of MTLE. It is observed that the minimum turning point of the three transmission-line-type models coincide at time t=1.3 x 10^{-6} s. Also the maximum turning point occurred at the same time, t = 2.2 x 10^{-6} s with slight variation in the current peak

Figure 4.6 revealed that in case of MTLL, a time delay of 2 x 10^{-6} s was observed in the wave form at z'=500m relative to that at z'=200m.The delay time of waveform was 5.3 x 10^{-6} s in case of channel height,z'=1km relative to that of z'=200m.It is also observed that peak current attenuates with increase in channel height (table 4.1 and figure 4.6).The same pattern of time delay in wave form was observed for both MTLE and TL. A linear relationship is established between the peak current, I_p and the channel height, z' (Figure.4.10).

4.2.2 Case B- High heights

Figures 4.7,4.8 and 4.9 represent return stroke current profiles as a function of time, t, within a window frame of 15 x 10^{-6} s and channel height ,z' =2 x 10^3 m, 3 x 10^3 m and 4km for MTLE,TL and MTLL models. The wave forms are the same for transmission-line-type models. The minimum and maximum turning points observed in current profiles at low heights are discontinuous at heights $z'=2 \times 10^3$ m and above. A rapid increase in the values of the current with height is observed

Table 4.2: The variation of induced voltage ,V with peak current, I_p (h=10m, t_f=5 x 10^{-6} s,β=0.3,y_0=100m,x=1000m)

Time.t(s) ($X10^{-6}$)	Induced voltagees, V(volt)					
	I_p=10kA	I_p=20kA	I_p=30kA	I_p=50kA	I_p=80kA	I_p=100kA
0.0	-	-	-	-	-	-
0.5	-	-	-	-	-	-
1.0	-	-	-	-	-	-
1.5	-	-	-	-	-	-
2.0	-	-	-	-	-	-
2.5	-	-	-	-	-	-
3.0	-	-	-	-	-	-
3.5	-	-	-	-	-	-
4.0	-	-	-	-	-	-
4.5	-	-	-	-	-	-
5.0	-	-	-	-	-	-
5.5	-	-	-	-	-	-
6.0	-	-	-	-	-	-
6.5	-	-	-	-	-	-
7.0	-	-	-	-	-	-
7.5	-	-	-	-	-	-
8.0	-	-	-	-	-	-
8.5	-2705.8	-5411.7	-8117.5	-13529.1	-21646.6	-27058.3
9.0	4500.4	9000.9	13501.3	22502.1	36003.4	45004.3
9.5	5865.5	11731.0	17596.5	29327.4	46923.9	58654.9
10.0	5965.2	11930.3	17895.5	29825.9	47721.4	59651.7
10.5	5727.2	11454.3	17181.5	28635.9	45817.4	57271.7
11.0	5415.7	10831.4	16247.1	27078.6	43325.7	54157.1
11.5	5110.0	10220.0	15329.9	25549.9	40879.8	51099.8
12.0	4832.3	9664.5	14496.8	24161.3	38658.0	48322.5
12.5	4586.3	9172.6	13759.0	22931.6	36690.6	45863.2
13.0	4370.1	8740.1	13110.2	21850.3	34960.5	43700.7
13.5	4179.8	8359.5	12539.3	20898.8	33438.1	41797.6
14.0	4011.6	8023.1	12034.7	20057.8	32092.5	40115.7
14.5	3862.0	7724.1	11586.1	19310.2	30896.4	38620.5

Table 4.3 : The variation of induced voltage ,V with specific velocity ,β (h =10m,t_f=5μs, I_p=10kA,y_0=100m,x=1000m)

Time.t(s) ($X10^{-6}$)	Induced voltages, V(volt)						
	β=0.2	β=0.3	β=0.4	β=0.5	β=0.6	β=0.7	β=0.8
0.0	-	-	-	-	-	-	-
0.5	-	-	-	-	-	-	-
1.0	-	-	-	-	-	-	-
1.5	-	-	-	-	-	-	-
2.0	-	-	-	-	-	-	-
2.5	-	-	-	-	-	-	-
3.0	-	-	-	-	-	-	-
3.5	-	-	-	-	-	-	-
4.0	-	-	-	-	-	-	-
4.5	-	-	-	-	-	-	-
5.0	-	-	-	-	-	-	-
5.5	-	-	-	-	-	-	-
6.0	-	-	-	-	-	-	-
6.5	-	-	-	-	-	-	-
7.0	-	-	-	-	-	-	-
7.5	-	-	-	-	-	-	-
8.0	-	-	-	-	-	-	-
	-	-					
8.5	11124.1	2705.8	275.3	1419.5	1792.2	1798.8	1619.0
9.0	1596.1	4500.4	4574.3	3976.5	3252.7	2562.0	1947.8
9.5	5449.0	5865.5	4898.2	3876.6	3013.3	2316.8	1759.0
10.0	6888.1	5965.2	4621.2	3534.9	2711.6	2087.6	1608.0
10.5	7350.9	5727.2	4274.4	3224.1	2469.5	1915.8	1499.3
11.0	7394.1	5415.7	3960.1	2971.0	2282.5	1786.9	1418.9
11.5	7256.9	5110.0	3693.2	2767.5	2136.4	1687.7	1357.0
12.0	7046.4	4832.3	3469.3	2602.5	2019.9	1609.1	1307.8
12.5	6811.9	4586.3	3280.9	2466.7	1925.1	1545.2	1267.3
13.0	6576.2	4370.1	3121.0	2353.3	1846.2	1491.9	1233.0
13.5	6349.5	4179.8	2983.9	2257.0	1779.5	1446.5	1203.4
14.0	6135.8	4011.6	2865.1	2174.2	1722.0	1407.1	1177.1
14.5	5936.6	3862.0	2761.0	2101.9	1671.7	1372.3	1153.5

Table 4.4 : The variation of induced voltage ,V with front time , t_f (h =10m, β=0.3,, I_p=10kA,y_0=100m,x=1000m)

Time.t(s) ($X10^{-6}$)	Induced voltagees, V (volt)							
	t_f=2μs	t_f=3μs	t_f=4μs	t_f=5μs	t_f=6μs	t_f=7μs	t_f=8μs	t_f=10μs
0.0	-	-	-	-	-	-	-	-
0.5	-	-	-	-	-	-	-	-
1.0	-	-	-	-	-	-	-	-
1.5	-	-	-	-	-	-	-	-
2.0	-	-	-	-	-	-	-	-
2.5	-	-	-	-	-	-	-	-
3.0	-	-	-	-	-	-	-	-
3.5	-	-	-	-	-	-8373.5	-7326.8	-5861.4
4.0	-	-	-	-	-	-	-11617.1	-9293.7
4.5	-	-	-	-	-	-	-12184.7	-9747.8
5.0	-	-	-	-	-	-	-	-9574.0
5.5	-16332	-	-	-	-	-	-	-9239.8
6.0	2227	-	-	-	-	-	-	-8877.1
6.5	6199	-8504.8	-	-	-	-	-	-8524.9
7.0	6962	3762.4	-	-	-	-	-	-
7.5	6823	6266.2	-4778.2	-	-	-	-	-
8.0	6443	6632.4	4315.0	-	-	-	-	-
8.5	6027	6409.8	6095.6	-2705.8	-	-	-	-
9.0	5638	6042.6	6284.8	4500.4	-	-	-	-
9.5	5292	5666.2	6043.6	5865.5	-1430.7	-	-	-
10.0	4989	5320.7	5703.6	5965.2	4531.5	-	-	-
10.5	4726	5014.9	5365.0	5727.2	5631.5	-589.0	-	-
11.0	4497	4747.6	5056.5	5415.7	5681.6	4493.3	-	-
11.5	4296	4514.2	4783.7	5110.0	5454.3	5411.3	-4.1	-
12.0	4119	4309.7	4544.5	4832.3	5169.0	5432.2	4423.5	-
12.5	3962	4129.6	4334.8	4586.3	4891.1	5217.5	5209.5	-
13.0	3821	3970.0	4150.4	4370.1	4638.9	4955.2	5212.2	-
13.5	3695	3827.6	3987.1	4179.8	4415.2	4700.9	5010.3	732.3
14.0	3581	3699.7	3841.6	4011.6	4217.8	4470.0	4767.8	4251.7
14.5	3476	3584.0	3711.2	3862.0	4043.5	4264.7	4533.5	4859.7

Table 4.5: The variation of Peak Induced Voltage (PIV),V_p with lightning parameters

Variation with peak crrent, I_p		Variation with specific velocity, **β**		Variation with front time, t_f	
I_p (kA)	V_p(volt)	**β**	V_p(volt)	t_f (μs)	V_p(volt)
10.0	5965.2	0.3	5965.2	2.0	6962.2
20.0	11930.3	0.4	4898.2	3.0	6632.4
30.0	17895.5	0.5	3976.5	4.0	6284.8
50.0	29825.9	0.6	3252.7	6.0	5681.7
80.0	47721.4	0.7	2562.0	7.0	5432.2
100.0	59651.7	0.8	1947.8	8.0	5212.2

Time,t(s) ($x10^{-6}$)	V_{s1} (volt)	V_1 (volt)	V_{s2} (volt)	V_2 (volt)	V_{s3} (volt)	V_3 (volt)
0.0	-	-	-	-	-	-
1.0	-	-	-	-	-	-
2.0	-	-	-	-	-	-
3.0	-	-	-	-	-	-
4.0	-	-	-	-	-	-
5.0	-	-	-	-	-	-
6.0	-	-	-	-	-	-
7.0	-	-	-	-	-	-
8.0	-	-	-	-	-	-
9.0	4500.4	8730.8	6147.6	10297.2	7790.2	11841.2
10.0	5965.2	11572.4	8148.4	13648.6	10325.7	15695.1
11.0	5415.7	10506.5	7397.9	12391.4	9374.6	14249.4
12.0	4832.3	9374.6	6600.9	11056.4	8364.6	12714.2
13.0	4370.1	8477.9	5969.5	9998.9	7564.6	11498.2
14.0	4011.6	7782.4	5479.8	9178.7	6944.0	10554.9
15.0	3728.3	7232.8	5092.8	8530.5	6453.6	9809.5
16.0	3498.5	6787.1	4778.9	8004.7	6055.9	9205.0
17.0	3307.3	6416.2	4517.8	7567.3	5724.9	8701.9
18.0	3144.5	6100.3	4295.3	7194.7	5443.1	8273.5
19.0	3003.0	5825.8	4102.1	6871.0	5198.2	7901.2
20.0	2877.9	5583.2	3931.2	6584.8	4981.7	7572.2
21.0	2765.8	5365.7	3778.1	6328.3	4787.6	7277.2
22.0	2664.1	5168.4	3639.2	6095.6	4611.6	7009.6
23.0	2571.0	4987.7	3511.9	5882.5	4450.3	6764.5
24.0	2485.0	4820.9	3394.5	5685.8	4301.5	6538.3
25.0	2405.1	4665.9	3285.4	5503.0	4163.2	6328.1
26.0	2330.5	4521.2	3183.5	5332.3	4034.1	6131.9
27.0	2260.6	4385.5	3087.9	5172.3	3913.0	5947.8
28.0	2194.7	4257.8	2998.0	5021.6	3799.1	5774.6
29.0	2132.6	4137.2	2913.1	4879.4	3691.5	5611.1
30.0	2073.8	4023.1	2832.8	4744.9	3589.7	5456.3
31.0	2018.0	3914.9	2756.6	4617.3	3493.1	5309.6
32.0	1965.0	3812.1	2684.2	4496.0	3401.4	5170.2
33.0	1914.6	3714.3	2615.3	4380.7	3314.2	5037.5
34.0	1866.6	3621.1	2549.7	4270.8	3231.0	4911.1
35.0	1820.7	3532.2	2487.1	4165.9	3151.7	4790.5
36.0	1776.9	3447.3	2427.3	4065.7	3075.9	4675.4
37.0	1735.1	3366.1	2370.1	3970.0	3003.5	4565.3
38.0	1695.0	3288.4	2315.4	3878.4	2934.1	4459.9
39.0	1656.7	3214.0	2263.0	3790.6	2867.7	4358.9
40.0	1619.9	3142.6	2212.8	3706.4	2804.1	4262.2

Table 4.6: Comparision of induced voltages on multiconductors for vertical configuration with single conductor equivalent.

Table 4.7: Peak induced voltages for vertical and horizontal configurations

Vertical configuration	conductor 1 h=10,0m	conductor 2 h=13.7m	conductor 3 h=17.3m
	Peak induced voltage, V_p(volt)		
Single	5965.2	8148.4	10325.7
Without earth wire	11572.4	13648.6	15695.1
With earth wire above	10558.4	12125	13010.4
With earth wire below	9961.9	12744.1	15075.5
Horizontal configuration	**conductor 1 h=10,0m**	**conductor 2 h=10,0m**	**conductor 3 h=10,0m**
	Peak induced voltage, V_p(volt)		
Single	5965.2	5965.2	5965.2
Without earth wire	8697.3	9395.2	8697.3
With 2 earth wires above	7050.9	6889.8	7050.9
With 2 earth wires below	7229.8	7516.2	7229.8

Table 4.8: Protective ratio values for vertical and horizontal configurations

Configuration	Profile	Conductor 1	Conductor 2	Conductor 3
Vertical	Earth wire above	0.912	0.890	0.827
	Earth wire below	0.861	0.934	0.960
Horizontal	Earth wires above	0.811	0.733	0.811
	Earth wires below	0.831	0.800	0.831

Table 4.9: Per-Unit Induced Voltages On 3-Conductor Lines

Earth wire radius= 3.16mm; conductor radius=9.46mm; earth wires sepration=3.66m;			
Vertical configuration	conductor 1 h=10.0m	conductor 2 h=13.7m	conductor 3 h=17.3m
	Per-unit induced voltage		
$\frac{V_n}{V_{sn}}$	$\frac{V_1}{V_{s1}}$	$\frac{V_2}{V_{s2}}$	$\frac{V_3}{V_{s3}}$
Without earth wire	1.94	1.68	1.52
With earth wire above,h=18.82m	1.77	1.49	1.26
With earth wire below,h=8.48m	1.67	1.56	1.46
Horizontal configuration	conductor 1 h=10.0m	conductor 2 h=10.0m	conductor 3 h=10.0m
	Per-unit induced voltage		
$\frac{V_n}{V_{sn}}$	$\frac{V_1}{V_{s1}}$	$\frac{V_2}{V_{s2}}$	$\frac{V_3}{V_{s3}}$
Without earth wire	1.46	1.58	1.46
With earth wire above,h=11.52m	1.18	1.16	1.18
With earth wire below,h=8.48m	1.21	1.26	1.21

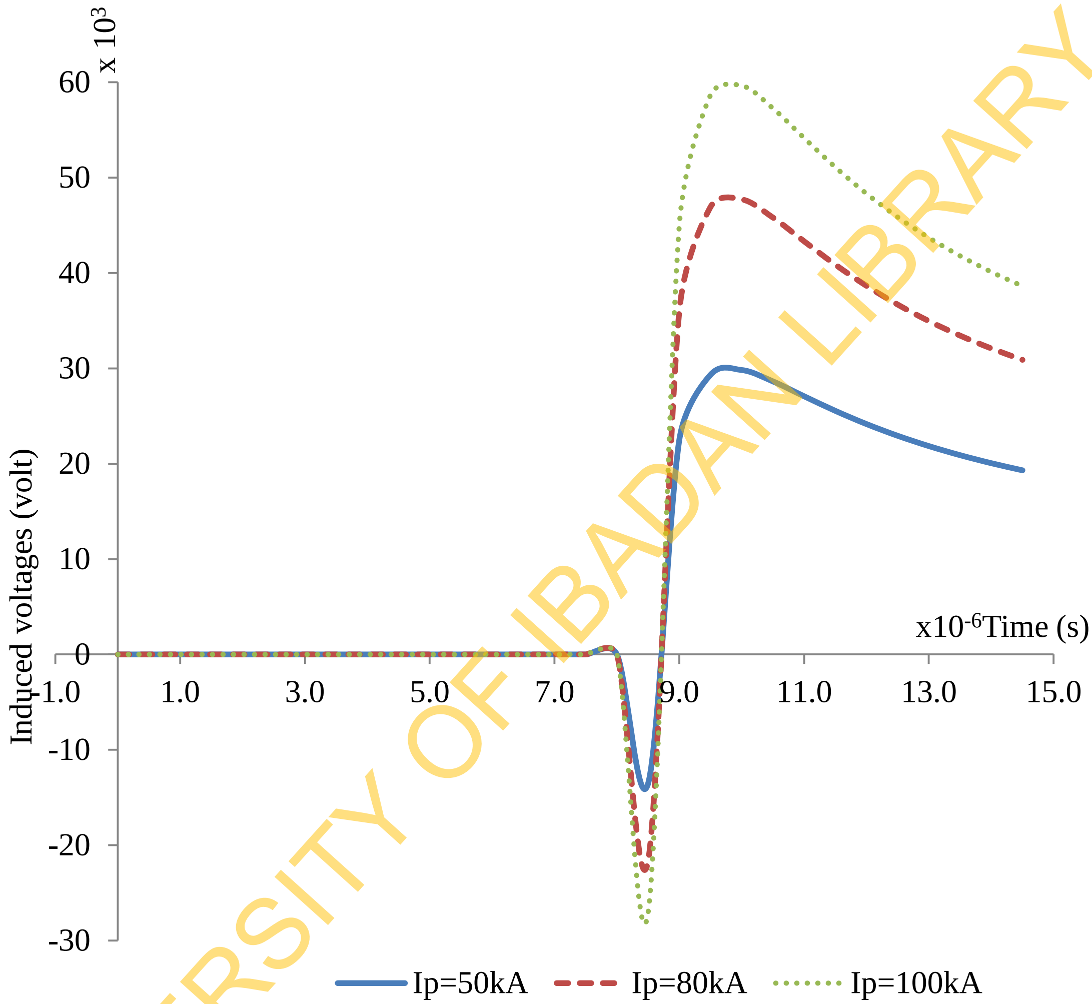

Fig. 4.11: Variation of induced voltages with return stroke peak current

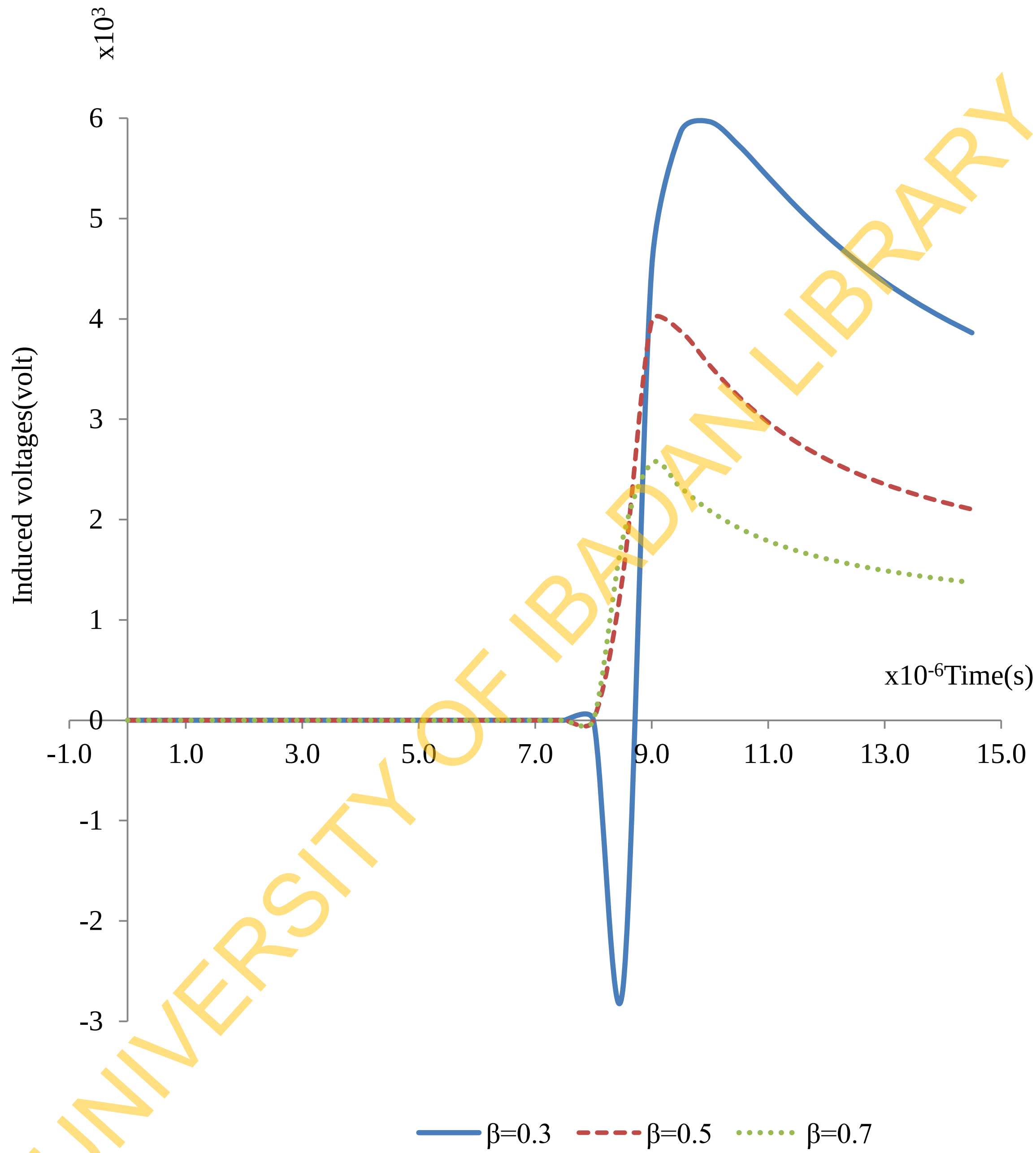

Fig. 4.12: Variation of induced voltages with return stroke specific velocity

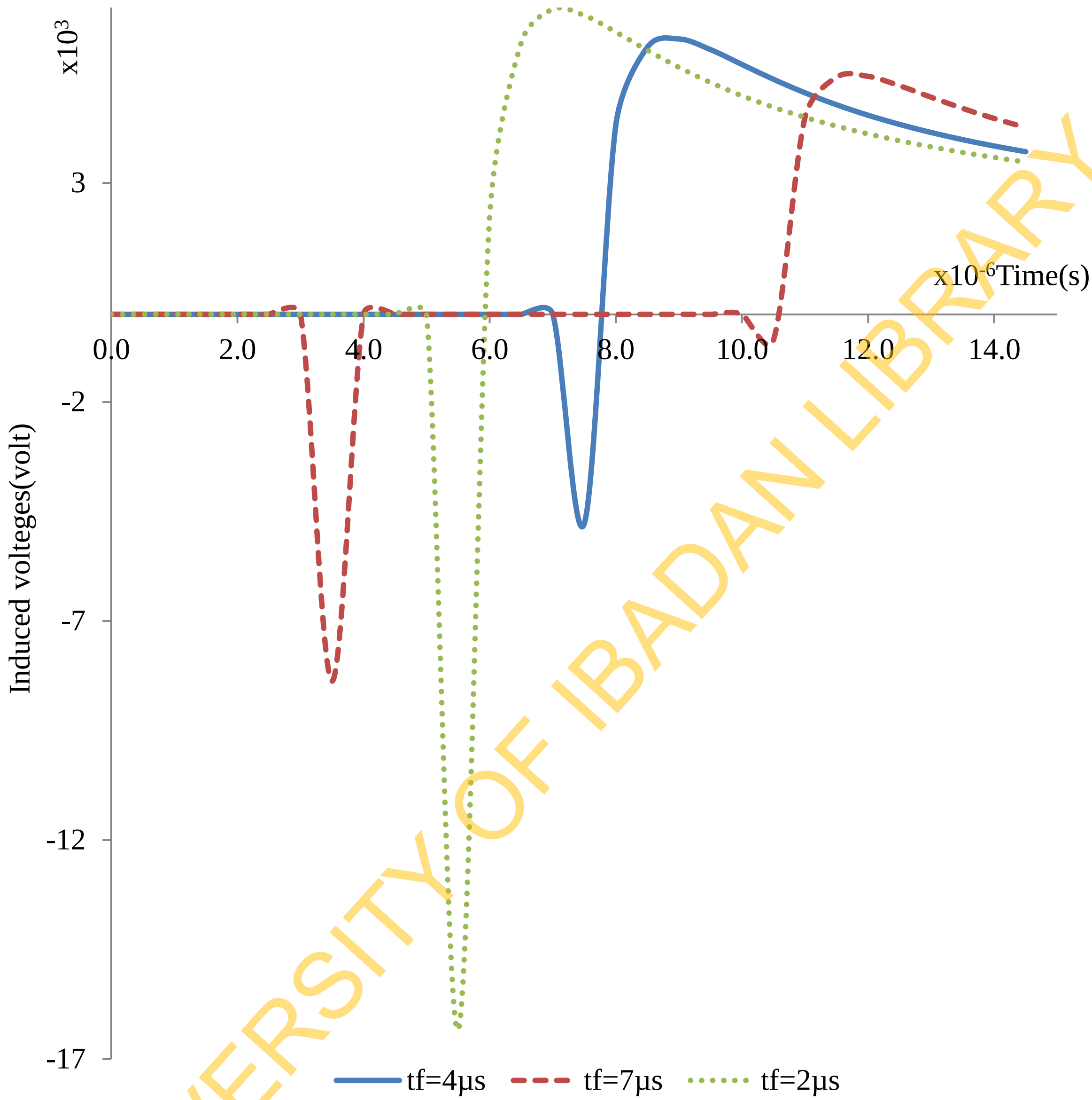

Fig. 4.13: Variation of induced voltages with return stroke front time

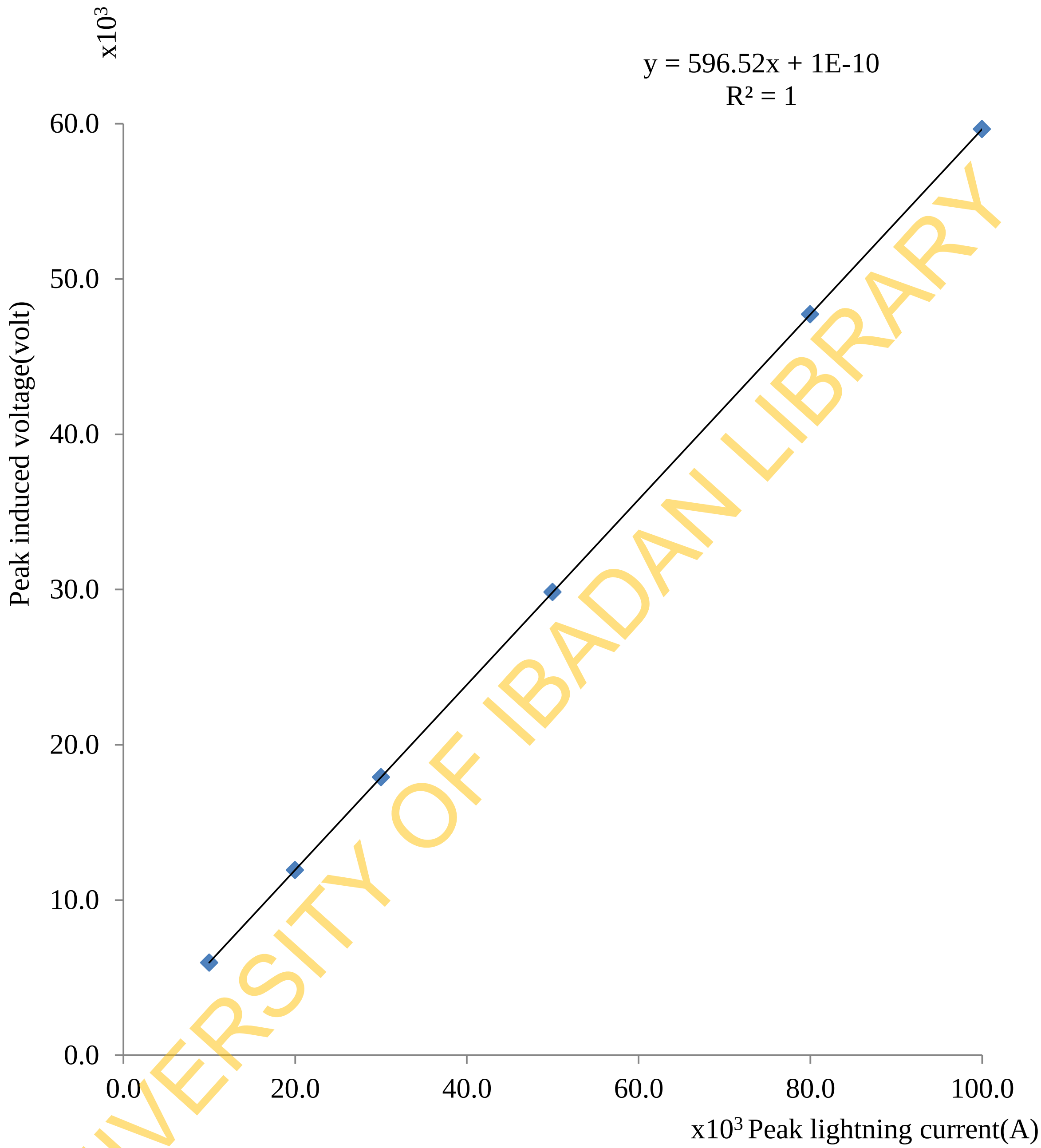

Fig. 4.14: Variation of peak induced voltages with return stroke peak current

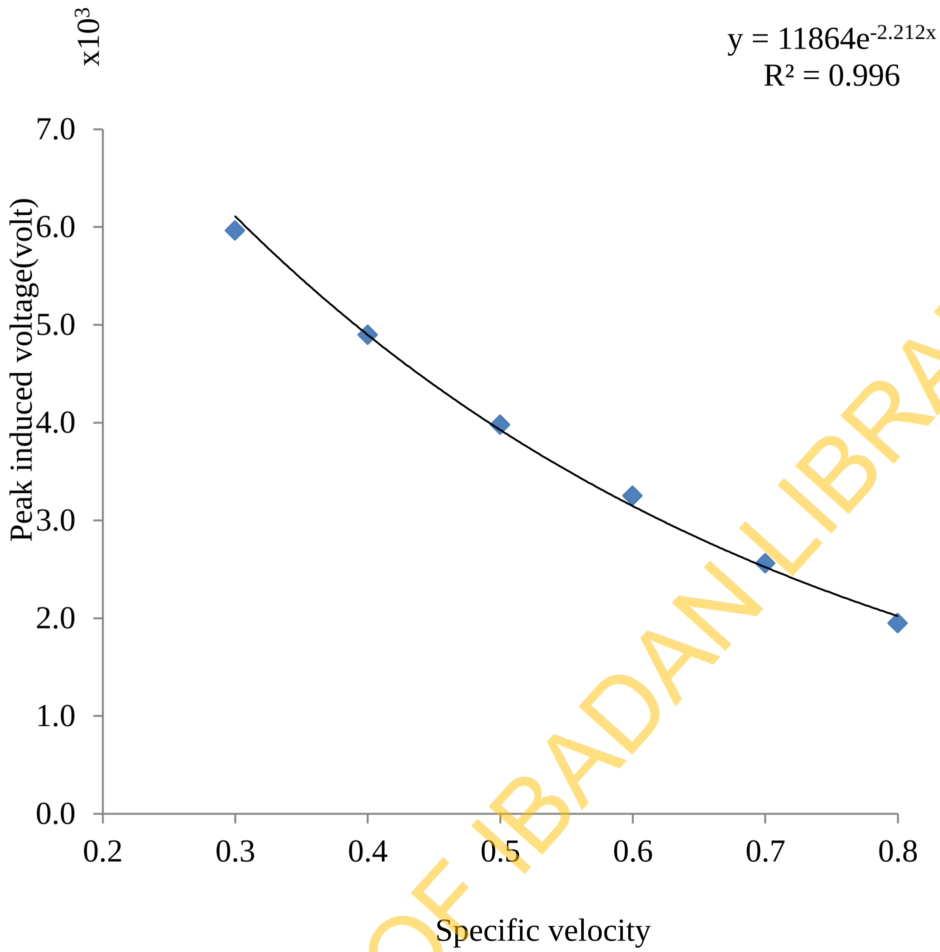

Fig.4.15: Variation of peak induced voltages with return stroke specific velocity

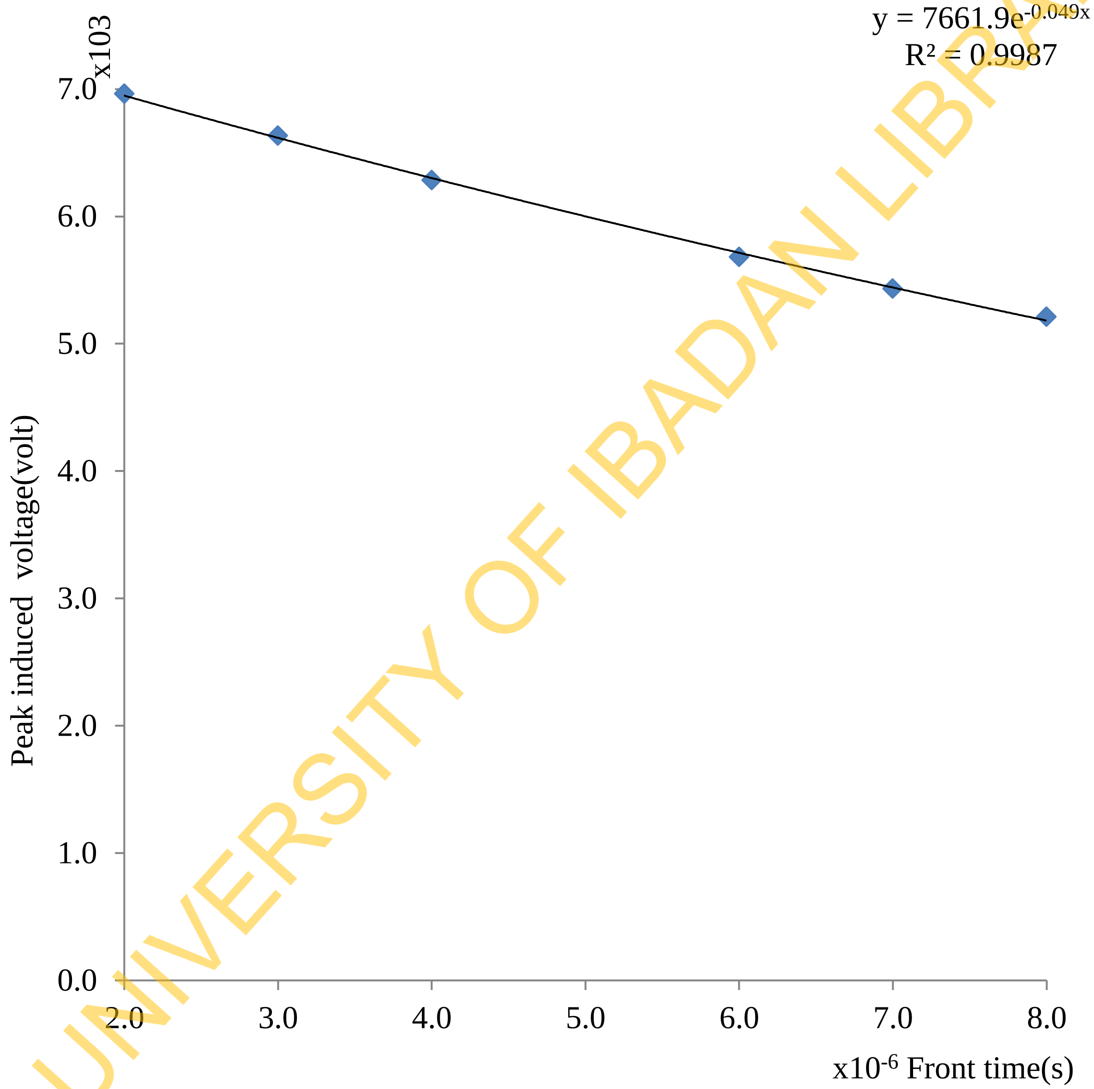

Fig.4.16: Variation of peak induced voltages with return stroke front time

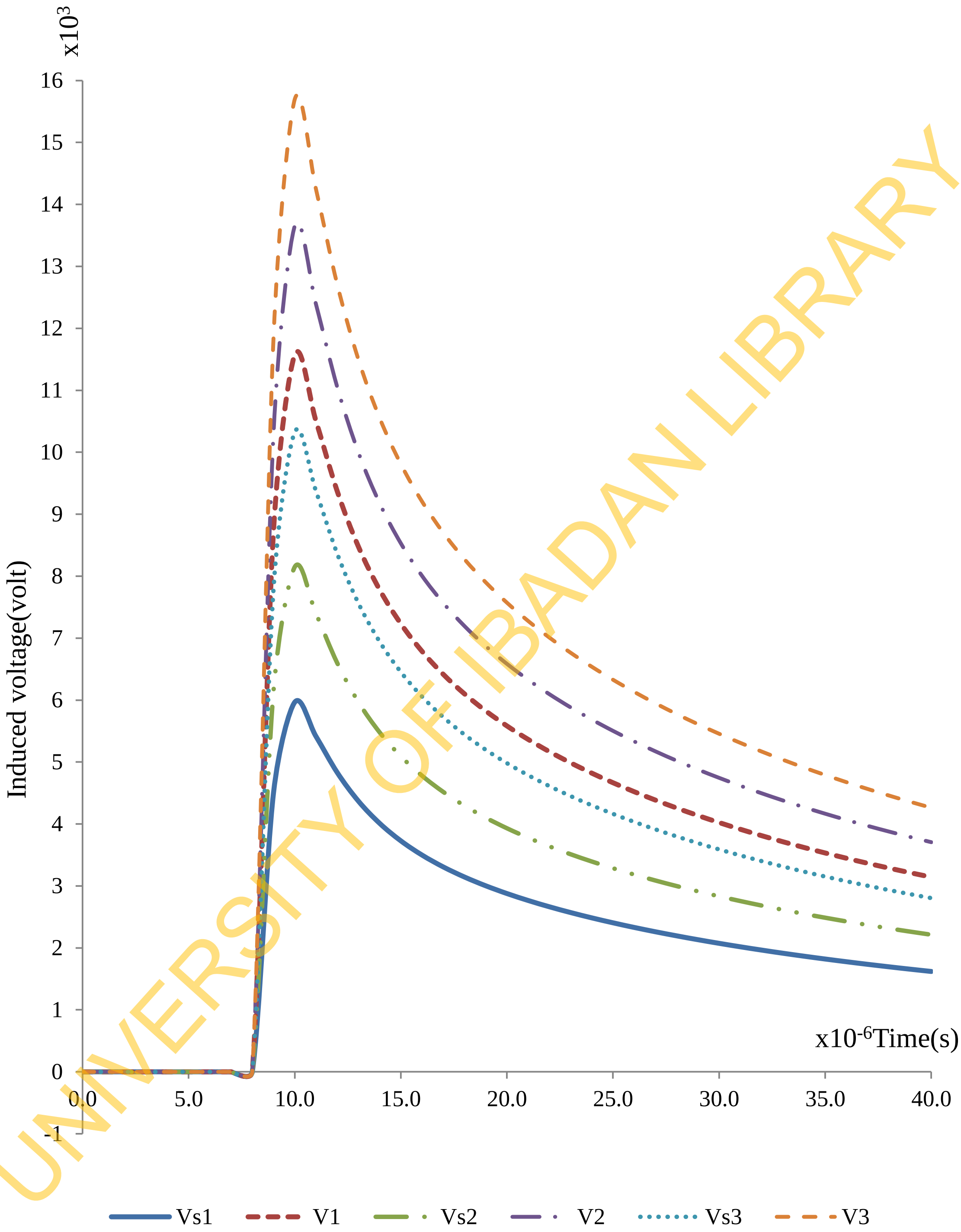

Fig.4.17: Comparing induced voltages for vertical configuration without earth wire with single conductor equivalent

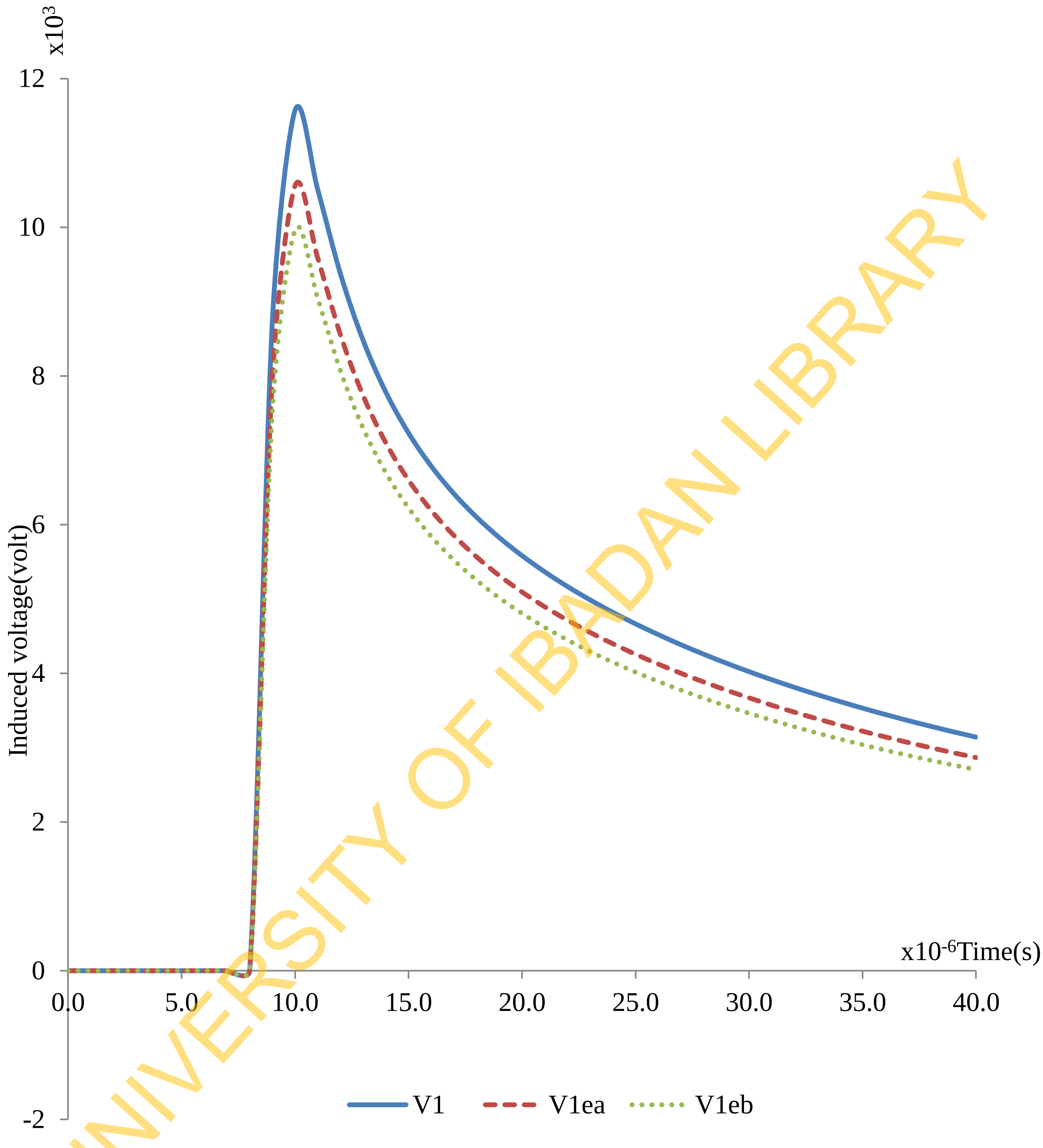

Fig.4.18: Induced voltage on lowest conductor for vertical configuration with and without earth wire (V1=without earth wire, V1ea= earth wire above, V1eb=earth wire below)

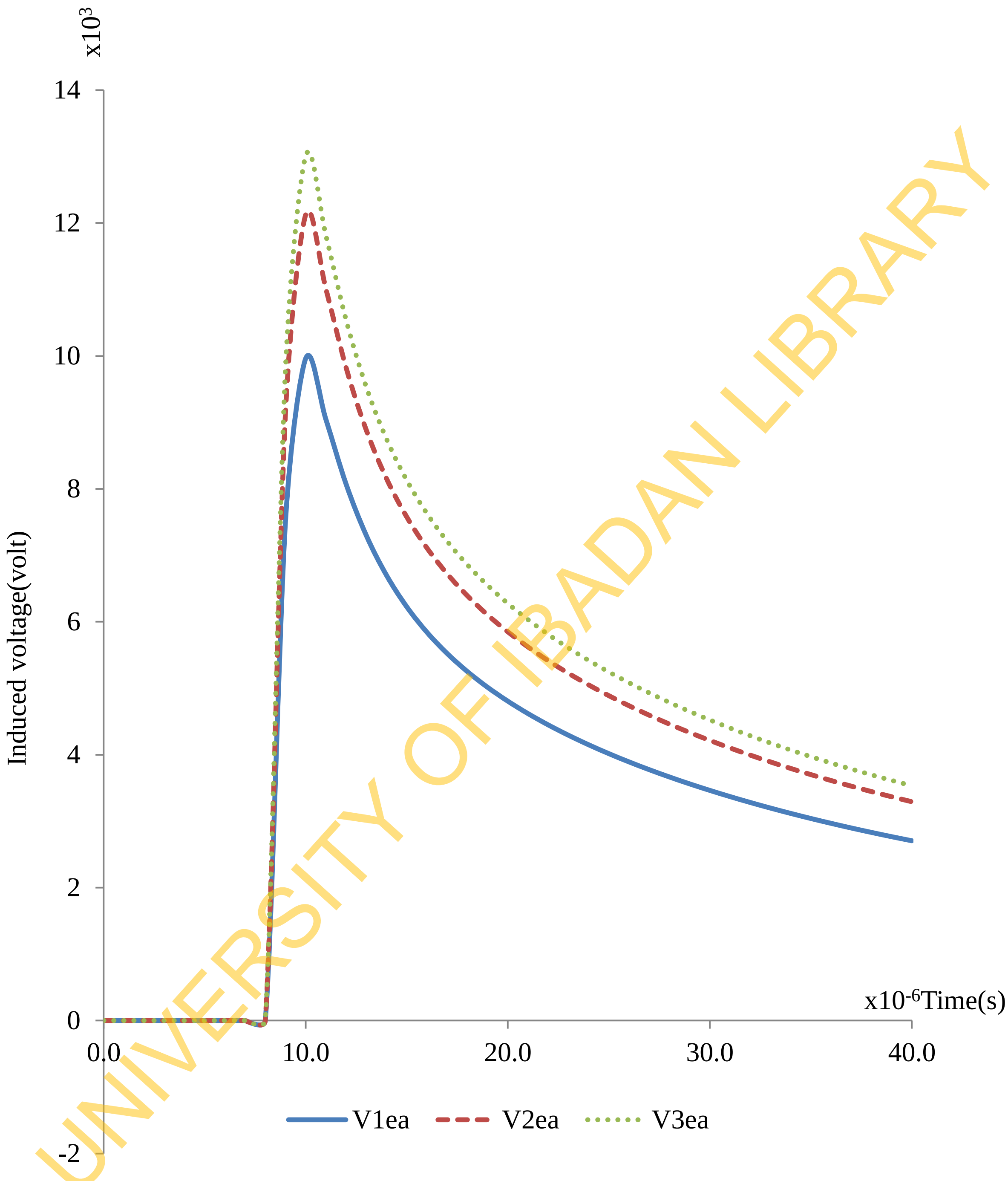

Fig.4.19: Induced voltage for vertical configuration with earth wires above conductors

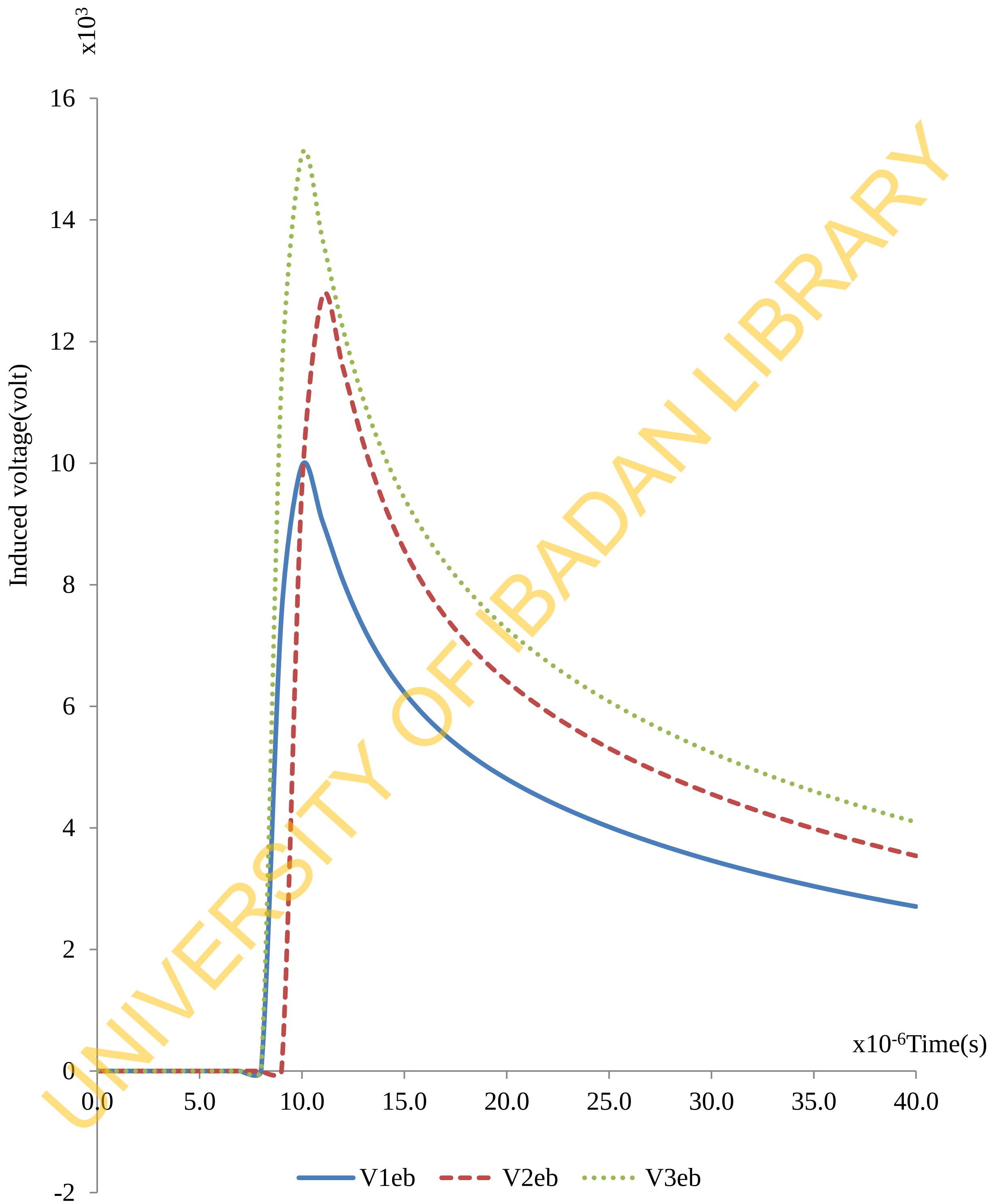

Fig.4.20: Induced voltage for vertical configuration with earth wire below conductors

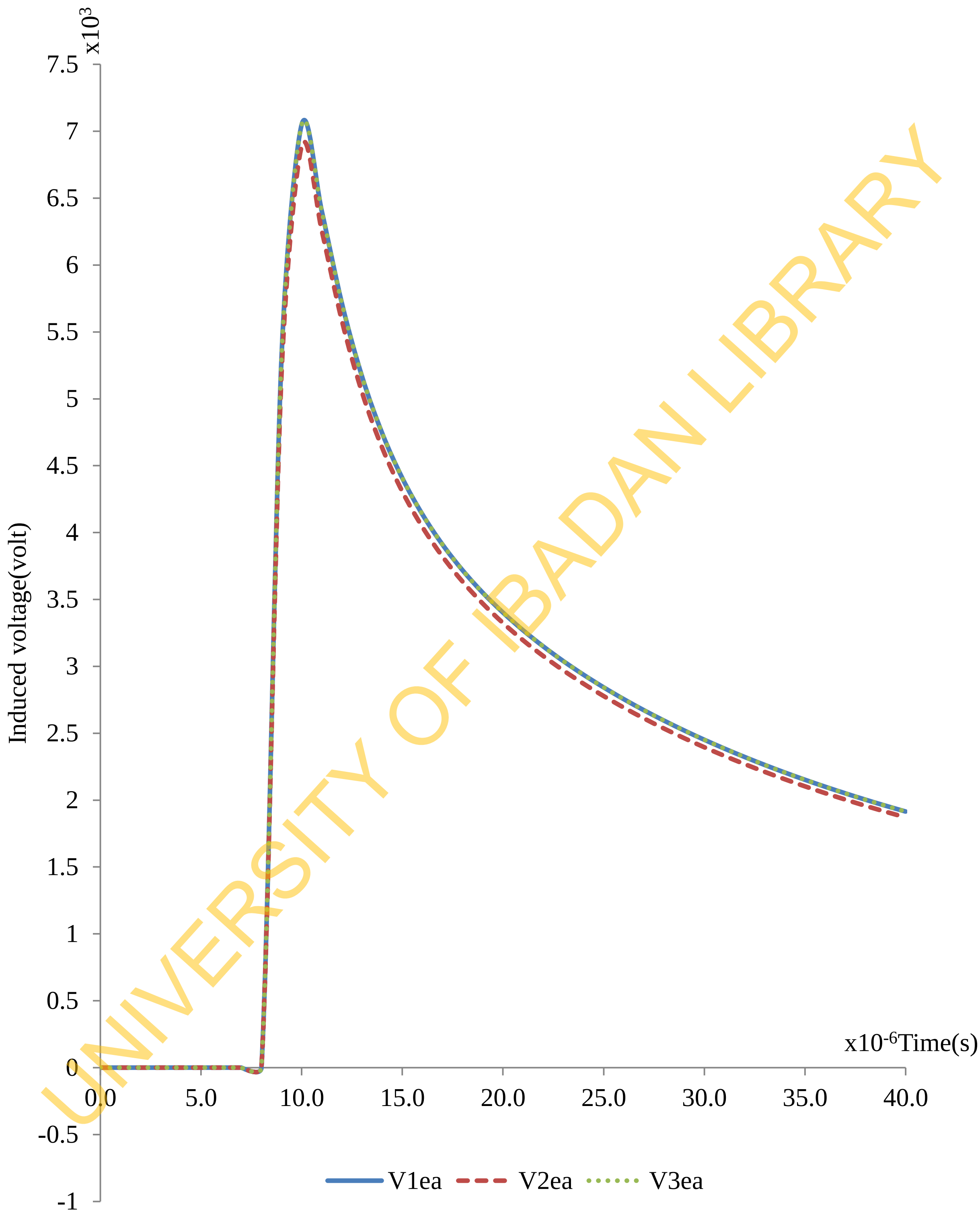

Fig.4.21: Induced voltage for horizontal configuration with earth wires above conductors

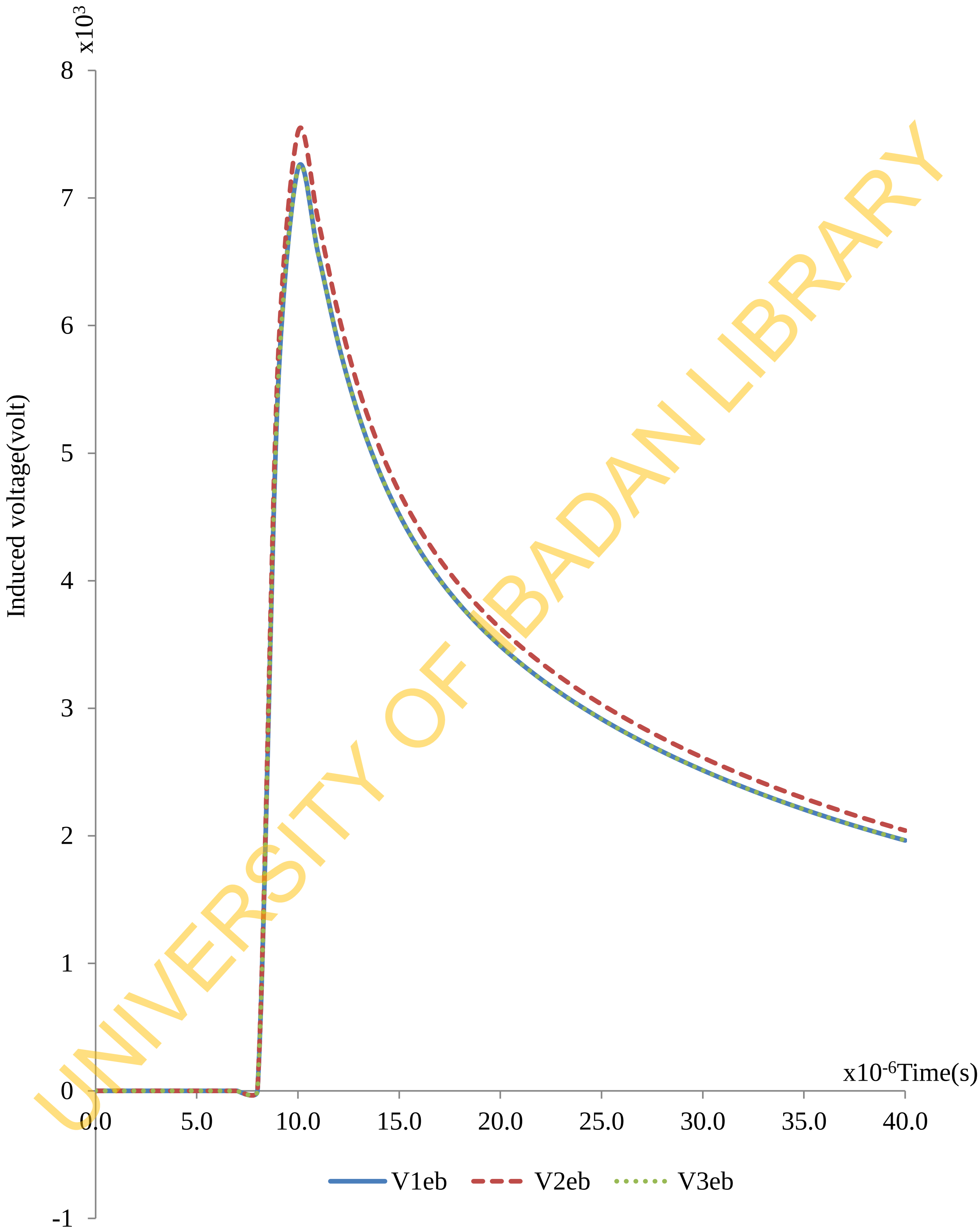

Fig.4.22: Induced voltage for horizontal configuration with earth wires below conductors

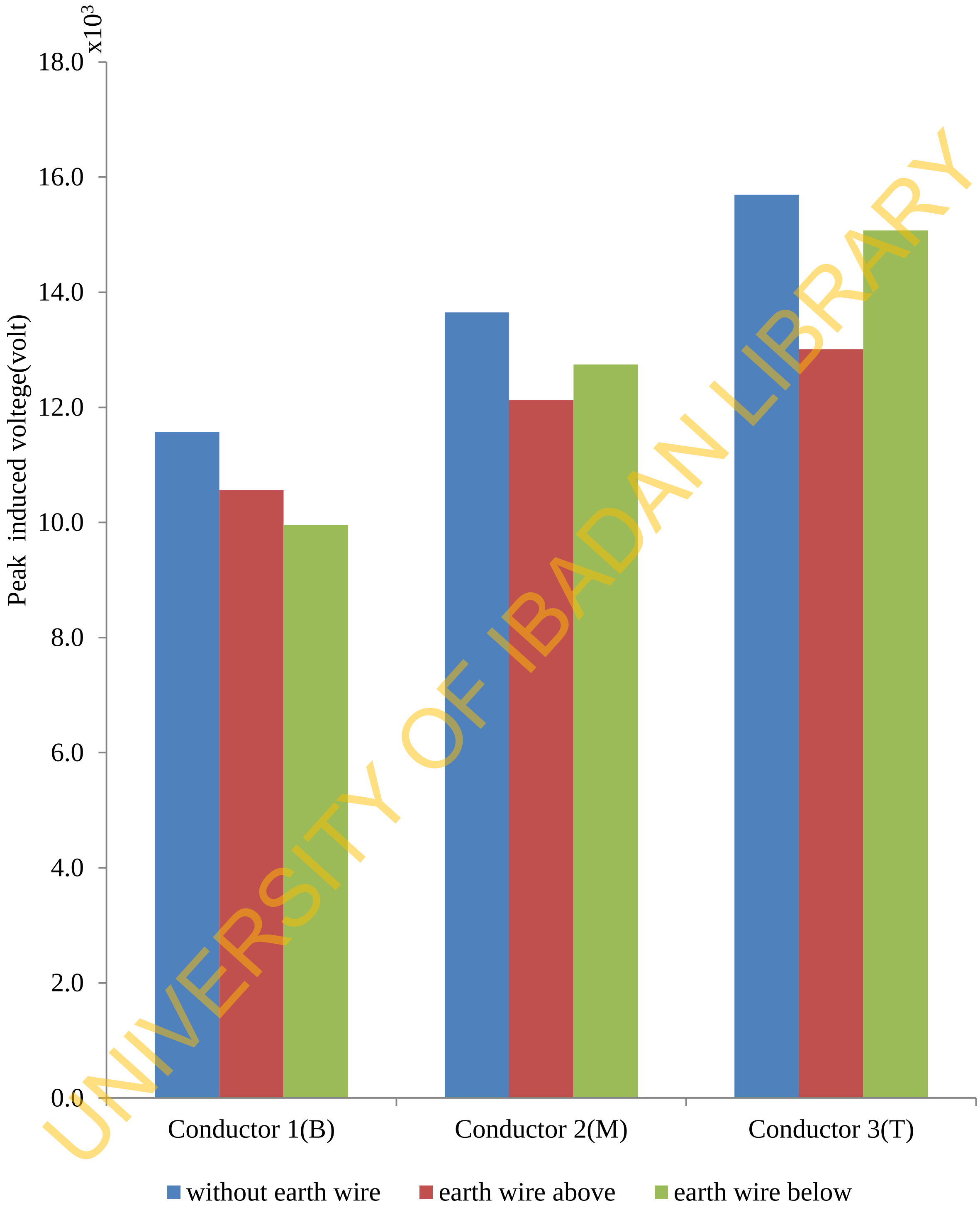

Fig. 4.23: Peak induced voltages for vertical configuration

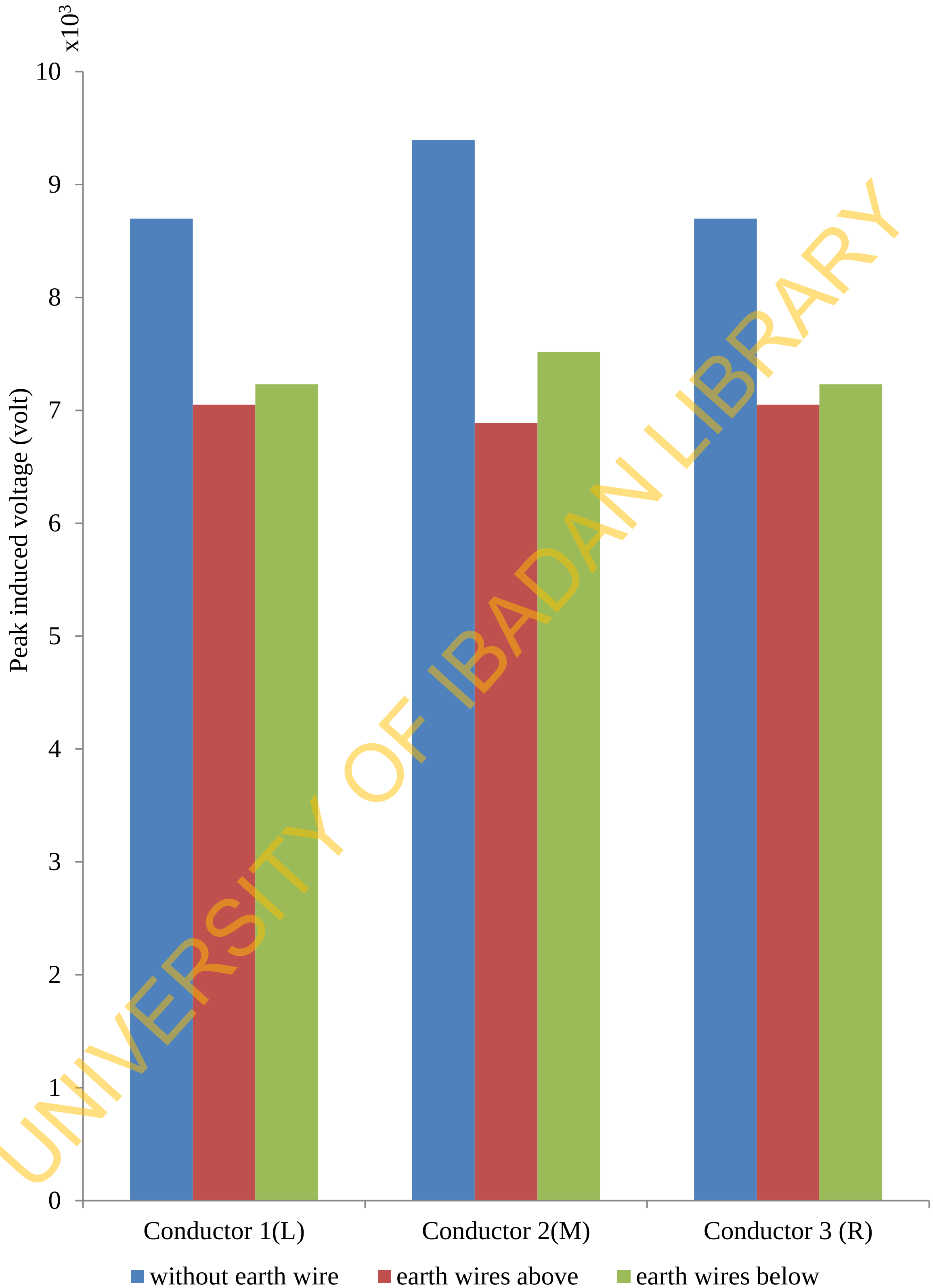

Fig. 4.24: Peak induced voltages for horizontal configuration

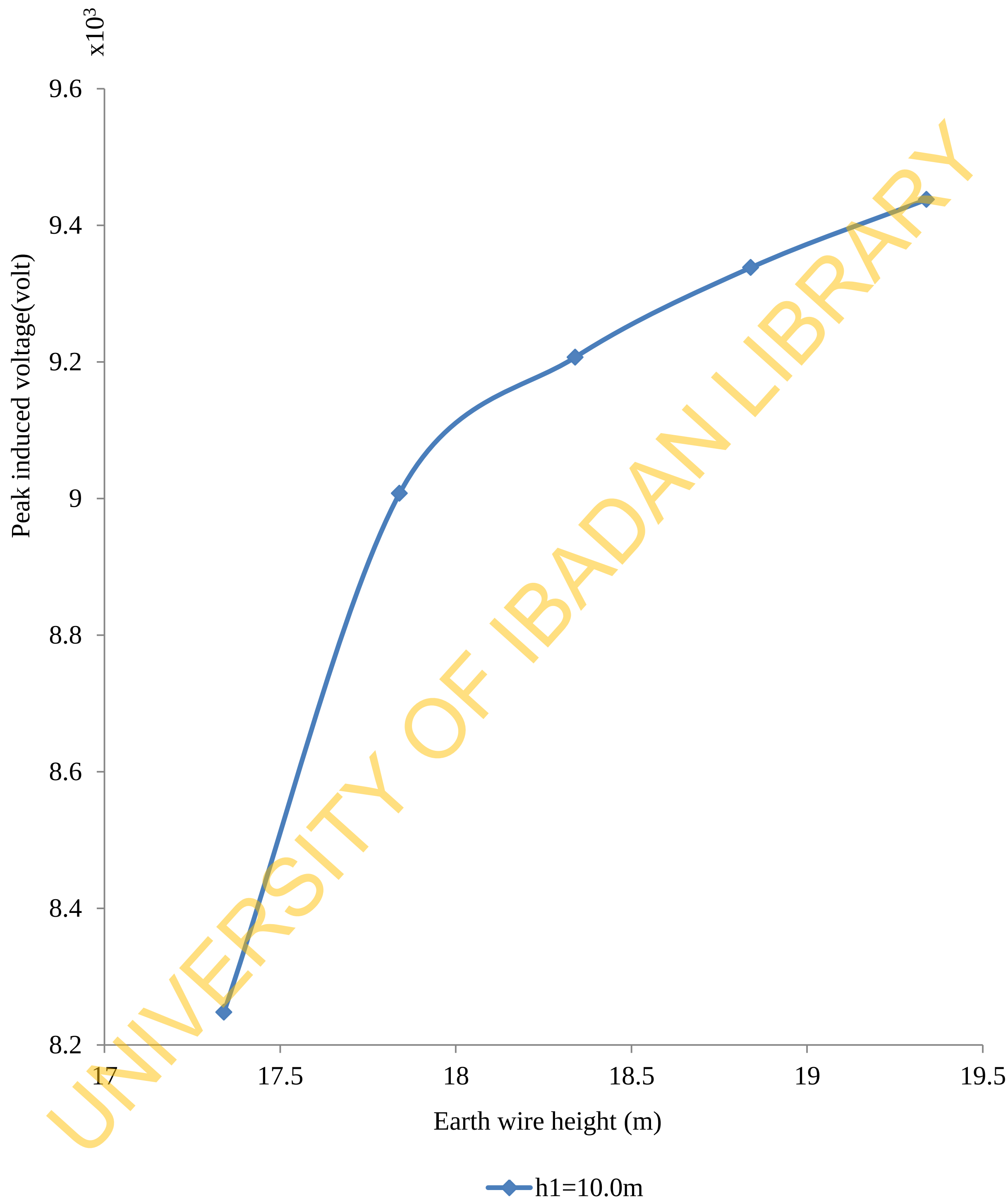

Fig.4.25 (a): Variation of peak induced voltage with earth wire height (conductor 1)

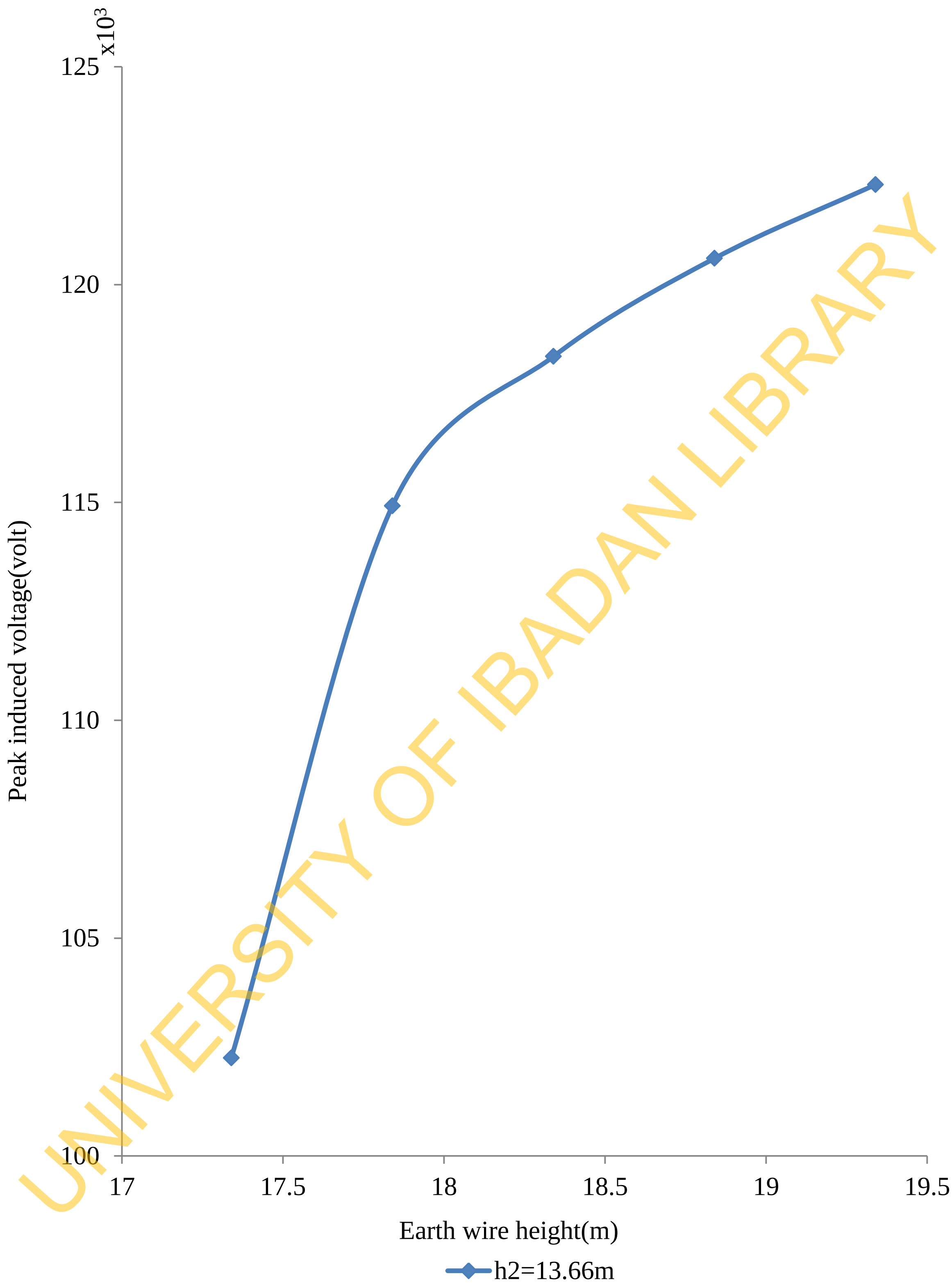

Fig.4.25 (b): Variation of peak induced voltage with earth wire height (conductor 2)

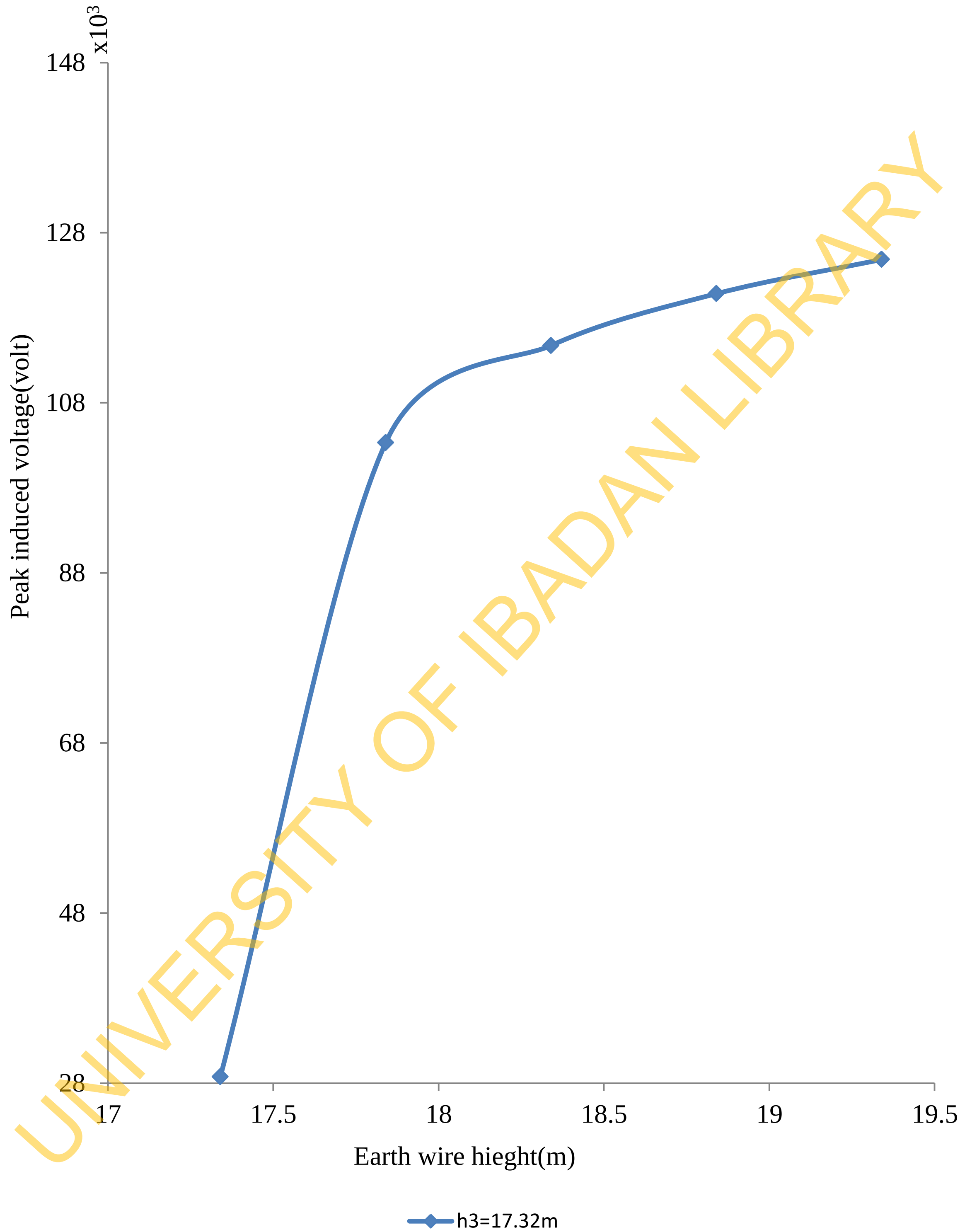

Figg.4.25 (c): Variation of peak induced voltage with earth wire height (conductor 3)

4.3 Influence of lightning parameters on lightning induced voltages

Table 4.2 showed the variation of the simulated values of lightning induced voltages (Volts), as a function of time, t (seconds) for various values of peak return stroke current, $I_{p,}$ keeping other lightning and line parameters constant. Fig. 4.11 revealed the profile of variation of induced voltage with time for various values of peak current, I_p. A linear relationship was established between the Peak Induced Voltage (PIV) and return stroke peak current, I_p ; as shown in Table 4.5 and Fig. 4.14. For instance, with I_p=50 x 10^3 A and 100 x 10^3 A, PIV were 30.0 x 10^3 V and 60.0 x 10^3 V respectively. Table 4.3 showed the variation of the simulated values of lightning induced voltages (Volts), as a function of time, t (microseconds) for various values of specific return stroke velocity ratio, β ,keeping other lightning and line parameters constant. Fig. 4.12 revealed the profile of variation of induced voltage with time for various values of specific return stroke velocity ratio, β. An exponential relationship whereby Peak Induced Voltage (PIV) decreased with increasing specific return stroke velocity ratio, β, was established as shown in Table 4.5 and Fig.4.15. For instance, with β=0.3 and 0.5, PIV were 6.0 x 10^3 V and 4.0 x 10^3 V respectively. The variation of the simulated values of lightning induced voltages (Volts), as a function of time, t (microseconds) for various values of front duration of return stroke current, t_f ,keeping other lightning and line parameters constant was shown in Table 4.4. Fig. 4.13 showed the profile of variation of induced voltage with time for various values of front duration of return stroke current, t_f. Likewise an exponential relationship whereby Peak Induced Voltage (PIV) decreased with increasing front duration of return stroke current, t_f, was established as shown in Table 4.5 and Fig. 4.16. For instance, with t_f=4.0 x 10^{-6} s and 7.0 x 10^{-6} s, PIV were 6.3 x 10^3 V and 5.4 x 10^3 V respectively.

4.4.1 Vertical configuration without shield wire

Table 4.6 showed the simulated values of induced voltages, at line height, h=10.0m, 13.66m and 17.31m ; with following lightning parameters kept constant at : β =0.3 , t_f =5.0 x 10^{-6} s , I_p=10 x 10^3 A as well as cloud height , h_c =3 x 10^3 m, y- coordinate of stroke from origin, y_0=100.0m and distance, x= 1x10^3 m along line. The single line equivalent values were also shown. Generally, the presence of other conductors increased the induced voltage of the conductor under consideration. The induced voltage on a single line equivalent of a multi conductor system is lesser in value. From Table 4.7 and Fig. 4.17 for example, in case of vertical configuration without earth wire, PIV for bottom, middle and topmost were 11.6 x 10^3 V, 13.7 x 10^3 V and 15.7 x 10^3 V respectively. While the corresponding values of single line equivalent were 6.0 x 10^3 V, 8.1 x 10^3 V and 10.3 x 10^3 V.

4.4.2 Vertical configuration with earth wire

The presence of other conductors in multiconductor system resulted in an increase in voltage amplitude of about 77% , 49% and 26% in case of vertical configuration with earth wire placed above topmost conductor ; for topmost ,middle and lowest conductors respectively compared with corresponding single line equivalent. This is in agreement with those reported by Chowdhuri(1969).

The presence of earth wire caused a reduction in the induced voltages on lines irrespective of the configuration. For vertical profile with earth wire above topmost conductor, PIV ranged from 10.0 x 10^3 V to 15.1 x 10^3 V with maximum reduction in PIV occurring on topmost conductor, with value 2.7 x 10^3 V. Figs.4.18 and 4.23 showed the comparison of induced voltage on bottom conductor without earth wire, with earth wire above and with earth wire below. The reduction in PIV was more prominent with earth wire below, having PIV value, 10.0 x 10^3 V than with earth wire above with PIV value, 10.6×10^3 V. Tab.4.7 revealed that the reduction in PIV value was more prominent in topmost conductor with earth wire above, having value 13.0×10^3 V than with earth wire below with PIV value, 15.0×10^3 V.The peak induced voltage reduced by a factor of about 10 to 27 % with the introduction of earthwires as shield wires. This is in line with results obtained by Rusck(as cited by Nucci & Rachidi, 1999) , Rachidi et al.(1997) and Yokoyama (1984).The lightning electric field induced current in all the overhead line conductors and earth wires ; which in turn produced magnetic field that coupled with all other conductors.This mutual coupling between conductors decreased the induced voltages. Table 4.9 revealed that the presence of other conductors increased the per-unit induced voltage (ratio of induced voltage on a line with others in place to that of single line equivalent of same height above ground level) of the conductor under consideration. The percentage increase ranged between 26 % and 94 % for vertical configuration. It was observed that there was appreciable reduction in the percentage of the per-umit induced voltage due to the introduction of earth wire on the system of conductors. In case of vertical configuration with earth wire above, the reduction was from 52% to 26% for the topmost conductor, from 68% to 49% for the middle conductor and from 94% to 77% for bottom conductor.

The variation of PIV on each conductor with height of earth wire followed the same trend as shown in Figs.4.25 (a) to (c) . The closer the earth wire is to the conductor, the lower the PIV; hence the better the shielding effect of the earth wire.

4.4.3 Horizontal configuration with and without earth wire

Table 4.7 showed the simulated values of induced voltages, at line height, $h_1= h_2= h_3=10.0$m , spacing between conductors 3.6m ;with following lightning parameters kept constant at : $\beta =0.3$, $t_f=5.0 \times 10^{-6}$ s , $I_p=10 \times 10^3$ A as well as cloud height , $h_c =3 \times 10^3$ m, y- coordinate of stroke from origin, y_0=100.0m and distance, x=1 x 10^3 m along line. Fig. 4.24 revealed that, for horizontal configuration without earth wires, PIV on middle conductor of the lines was 9.4 x 10^3 V, while the outer conductors each had 8.7 x 10^3 V. The result was closely related to the experimental value of 8.7 x 10^3 V obtained in De la Rossa (1985). In case of horizontal profile with two earth wires symmetrically placed from the center above, PIV ranged from 6.9 x 10^3 V to 7.5 x 10^3 V. The PIV on middle conductor of horizontal profile with earth wires above was 6.9 x 10^3 V, while the outer conductors each had 7.1 x 10^3 V. For horizontal profile with earth wire above, PIV ranged from 6.9 x 10^3 V to 7.5 x 10^3 V. As displayed in Fig.4.21 and Table 4.7, the PIV on middle conductor of horizontal profile with earth wires above was 6.9 x 10^3 V, while the outer conductors each had 7.1 x 10^3 V. Figs.4.22 and 4.24 showed that the PIV on middle conductor of horizontal profile with earth wires below was 7.5 x 10^3 V, while the outer conductors each had 7.3 x 10^3 V.

Thus the horizontal configuration with earth wires above , is preffered for maximum reduction experienced in PIV, compared to oter configurations considered. When the lines were energized, there was at least a 25% reduction in all the PIV`s. Table 4.9 showed that the per-unit induced voltage ranged between 16 % and 58 % for horizontal configuration. It was also observed that there was appreciable reduction in the percentage of the per-umit induced voltage due to the introduction of earth wires on the system of conductors. In case of horizontal configuration, the reduction was from 58% to 16% for the middle conductor; and from 46% to 18% for the outer conductors. The best option of the considered profiles is that of horizontal configuration with eatth wires above the conducting lines; with per-unit induced voltage of 1.16 for the conductor in the middle and 1.18 for the outer conductors.

4.5 Protective Ratio

The protective ratio (PR) , is the ratio of induced voltage on the conductor with the earth wires in place to induced voltage on the conductor without the earth wires . It was observed from Table 4.8 that in case of vertical configuration, the PR for the vertical configuration ranged between 0.861 and 0.96. The closer the conductor to earth wires the better its protection. Thus, the best protected conductor for vertical configuration with earth wire above was the topmost conductor, with PR value of 0.827. While in case of profile with earth wire below, the bottom wire was most protected with PR value of 0.861. The PR of each conductor for the horizontal configuration with earth wires placed above conductors was lowest among the cases considered, with values 0.811 for each of the outer conductors and 0.733 for the middle conductor. The PR of each of the outer conductors for the horizontal configuration with earth wires placed below conductors was with values 0.831 and 0.800 for the middle conductor.

In practice, it is not possible the earth wires at earth potentials at all points along their lengths as assumed in the calculation.

CHAPTER FIVE

CONCLUSION AND RECOMMENDATIONS

5.1 Conclusion

The proportion of outages arising from lightning induced voltages was considered on one hand. The study on the other hand considered a model of the interaction between lightning current and overhead multiconducting lines. The lightning induced voltages on infinitely long distribution lines with different configurations were calculated with the model.

Only 10% of the power outages recorded in Nigeria was induced by lightning. The magnitudes of the induced voltages were considerably higher on multiconductor lines than on a single-conductor line of the same height above ground. Earth wires acting as shield against lightning, reduce the magnitude of the induced voltages on overhead conductors. The reduction in case of horizontal configuration with two earth wires above conducting lines ranged between 19 to 27%. In case of vertical configuration with one earth wire above topmost conductor, reduction in induced voltage was 17% for conductor closest to earth wire. Apart from configuration, a construction that allows shorter height for the conductors experience higher reduction in induced voltages. Thus, horizontal configuration of overhead conductors is preferred to vertical configuration with its lowest conductor being at the same height above ground with that of horizontal arrangement.

It is observed that in Nigeria, only high tension transmission overhead power lines are protected from lightning by earth wires. Traditionally, the distribution lines do not have earth wire installed over them. Thus the distribution lines are more prone to lightning interaction, resulting in damage of circuits and gadgets; and sometimes line outages. We hereby recommend that overhead distribution conducting lines be protected from lightning by installing earth wires, that is, horizontal configuration with two earth wires is preferred.

Other sources apart from lightning accounted for the lion's shear of power problem of Power Holding Company of Nigeria (PHCN). While attempts need be made to improve lightning protection, probably by installing underground cables instead of overhead lines, or by installing lightning arresters on our lines; PHCN cannot overrule exploring some other areas such as replacement of old equipment and improvement of the quality of the management staff.

REFERENCES

Anderson, R. B., & Eriksson, A. J. (1980) . Lightning parameters for engineering applications. *Electra*, *69*, 65–102. In Parameters of Lightning Strokes: A Review Lightning and Insulator Subcommittee of the T&D Committee. *IEEE Transactions On Power Delivery, 20, 1, 2005*

Andersson, G., Donalek, P., Farmer, R., Hatziargyriou, N., Kamwa, I., Kundur, P., …. Vittal, V. (2005). Causes of the 2003 major grid blackout in North America and Europe, and recommended means to improve system dynamic performance.*IEEE transactions over power systems* 20(4).1922-1928.

Ajayi, N.O. (1970). *Acoustics of thunder*. PhD. thesis in Physics department of University of Ibadan, Nigeria.

Berger, K., Anderson, R. B. & Kroninger, H. (1975) . Parameters of lightning flashes. *Electra*, 41, 23–37, 1975. In Parameters of Lightning Strokes: A Review Lightning and Insulator Subcommittee of the T&D Committee *IEEE Transactions On Power Delivery, 20, 1, 2005*

Braunstein, A. (1970). Lightning strokes to power transmission lines and the shielding effects of ground wires. *IEEE Trans.* ***PAS-89***,1900-1910

Brown, G.W. and Whitehead, E. R. (1969). Field and analytical studies of transmission line shielding. *IEEE Trans.* ***PAS-88****, 617-626.*

Brook, M., Kitagawa, N., Workman, E.J., (1962) “Quantitative study of strokes and continuing currents lightning discharges to ground”, sJ. Geophys. Res. 67 , 649–659.

Bruce, C. E.R., & Golde, R.H. (1941).The lightning discharge. *J. IEE. London* **88 (pt *2)*** 487-524 . In Uman, M.A. and McLain, D.K. (1969). Magnetic field of lightning return stroke. *J. Geophys. Res.* **74, 28**, 6899-6910.

Chowdhuri, P. (1996). *Electromagnetic transients in power systems* .Research Studies Press Ltd.

Chowdhuri, P., Li, *S.*, & Yan, P. (2002). Rigorous analysis of back-flashover outages caused by direct lightning strokes to overhead power lines. *IEE Proc.-Gen. Transm. Distrib. 149,1, 58-68*

Chowdhuri, P., & Gross, E.T.B. (1967). Voltage surges induced on overhead lines by lightning strokes. *Proc. of Instn. Elect. Engrs.* ***114,***1899-1967.

Chowdhuri, P., & Gross, E.T.B. (1969). Voltages induced on overhead multiconductor lines by lightning strokes. *PROC. IEE, 116, . 4, 561-565.*

Dennis, A.S. & Pierce, E.T. (1964): *Radio Science* ***68 D,*** *777*

Deindorfer, G. & Uman, M. A., (1990), An improved return stroke model with specified channel base current, *J.Geophys. Res., 95*, 13,621-13,644.

De la Rossa, F . (1985). Inducing effect of lightning on an experimental power distribution line in Mexico. ISSN 0349-8352 Uppsala.

Driscoll, K. T., Christian, H. J., Blakeslee, R. J., Boccippio, D. J., Boeck, W. L., Buechler, D. E., ….. Stewart, M. F.(2003) : Global frequency and distribution of lightning as observed from space by the Optical Transient Detector, *J. Geophys. Res.,* 108(D1), 4005, doi:10.1029/2002JD002347.

Eriksson, A. J.(1987) .The incidence of lighting strikes to power lines. *IEEE Trans. on Power Delivery* , PWRD- 2(2), 859–870.

Eriksson, A.J. & Meal, D.V. (1982) . Lightning Performance and overvoltage surge studies on a rural distribution line. *IEE Proc.* ***129, Pt C*** *, 2.*

Electric Power Research Institute –EPRI (1997). Performance Evaluation of the National Lightning Detection Network in the Vicinity of Albany, New York, Palo Alto, CA, Rep. TR-109 544.

Golde, R.H.(1954). Lightning surges on overhead distribution lines caused by indirect and direct lightning strokes. *Trans. Am. 1st elect.Engrs.**73 Pt.III**,437-447.*

Golde, R.H.(1973) .*Lightning protection* .Edward Arnold.

Golde,R.H . (1977a). *Lightning Vol.1*. New York.Academic Press.

Golde,R.H . (1977b). *Lightning Vol.2*. New York.Academic Press.

Gomes, C. & Cooray, V. (2000). Concepts of Lightning Return Stroke Models. IEEE *Trans. on EMC, 42, 1, 82-96.*

Heidler, F., (1985). Traveling current source model for LEMP calculation. 6th International Symposium on Electromagnetic Compatibility, Swiss Fed. Inst. of Technol., Zurich, Switzerland. In Schoene, J., Uman, M.A., Rakov, V.A., Rambo, K.J. , Jerauld, J. and Schnetzer , G.H. (2003) .Test of the transmission line model and the traveling current source model with triggered lightning return strokes at very close range *Journal Of Geophysical Research, 108, D23, 4737, Doi: 10.1029/2003jd003683.*

IEEE Standard 493-1990, (1990). IEEE Reccommended Practice for Design of Reliable Industrial and Commercial Power System, 54, 75,204.

Izraeli, I. & Brasuntein, A. (1983).Analysis and design of protection systems for structures against direct lightning strokes. Part 1 :Theory. *IEE Proc.**130 Pt.A,3,***140-144.

Krider, E. P., Leteinturier, C. and Willett, J.C. (1996). Submicrosecond fields radiated during the onset of first return strokes in cloud-to-ground lightning, *J. Geophys. Res., 101, 1589–1597*. In Schoene, J., Uman, M.A., Rakov, V.A., Rambo, K.J. , Jerauld, J. and Schnetzer, G.H. (2003). Test of the transmission line model and the traveling current source model with triggered lightning return strokes at very close range *Journal Of Geophysical Research. 108, D23, 4737, Doi: 03jd003683.*

Lin, Y.T. , Uman, M.A. ,Titler, J.A. , Brantley, R.D. , Beasley, W.H. , Krider, E.P. and Wiedein, C.D. (1979): Characterization of lightning return stroke electric and magnetic fields from simultaneously two-station measurement. *J. Geophys. Res.* 8**4,** 6307-6314.

Lin, Y.T, Uman, M.A. and Standler, R.B.(1980): Lightning Return Strokes Models. *J. Geophys. Res.* **85, C3,** 1571-1583.

Matsubara,I. and Sekioka,S. (2009). Analytical Formulas for Induced Surges on a Long Overhead Line Caused by Lightning With an Arbitrary Channel Inclination. *IEEE transactions on electromagnetic compatibility, 51, 3.*

National Electric Power Authority (NEPA) 2002 Annual Report and Accounts.

Norinder, H. & Dahle ,O. (1945) . Measurements by frame aerials of current variations in lightning discharge .*Ark. Mat. Astron. Fys.32 A* 1-70 .In Uman,M. A. and Mc Lain, D..K. (1970). Lightning Return Stroke Current from Magnetic and Radiation Field Measurements. *J. Geophys. Res.* ***75, 27***, 5143-5147.

Nucci, C.A., Mazzetti, C., Rachidi, F., & Ianoz, M. (1988). On lightning return stroke models for LEMP calculations. *Proc. of the 19th International Conference on Lightning protection, Graz.*In Paopone, M.(2001) . Modeling Of Lightning-Induced Voltages On

Distribution Networks For The Solution Of Power Quality Problems, And Relevant Implementation In A Transient Program. PhD Thesis in Department of Electrical Engineering, University of Bologna.

Nucci, C.A. and Rachidi F.(1989). Experimental validation of a modification to the Transmission Line model for LEMP calculations, Proc. of the 8th International Symposium and Technical Exhibition on Electromagnetic Compatibilty,389- 394, Zurich.

Nucci, C.A. and Rachidi F.(1999). Lightning-Induced Overvoltages. IEEE *Transmission and Distribution Conference, Panel Session.*Distribution Lightning Protection.

Nucci, C.A., Diendorfer G., Uman M.A., Rachidi F., & Mazzetti, C.(1990). Lightning return-stroke models with channel-base specified current: a review and comparison., *Journal of Geophysical Research*, ***95**, **D12**, 20395-20408.*

Nucci, C.A., Rachidi F., Ianoz M., & Mazzetti, C.(1993). Lightning-induced overvoltages on overhead lines. *IEEE Trans. on EMC, Vol.* ***35****, No. 1, 75-86.*

Oladiran, E.O., Aina, J. I. & Israelsson, S. (1988). Lightning Flash-rate Characteristics of the Tropical thunder Cloud . *Proceedings of 8th International Conference of Atmospheric Electricity*.757-765.

Oladiran,E.O. , Pisler, E. , & Israelsson, S. (1998). New lightning flash counter and calibration circuit with improved discrimination of cloud and ground discharges. *IEE Proceedings* . *135 Pt. A* 1 , 22-28.

Rachidi, F., & Nucci. C. A.,(1990). On the Master, Uman, Lin, Standler and the modified transmission line return stroke current models, *J. Geophys. Res., 95*,20389 – 20393, Rachidi, F., Nucci. C. A.,Ianoz, M. & Mazzetti, C. (1997). Response of multiconductor power lines to nearby to lightning return stroke electromagnetic fields. *IEEE Trans. On Power Delivery , 12, 1404-1411* .

Rachidi, F., Rakov, V.A. , Nucci,C.A. & Bermudez, J. L. (2002). The effect of vertically extended strike object on the distribution of current along the lightning channel, *J. Geophys. Res., 107(D23), 4699, doi:10.1029/ 2002JD002119.*

Rakov, V.A. (1997). Lightning electromagnetic fields: Modeling and measurements, in *Proc. 12th Int. Zurich Symp. Electromagn. Compat.*, . 59–64.

Rakov, V. A, and Uman, M.A. (1998). Review and Evaluation of Lightning Return Stroke Models Including Some Aspects of Their Application. *IEEE Transactions On Electromagnetic Compatibility, 40,. 4, 403– 426.*

Raul, Montano (2006). The effect of lightning on low voltage power networks *Dissertation* Acta Universitatis Upsaliensis Uppsala.

Rusck , S. (1958). Induced over-voltages on power-transmission lines with special reference to the over-voltage protection of low-voltage networks. *Trans. SRoyal Inst. Tech.*, Stockholm, Sweden, 120, 1–118.

Schoene, J., Uman, M. A., Rakov, V. A., Rambo, K. J., Jerauld, J. , & Schnetzer, G. H. (2003).Test of the transmission line model and the traveling current source model with triggered lightning return strokes at very close range *Journal Of Geophysical Research, 108, D23, 4737, doi:10.1029/2003JD003683.*

Simpson, G. **C.** and Robinson, G. D. (1941).The distribution of electricity in the thunderclouds, Part 11 . ***Pmc. R. Soc.,*** vol. A177, p. 281 . In Umaan, M.A. (1994). Natural lightning *IEEE Transactions On Industry Applications, 30, 3 ,785-790.*

Simpson, G. **S.** and Scrase , F. J. (1937). The distribution of electricity in Thunderclouds. ***Proc. R. Soc.,*** A161, 309 . In Montano ,Raul (2005). The effect of lightning on low voltage power networks . PhD. Thesis of Upsala University .

Summerfield,A.(1952): *Lectures in Theoretical Physics Vol.III (Electrodynamics)*. New York. Academic Press.

Thottappillil, R., Rakov, V.A. & Uman, M.A. (1997). Distribution of charge along the lightning channel: Relation to remote electric and magnetic fields and to return-stroke models. *J. Geophys. Res.*, 102, D6, 6987–7006.

Thottappillil R. and Uman M.A.(1993). Comparison of lightning return-stroke models, *Journal of Geophysical Research, 93, 98, 22,903-22,914.*

Thurman, B.N., & Edgar, B.C. (1982). Global lightning distribution of damn and dusk. . *J. Geophys. Res.* 87, C2, 1191-1206.

Uman, M.A. (1969). *Lightning* . New York : McGraw-Hill.

Uman, M.A., & McLain, D.K (1969). Magnetic field of lightning return stroke. *J. Geophys. Res.* **74, 28**, 6899-6910.

Uman, M.A., & McLain, D.K. (1970 a). Radiation field and current of the lightning stepped leader. *J. Geophys. Res.* **75, 6,** 1058-1066.

Uman ,M.A. and McLain, D.K (1970 b). Lightning Return Stroke Current from Magnetic and Radiation Field Measurements. *J. Geophys. Res.* **75, 27**, 5143-5147.

Uman, M.A. (1987). *Lightning Discharge*. San Diego, Califonia: Academic Press.

Uman, M.A. (1994). Natural Lightning. *IEEE Transactions on Industry Applications, 30, 3, 785-790.*

Volland, H. (1981). A wave guide mode of lighting currents *.Jour. of Atmp. and Terr.Phys*.**43,3,**191-204.

Weidman, C. D., and Krider, E.P. (1980). Submicrosecond risetimes in lightning return-stroke fields, Geophys. Res. Lett., 7, 955–958 . In Schoene, J. & Uman M.A.(1987) . *The lightning discharge*. Orlando Florida: Academic Press.

Wood, T.G. (2004). Geo-location of individual lightning discharges using impulsive vlf electromagnetic waveforms. A dissertation for the degree of doctor of philosophy

Yokoyama, S.(1984). Calculation of lightning-induced voltages on overhead multiconductor systems. *IEEE Transactions on Power Apparatus and Systems, PAS-103, 1,* 100-108.

Appendix I

MAPLE 13 program for solving induced voltage ,v(x,t)

```
> restart :
> with(plots) :
> with(inttrans) :
> q(t) := 0 :
> f(x) := 0 :
> f(v) := subs(x = u, f(x)) :
> g(x) := 0 :
> g(v) := subs(x = u, g(x)) :
>
```

$$LC := L_{11}\cdot C_{11} + L_{12}\cdot C_{22} + L_{13}\cdot C_{33} \ : c := 3\cdot 10^{8} \ : \beta := 0.5 \ : y_0 := 1000 : x_0 := 1000 : \ i_0 := 5000 : h_p := 10 : h_c := 5000 : L_{11} := 1.540\cdot 10^{-6} :$$

$$L_{12} := 0.343\cdot 10^{-6} \ : L_{13} := \ 0.214\cdot 10^{-6} : C_{11} := 7.7\cdot 10^{-12} \ : \ C_{22} := 7.94\cdot 10^{-12} \ : \ C_{33} := 7.7 \cdot 10^{-12} \ :$$

$$> t_0 := \frac{\left(\left(x - x_0\right)^2 + y_0^2\right)^{0.5}}{c} :$$

```
> if t = t0 then a := 0 else a := 1 end if :
>
```

$$> r := \left(\left(x - x_0\right)^2 + y_0^2\right)^{0.5} \ :$$

$$> \operatorname{psi}(x, t) := -\left(\frac{\left(60\cdot i_0\cdot h_p\right)}{\beta}\right) \cdot \left(\frac{\left(1 - \beta^2\right)}{\left(\beta^2\cdot \ c^2\cdot t^2 + \left(1 - \beta^2\right)\cdot r^2\right)^{0.5}} - \frac{1}{\left(h_c^2 + r^2\right)^{0.5}}\right);$$

$$\psi(x,t) := -\frac{4.50000000010^{6}}{\left(2.25000000010^{16}\,t^2 + 0.75\left((x-1000)^2 + 1000000\right)^{1.0}\right)^{0.5}} + \frac{6.00000000010^{6}}{\left(25000000 + \left((x-1000)^2 + 1000000\right)^{1.0}\right)^{0.5}}$$

```
> h(x, t) := LC·diff((psi(x, t)·a), t, t);
```

$$h := (x,t) \rightarrow LC\left(\frac{\partial^2}{\partial t^2}\left(\psi(x,t)\,a\right)\right)$$

```
> diff(v(x, t), t, t) = c^2·diff(v(x, t), x, x) + h(x,
    t);
```

$$\frac{\partial^2}{\partial t^2} v(x,t) = 90000000000000000\left(\frac{\partial^2}{\partial x^2} v(x,t)\right) - \left(1.10916575410^{23}\,t^2\right) \Big/ \left(2.25000000010^{16}\,t^2 + 0.75\left((x-10 + 1000000\right)^{1.0}\right)^{2.5} + \left(1.64320852510^{6}\right) \Big/ \left(2.25000000010^{16}\,t^2 + 0.75\left((x-1000) + 1000000\right)^{1.0}\right)^{1.5}$$

Laplace transform of the induced voltage equation

```
> diff(V(x, s), x, x) − s^2/c^2*V(x, s) =−s*f(x)
    /c^2 − g(x)/c^2 − H(x, s)/c^2;
```

$$\frac{\partial^2}{\partial x^2} V(x,s) - \frac{1}{90000000000000000} s^2\,V(x,s) = -\frac{1}{90000000000000000} H(x,s)$$

Transformed boun dary condition

```
> Q(s) := Int(q(t)*exp(−s*t), t = 0 ..infinity);
```

$$Q(s) := \int_0^{\infty} 0\,\mathrm{d}t$$

```
> Q(s) := value(%);
```

$$Q(s) := 0$$

Transformed source term

```
> H(x, s) := Int(h(x, t)*exp(-s*t), t = 0
    ..infinity);
```

$$H(x,s) := \int_0^{\infty} \Bigg(-\frac{1.10916575410^{23}\, t^2}{\left(2.25000000010^{16}\, t^2 + 0.75\left((x-1000)^2 + 1000000\right)^{1.0}\right)^{2.5}} + \left(1.64320852510^{6}\right) \Big/ \left(2.25000000010^{16}\, t^2 + 0.75\left((x-1000)^2 + 1000000\right)^{1.0}\right)^{1.5} \Bigg)\, e^{-s\,t}\, dt$$

```
> H(x, s) := laplace(h(x, t), t, s);
```

$$H(x,s) := 7.64783974710^{-19}\, s^{2.}\, \Big(1.\,\mathrm{BesselY}\big(0.,\, 3.33333333310^{-9}\, s^{1.}\, (3.\,x^{2.} - 6000.\,x + 6.00000010^{6})^{0.5000000000}\big) - 1.\,\mathrm{StruveH}\big(0.,\, 3.33333333310^{-9}\, s^{1.}\, (3.\,x^{2.} - 6000.\,x + 6.00000010^{6})^{0.5000000000}\big)\Big)^{1.} + \Big(2.46913580210^{-20}\, \big(5.91555068810^{9} - 3.141592654\mathrm{StruveH}(\ldots + 6.00000010^{6})^{0.5000000000}\big)^{1.} - 3.141592654\mathrm{BesselY}\big(1.,\, 3.33333333310^{-9}\, s^{1.}\, (3.\,x^{2.} - 6000.\,x + 6.00000010^{6})^{0.5000000000}\big)^{1.}\big)^{1.}\, s^{1.}\Big) \Big/ \left(3.\,x^{2.} - 6000.\,x + 6.00000010^{6}\right)^{0.5000000000}$$

```
> H(u, s) := subs(x = u, H(x, s));
```

$$H(u,s) := 7.64783974710^{-19}\, s^{2.}\, \Big(1.\, \mathrm{BesselY}\Big(0., 3.33333333310^{-9}\, s^{1.}\, \big(3.\, u^{2.} - 6000.\, u + 6.00000010^{6}\big)^{0.5000000000}\Big) - 1.\, \mathrm{StruveH}\Big(0., 3.33333333310^{-9}\, s^{1.}\, \big(3.\, u^{2.} - 6000.\, u + 6.00000010^{6}\big)^{0.5000000000}\Big)\Big)^{1.} + \Big(2.46913580210^{-20}\, \big(5.91555068810^{9} - 3.141592654\mathrm{StruveH}\big(+ 6.00000010^{6}\big)^{0.5000000000}\big)^{1.} - 3.141592654\mathrm{BesselY}\Big(1., 3.33333333310^{-9}\, s^{1.}\, \big(3.\, u^{2.} - 6000.\, u + 6.00000010^{6}\big)^{0.5000000000}\big)^{1.}\Big)^{1.}\, s^{1.}\Big) \Big/ \big(3.\, u^{2.} - 6000.\, u + 6.00000010^{6}\big)^{0.5000000000}$$

```
> H(u, s) := value(%);
```

$$H(u,s) := 7.64783974710^{-19}\, s^{2.}\, \Big(1.\, \mathrm{BesselY}\Big(0., 3.33333333310^{-9}\, s^{1.}\, \big(3.\, u^{2.} - 6000.\, u + 6.00000010^{6}\big)^{0.5000000000}\Big) - 1.\, \mathrm{StruveH}\Big(0., 3.33333333310^{-9}\, s^{1.}\, \big(3.\, u^{2.} - 6000.\, u + 6.00000010^{6}\big)^{0.5000000000}\Big)\Big)^{1.} + \Big(2.46913580210^{-20}\, \big(5.91555068810^{9} - 3.141592654\mathrm{StruveH}\big(+ 6.00000010^{6}\big)^{0.5000000000}\big)^{1.} - 3.141592654\mathrm{BesselY}\Big(1., 3.33333333310^{-9}\, s^{1.}\, \big(3.\, u^{2.} - 6000.\, u + 6.00000010^{6}\big)^{0.5000000000}\big)^{1.}\Big)^{1.}\, s^{1.}\Big) \Big/ \big(3.\, u^{2.} - 6000.\, u + 6.00000010^{6}\big)^{0.5000000000}$$

Basis vectors

```
> assume(x > 0) ; phi[1](x, s) := exp(-s / c * x);
    phi[1](u, s) := subs(x = u, phi[1](x, s)) :
    phi[2](x, s) := exp(s / c * x); phi[2](u, s)
    := subs(x = u, phi[2](x, s)) :
```

$$\phi_1(x\sim, s) := \mathrm{e}^{-\frac{1}{300000000}\, s\, x\sim}$$

$$\phi_2(x\sim, s) := e^{\frac{1}{300000000} s\, x\sim}$$

Evaluation of theWronskian

```
> W(phi[1](u, s), phi[2](u, s))
    := simplify(phi[1](u, s) * diff(phi[2](v, s),
    u)-phi[2](u, s) *
  diff(phi[1](u, s), u));
```

$$W\left(e^{-\frac{1}{300000000} s\, u}, e^{\frac{1}{300000000} s\, u}\right) := \frac{1}{300000000} s$$

Evaluation of the Green's function

```
> G(x, u, s) := (phi[1](u, s) * phi[2](x, s)
    + phi[1](x, s) * phi[2](u, s)) / W(phi[1](u,
    s), phi[2](u, s));
```

$$G(x\sim, u, s) := \frac{1}{s}\left(300000000\left(e^{-\frac{1}{300000000} s\, u}\, e^{\frac{1}{300000000} s\, x\sim} + e^{-\frac{1}{300000000} s\, x\sim}\, e^{\frac{1}{300000000} s\, u}\right)\right)$$

Particular solution

```
> V[p](x, s) :=-Int(G(x, u, s) * (s * f(u) + g(u)
    + H(u, s)) / c^2, u);
```

$$V_p(x\sim, s) := -\left(\int \frac{1}{300000000}\,\frac{1}{s}\left(\left(e^{-\frac{1}{300000000}\,s\,u}\,e^{\frac{1}{300000000}\,s\,x\sim}\right.\right.\right.$$

$$+\,e^{-\frac{1}{300000000}\,s\,x\sim}\,e^{\frac{1}{300000000}\,s\,u}\Big)\Big(s\,f(u) + g(u)$$

$$+\,7.647839747\,10^{-19}\,s^{2.}\,\Big(1.\,\mathrm{BesselY}\Big(0.,$$

$$3.333333333\,10^{-9}\,s^{1.}\,\big(3.\,u^{2.} - 6000.\,u$$

$$+\,6.000000\,10^{6}\big)^{0.5000000000}\Big) - 1.\,\mathrm{StruveH}\Big(0.,$$

$$3.333333333\,10^{-9}\,s^{1.}\,\big(3.\,u^{2.} - 6000.\,u$$

$$+\,6.000000\,10^{6}\big)^{0.5000000000}\Big)\Big)^{1.}$$

$$+\,\Big(2.469135802\,10^{-20}\,\Big(5.915550688\,10^{9} - 3.141592654\,\mathrm{StruveH}\Big($$

$$+\,6.000000\,10^{6}\big)^{0.5000000000}\Big)^{1.} - 3.141592654\,\mathrm{BesselY}\Big(1.,$$

$$3.333333333\,10^{-9}\,s^{1.}\,\big(3.\,u^{2.} - 6000.\,u$$

$$+\,6.000000\,10^{6}\big)^{0.5000000000}\Big)^{1.}\Big)^{1.}\,s^{1.}\Big)\Big/\Big(3.\,u^{2.} - 6000.\,u$$

$$+\,6.000000\,10^{6}\big)^{0.5000000000}\Big)\Big)\,\mathrm{d}u\Big)$$

```
> V_p(x, s) := simplify(subs(u = x, value(%)));
```

$$
\begin{aligned}
V_p(x\sim, s) := -\frac{1}{s}\Big(6.66666666710^{-38}\Big(\int\Big(-\Big(1.\Big(\\
&-1.00000000010^{29}\, s\, f(x\sim)\sqrt{3.\,x\sim^2-6000.\,x\sim+6.00000010^6} \\
&-1.00000000010^{29}\, g(x\sim)\sqrt{3.\,x\sim^2-6000.\,x\sim+6.00000010^6} \\
&-7.64783974710^{10}\, s^2\, \mathrm{BesselY}\Big(0., \\
&3.33333333310^{-9}\, s\sqrt{3.\,x\sim^2-6000.\,x\sim+6.00000010^6}\Big) \\
&\sqrt{3.\,x\sim^2-6000.\,x\sim+6.00000010^6} \\
&+7.64783974710^{10}\, s^2\, \mathrm{StruveH}\Big(0., \\
&3.33333333310^{-9}\, s\sqrt{3.\,x\sim^2-6000.\,x\sim+6.00000010^6}\Big) \\
&\sqrt{3.\,x\sim^2-6000.\,x\sim+6.00000010^6} - 1.46062979910^{19}\, s \\
&+7.75701889710^{9}\, s\, \mathrm{StruveH}\Big(-1., \\
&3.33333333310^{-9}\, s\sqrt{3.\,x\sim^2-6000.\,x\sim+6.00000010^6}\Big) \\
&+7.75701889710^{9}\, s\, \mathrm{BesselY}\Big(1., \\
&3.33333333310^{-9}\, s\sqrt{3.\,x\sim^2-6000.\,x\sim+6.00000010^6}\Big)\Big)\Big)\Big/ \\
&\sqrt{3.\,x\sim^2-6000.\,x\sim+6.00000010^6}\Big)\,dx\sim\Big)\Big)
\end{aligned}
$$

General solution

```
> V(x, s) := C1(s) * exp(-s / c * x) + C2(s) * exp(s / c
      * x) + V_p(x, s);
```

$$V(x\sim, s) := C1(s)\, e^{-\frac{1}{300000000} s\, x\sim} + C2(s)\, e^{\frac{1}{300000000} s\, x\sim}$$

$$- \frac{1}{s}\Big(6.666666667\,10^{-38} \Big(\int\Big(-\big(1. \big(-1.000000000\,10^{29}\, s\, f(x\sim)\, \sqrt{3.\, x\sim^2 - 6000.\, x\sim + 6.000000\,10^{6}}$$

$$- 1.000000000\,10^{29}\, g(x\sim)\, \sqrt{3.\, x\sim^2 - 6000.\, x\sim + 6.000000\,10^{6}}$$

$$- 7.647839747\,10^{10}\, s^2\, \mathrm{BesselY}\big(0., 3.333333333\,10^{-9}\, s\, \sqrt{3.\, x\sim^2 - 6000.\, x\sim + 6.000000\,10^{6}}\big) \sqrt{3.\, x\sim^2 - 6000.\, x\sim + 6.000000\,10^{6}}$$

$$+ 7.647839747\,10^{10}\, s^2\, \mathrm{StruveH}\big(0., 3.333333333\,10^{-9}\, s\, \sqrt{3.\, x\sim^2 - 6000.\, x\sim + 6.000000\,10^{6}}\big) \sqrt{3.\, x\sim^2 - 6000.\, x\sim + 6.000000\,10^{6}} - 1.460629799\,10^{19}\, s$$

$$+ 7.757018897\,10^{9}\, s\, \mathrm{StruveH}\big(-1., 3.333333333\,10^{-9}\, s\, \sqrt{3.\, x\sim^2 - 6000.\, x\sim + 6.000000\,10^{6}}\big)$$

$$+ 7.757018897\,10^{9}\, s\, \mathrm{BesselY}\big(1., 3.333333333\,10^{-9}\, s\, \sqrt{3.\, x\sim^2 - 6000.\, x\sim + 6.000000\,10^{6}}\big)\big)\big)\Big) \Big/ \sqrt{3.\, x\sim^2 - 6000.\, x\sim + 6.000000\,10^{6}}\Big)\, dx\sim\Big)\Big)$$

Substituting the boundary conditions at x = 0 and as x approaches infinity, for Re{s} > 0, we get

```
> C[2](s) := 0;
```

$$C_2(s) := 0$$

```
> C[1](s) := solve(eq, C1(s));
```

$$C_1(s) :=$$

Transformed solution for V(x, s)

```
> V(x, s) := eval(V(x, s));
```

$$V(x\sim, s) := C1(s)\,\mathrm{e}^{-\frac{1}{300000000} s\,x\sim} + C2(s)\,\mathrm{e}^{\frac{1}{300000000} s\,x\sim}$$
$$- \frac{1}{s}\Bigg(6.66666666710^{-38} \bigg(\int\Big(-\Big(1.\,\Big($$
$$-1.00000000010^{29}\, s\, f(x\sim)\,\sqrt{3.\,x\sim^2 - 6000.\,x\sim + 6.00000010^6}$$
$$- 1.00000000010^{29}\, g(x\sim)\,\sqrt{3.\,x\sim^2 - 6000.\,x\sim + 6.00000010^6}$$
$$- 7.64783974710^{10}\, s^2\, \mathrm{BesselY}\Big(0.,$$
$$3.33333333310^{-9}\, s\,\sqrt{3.\,x\sim^2 - 6000.\,x\sim + 6.00000010^6}\Big)$$
$$\sqrt{3.\,x\sim^2 - 6000.\,x\sim + 6.00000010^6}$$
$$+ 7.64783974710^{10}\, s^2\, \mathrm{StruveH}\Big(0.,$$
$$3.33333333310^{-9}\, s\,\sqrt{3.\,x\sim^2 - 6000.\,x\sim + 6.00000010^6}\Big)$$
$$\sqrt{3.\,x\sim^2 - 6000.\,x\sim + 6.00000010^6} - 1.46062979910^{19}\, s$$
$$+ 7.75701889710^{9}\, s\, \mathrm{StruveH}\Big(-1.,$$
$$3.33333333310^{-9}\, s\,\sqrt{3.\,x\sim^2 - 6000.\,x\sim + 6.00000010^6}\Big)$$
$$+ 7.75701889710^{9}\, s\, \mathrm{BesselY}\Big(1.,$$
$$3.33333333310^{-9}\, s\,\sqrt{3.\,x\sim^2 - 6000.\,x\sim + 6.00000010^6}\Big)\Big)\Big)\Big) \Big/$$
$$\sqrt{3.\,x\sim^2 - 6000.\,x\sim + 6.00000010^6}\Big)\, \mathrm{d}x\sim\bigg)\Bigg)$$

Solution is the inverse Laplace of V(x, s)

```
> v(x, t) := invlaplace(V(x, s), s, t);
```

$$
\begin{aligned}
v(x\sim, t) := {} & \mathit{invlaplace}\left(\mathit{C1}(s)\,\mathrm{e}^{-\frac{1}{300000000}\,s\,x\sim}, s, t\right) \\
& + \mathit{invlaplace}\left(\mathit{C2}(s)\,\mathrm{e}^{\frac{1}{300000000}\,s\,x\sim}, s, t\right) \\
& - 6.666666667\,10^{-38}\,\mathit{invlaplace}\Bigg(\frac{1}{s}\Bigg(\\
& \int\Bigg(1000000000000000000000000000000\,s\,f(x\sim) \\
& + 1000000000000000000000000000000\,g(x\sim) \\
& + 7647839747\,0\,s^{2}\Bigg(\mathrm{BesselY}\Bigg(0, \\
& \frac{3333333333}{1000000000000000000}\,s\,\sqrt{3\,x\sim^{2} - 6000\,x\sim + 6000000}\Bigg) \\
& - \mathrm{StruveH}\Bigg(0, \\
& \frac{3333333333}{1000000000000000000}\,s\,\sqrt{3\,x\sim^{2} - 6000\,x\sim + 6000000}\Bigg)\Bigg) \\
& + \frac{1}{\sqrt{3\,x\sim^{2} - 6000\,x\sim + 6000000}}\Bigg(\Bigg(14606297990000000000 \\
& - 7757018897\,\mathrm{StruveH}\Bigg(-1, \\
& \frac{3333333333}{1000000000000000000}\,s\,\sqrt{3\,x\sim^{2} - 6000\,x\sim + 6000000}\Bigg) \\
& - 7757018897\,\mathrm{BesselY}\Bigg(1, \\
& \frac{3333333333}{1000000000000000000}\,s\,\sqrt{3\,x\sim^{2} - 6000\,x\sim + 6000000}\Bigg)\Bigg)\,s\Bigg)\Bigg) \\
& \mathrm{d}x\sim\Bigg), s, t\Bigg)
\end{aligned}
$$

Appendix II

C-sharp Application Programme Interface (API) to determine lightning induced voltages

```
using System;
 using System.Collections.Generic;
 using System.Linq;
 using System.Text;

 namespace Voltage_Calculator
 {
     public class Calculator
     {
         GraphPointList megaCoordinateList;

         public GraphPointList MegaCoordinateList
         {
             get { return megaCoordinateList; }
             set { megaCoordinateList = value; }
         }
         ProbabilityList megaProbabilityList;

         public ProbabilityList MegaProbabilityList
         {
             get { return megaProbabilityList; }
             set { megaProbabilityList = value; }
         }

         ResponseOfCalculateMethod resultOutput = new ResponseOfCalculateMethod();
         ResponseOfCalculateMethod output = new ResponseOfCalculateMethod();

         List<double> tList = new List<double>();
         List<double> vList = new List<double>();
```

```
//GraphPointList graphpoints;
//MultiLevelGraphPointList multiLevelGraphPoints;
Probability moi;
double tf, ttf, f3, f4, f5, f6, f7, f8, f9, f10, f11, f12, f13, f14, f15, bo, tof, f1a, f2a, f3a, f4a,
f5a, f6a, f7a, f8a, f9a, f10a, f11a, f12a, f13a, f14a, f15a;
double Ip, h, hc, beta, mo, m1a, n1a, no, n1, t0, c, t, x, rs, yo1, m1, f1, fo, U_t_to,
U_t_tof;
long i;
double v1, v2, v;
double alpha, rho, gamma, Ipmin, Ipmax, Ipstep;
double z;
double p, p1, p2, p3, p4, p5, g, y, e, w, q, inP1, inP2, inP3, inP, nfod;
double bIL, yo2, ip2, a, ng, nfo, tfstep, tfMin, tfMax, tfCounter;
double coEffOfTd, poWerOfTd, tD;

public double TD
{
   get { return tD; }
   set { tD = value; }
}

public double PoWerOfTd
{
   get { return poWerOfTd; }
   set { poWerOfTd = value; }
}

public double CoEffOfTd
{
   get { return coEffOfTd; }
   set { coEffOfTd = value; }
```

```
}

public double TfMax
{
   get { return tfMax; }
   set { tfMax = value; }
}

public double TfMin
{
   get { return tfMin; }
   set { tfMin = value; }
}

public double Tfstep
{
   get { return tfstep; }
   set { tfstep = value; }
}

public double Nfo
{
   get { return nfo; }
   set { nfo = value; }
}

public double Ng
{
   get { return ng; }
   set { ng = value; }
}
```

```
public double A
{
   get { return a; }
   set { a = value; }
}
public double Ip2
{
   get { return ip2; }
   set { ip2 = value; }
}
public double Yo2
{
s        get { return yo2; }
   set { yo2 = value; }
}

public double BIL
{
   get { return bIL; }
   set { bIL = value; }
}
public double Nfod
{
   get { return nfod; }
   set { nfod = value; }
}

public double InP
{
   get { return inP; }
```

```
    set { inP = value; }
}

public double InP3
{
    get { return inP3; }
    set { inP3 = value; }
}

public double InP2
{
    get { return inP2; }
    set { inP2 = value; }
}

public double InP1
{
    get { return inP1; }
    set { inP1 = value; }
}

public double Q
{
    get { return q; }
    set { q = value; }
}

public double W
{
    get { return w; }
    set { w = value; }
```

```
}

public double E
{
   get { return e; }
   set { e = value; }
}

public double Y
{
   get { return y; }
   set { y = value; }
}

public double G
{
   get { return g; }
   set { g = value; }
}

public double P4
{
   get { return p4; }
   set { p4 = value; }
}

public double P3
{
   get { return p3; }
   set { p3 = value; }
}
```

```
public double P2
{
   get { return p2; }
   set { p2 = value; }
}

public double P1
{
   get { return p1; }
   set { p1 = value; }
}

public double P
{
   get { return p; }
   set { p = value; }
}

public double Ipstep1
{
   get { return Ipstep; }
   set { Ipstep = value; }
}

public double Ipmax1
{
   get { return Ipmax; }
   set { Ipmax = value; }
}
```

```
public double Ipmin1
{
    get { return Ipmin; }
    set { Ipmin = value; }
}

public double Gamma
{
    get { return gamma; }
    set { gamma = value; }
}

public double Rho
{
    get { return rho; }
    set { rho = value; }
}

public double Alpha
{
    get { return alpha; }
    set { alpha = value; }
}

public double V
{
    get { return v; }
    set { v = value; }
}
double f2, tStep, tMin, tMax;
```

```
public double TMax
{
   get { return tMax; }
   set { tMax = value; }
}

public double TMin
{
   get { return tMin; }
   set { tMin = value; }
}

public double TStep
{
   get { return tStep; }
   set { tStep = value; }
}

public double F2
{
   get { return f2; }
   set { f2 = value; }
}

public double V2
{
   get { return v2; }
   set { v2 = value; }
}

public double V1
```

```
{
   get { return v1; }
   set { v1 = value; }
}

public long I
{
   get { return i; }
   set { i = value; }
}

public double U_t_tof1
{
   get { return U_t_tof; }
   set { U_t_tof = value; }
}

public double U_t_to1
{
   get { return U_t_to; }
   set { U_t_to = value; }
}

public double Fo
{
   get { return fo; }
   set { fo = value; }
}

public double F1
{
```

```
    get { return f1; }
    set { f1 = value; }
}

public double M1
{
    get { return m1; }
    set { m1 = value; }
}

public double Yo1
{
    get { return yo1; }
    set { yo1 = value; }
}

public double Rs
{
    get { return rs; }
    set { rs = value; }
}

public double X
{
    get { return x; }
    set { x = value; }
}

public double T
{
    get { return t; }
```

```
    set { t = value; }
}

public double C
{
    get { return c; }
    set { c = value; }
}

public double T01
{
    get { return t0; }
    set { t0 = value; }
}

public double T0
{
    get { return t0; }
    set { t0 = value; }
}

public double N1
{
    get { return n1; }
    set { n1 = value; }
}

public double No
{
    get { return no; }
    set { no = value; }
```

```
}

public double N1a
{
   get { return n1a; }
   set { n1a = value; }
}

public double M1a
{
   get { return m1a; }
   set { m1a = value; }
}

public double Mo
{
   get { return mo; }
   set { mo = value; }
}

public double Beta
{
   get { return beta; }
   set { beta = value; }
}

public double Hc
{
   get { return hc; }
   set { hc = value; }
}
```

```
public double H
{
   get { return h; }
   set { h = value; }
}

public double Ip1
{
   get { return Ip; }
   set { Ip = value; }
}

public double F15a
{
   get { return f15a; }
   set { f15a = value; }
}

public double F14a
{
   get { return f14a; }
   set { f14a = value; }
}

public double F13a
{
   get { return f13a; }
   set { f13a = value; }
}
```

```
public double F12a
{
    get { return f12a; }
    set { f12a = value; }
}

public double F11a
{
    get { return f11a; }
    set { f11a = value; }
}

public double F10a
{
    get { return f10a; }
    set { f10a = value; }
}

public double F9a
{
    get { return f9a; }
    set { f9a = value; }
}

public double F8a
{
    get { return f8a; }
    set { f8a = value; }
}

public double F7a
```

```
{
    get { return f7a; }
    set { f7a = value; }
}

public double F6a
{
    get { return f6a; }
    set { f6a = value; }
}

public double F5a
{
    get { return f5a; }
    set { f5a = value; }
}

public double F4a
{
    get { return f4a; }
    set { f4a = value; }
}

public double F3a
{
    get { return f3a; }
    set { f3a = value; }
}

public double F2a
{
```

```
    get { return f2a; }
    set { f2a = value; }
}

public double F1a
{
    get { return f1a; }
    set { f1a = value; }
}

public double Tof
{
    get { return tof; }
    set { tof = value; }
}

public double Bo
{
    get { return bo; }
    set { bo = value; }
}

public double F15
{
    get { return f15; }
    set { f15 = value; }
}

public double F14
{
    get { return f14; }
```

```
    set { f14 = value; }
}

public double F13
{
    get { return f13; }
    set { f13 = value; }
}

public double F12
{
    get { return f12; }
    set { f12 = value; }
}

public double F11
{
    get { return f11; }
    set { f11 = value; }
}

public double F10
{
    get { return f10; }
    set { f10 = value; }
}

public double F9
{
    get { return f9; }
    set { f9 = value; }
```

```
}

public double F8
{
   get { return f8; }
   set { f8 = value; }
}

public double F7
{
   get { return f7; }
   set { f7 = value; }
}

public double F6
{
   get { return f6; }
   set { f6 = value; }
}

public double F5
{
   get { return f5; }
   set { f5 = value; }
}

public double F4
{
   get { return f4; }
   set { f4 = value; }
}
```

```
public double F3
{
    get { return f3; }
    set { f3 = value; }
}

public double Ttf
{
    get { return ttf; }
    set { ttf = value; }
}

public double Tf
{
    get { return tf; }
    set { tf = value; }
}

public Calculator()
{

}

public Calculator(float I_p, double t_f, double y_0, double x_, double h_, double h_c,
double beta_, double t_min, double t_max, double t_step)
{
    Ip = (double)I_p;
    tf = t_f;
    h = h_;
    x = x_;
```

```
    hc = h_c;
    beta = beta_;
    yo1 = y_0;
    tMin = t_min;
    tMax = t_max;
    tStep = t_step;
}

public Calculator(float I_p, double t_f, double y_0, double x_, double r_s, double h_, double h_c, double beta_, double t_min, double t_max, double t_step)
{
    Ip = (double)I_p;
    tf = t_f;
    h = h_;
    x = x_;
    hc = h_c;
    beta = beta_;
    rs = r_s;
    yo1 = y_0;
    tMin = t_min;
    tMax = t_max;
    tStep = t_step;
}

public Calculator(double I_p, double t_f, double x_, double r_s, double rho_, double h_, double h_c, double beta_, double t_min, double t_max, double t_step)
{
    Ip = I_p;
    tf = t_f;
    h = h_;
    x = x_;
```

```
        hc = h_c;
        beta = beta_;
        rs = r_s;
        rho = rho_;
        tMin = t_min;
        tMax = t_max;
        tStep = t_step;
    }

    public Calculator(float I_p, double t_f, float x_, double alpha_, double rho_, double gamma_, double h_, double h_c, double beta_, double t_min, double t_max, double t_step)
    {
        Ip = (double)I_p;
        tf = t_f;
        h = h_;
        x = (double)x_;
        hc = h_c;
        beta = beta_;
        alpha = alpha_;
        rho = rho_;
        gamma = gamma_;
        tMin = t_min;
        tMax = t_max;
        tStep = t_step;
    }

    public Calculator(float I_pmin, double I_pmax, double I_pstep, double t_fMin, double t_fMax, double t_fStep, double t_min, double t_max, double t_step, double _Ng, double y_0, double x_, double h_, double h_c, double beta_, double _BIL)
    {
        Ipmin = (double)I_pmin;
```

```
            Ipmax = I_pmax;
            Ipstep = I_pstep;
            tfMin = t_fMin;
            tfMax = t_fMax;
            tfstep = t_fStep;
            ng = _Ng;
            bIL = _BIL;
            h = h_;
            x = x_;
            hc = h_c;
            beta = beta_;
            yo1 = y_0;
            tMin = t_min;
            tMax = t_max;
            tStep = t_step;
        }

        public Calculator(float I_pmin, double I_pmax, double I_pstep, double t_fMin, double
t_fMax, double t_fStep, double t_min, double t_max, double t_step, double _td, double _coEfftd,
double _powerTd, double y_0, double x_, double h_, double h_c, double beta_, double _BIL)
        {
            Ipmin = (double)I_pmin;
            Ipmax = I_pmax;
            Ipstep = I_pstep;
            tfMin = t_fMin;
            tfMax = t_fMax;
            tfstep = t_fStep;
            tD = _td;
            coEffOfTd = _coEfftd;
            poWerOfTd = _powerTd;
            bIL = _BIL;
```

```
        h = h_;
        x = x_;
        hc = h_c;
        beta = beta_;
        yo1 = y_0;
        tMin = t_min;
        tMax = t_max;
        tStep = t_step;
    }

    public Calculator(float I_pmin, double I_pmax, double I_pstep, double t_fMin, double t_fMax, double t_fStep, double t_min, double t_max, double t_step, double _Ng, double y_0, double x_, double r_s, double h_, double h_c, double beta_, double _BIL)
    {
        Ipmin = (double)I_pmin;
        Ipmax = I_pmax;
        Ipstep = I_pstep;
        tfMin = t_fMin;
        tfMax = t_fMax;
        tfstep = t_fStep;
        ng = _Ng;
        bIL = _BIL;
        h = h_;
        x = x_;
        hc = h_c;
        beta = beta_;
        rs = r_s;
        yo1 = y_0;
        tMin = t_min;
        tMax = t_max;
        tStep = t_step;
```

```
}

public Calculator(float I_pmin, double I_pmax, double I_pstep, double t_fMin, double
t_fMax, double t_fStep, double t_min, double t_max, double t_step, double _td, double _coEfftd,
double _powerTd, double y_0, double x_, double r_s, double h_, double h_c, double beta_,
double _BIL)
{
    Ipmin = (double)I_pmin;
    Ipmax = I_pmax;
    Ipstep = I_pstep;
    tfMin = t_fMin;
    tfMax = t_fMax;
    tfstep = t_fStep;
    tD = _td;
    coEffOfTd = _coEfftd;
    poWerOfTd = _powerTd;
    bIL = _BIL;
    h = h_;
    x = x_;
    hc = h_c;
    beta = beta_;
    rs = r_s;
    yo1 = y_0;
    tMin = t_min;
    tMax = t_max;
    tStep = t_step;
}

public Calculator(double I_pmin, double I_pmax, double I_pstep, double t_fMin, double
t_fMax, double t_fStep, double t_min, double t_max, double t_step, double _Ng, double x_,
double rho_, double r_s, double h_, double h_c, double beta_, double _BIL)
```

```
{
    Ipmin = I_pmin;
    Ipmax = I_pmax;
    Ipstep = I_pstep;
    tfMin = t_fMin;
    tfMax = t_fMax;
    tfstep = t_fStep;
    ng = _Ng;
    bIL = _BIL;
    h = h_;
    x = x_;
    hc = h_c;
    beta = beta_;
    rs = r_s;
    rho = rho_;
    tMin = t_min;
    tMax = t_max;
    tStep = t_step;
}

public Calculator(double I_pmin, double I_pmax, double I_pstep, double t_fMin, double t_fMax, double t_fStep, double t_min, double t_max, double t_step, double _td, double _coEfftd, double _powerTd, double x_, double rho_, double r_s, double h_, double h_c, double beta_, double _BIL)
{
    Ipmin = I_pmin;
    Ipmax = I_pmax;
    Ipstep = I_pstep;
    tfMin = t_fMin;
    tfMax = t_fMax;
    tfstep = t_fStep;
```

```
        tD = _td;
        coEffOfTd = _coEfftd;
        poWerOfTd = _powerTd;
        bIL = _BIL;
        h = h_;
        x = x_;
        hc = h_c;
        beta = beta_;
        rs = r_s;
        rho = rho_;
        tMin = t_min;
        tMax = t_max;
        tStep = t_step;
    }

    public Calculator(double I_pmin, double I_pmax, double I_pstep, double t_fMin, double t_fMax, double t_fStep, double t_min, double t_max, double t_step, double _Ng, double x_, double alpha_, double rho_, double gamma_, double h_, double h_c, double beta_, double _BIL)
    {
        Ipmin = I_pmin;
        Ipmax = I_pmax;
        Ipstep = I_pstep;
        tfMin = t_fMin;
        tfMax = t_fMax;
        tfstep = t_fStep;
        ng = _Ng;
        bIL = _BIL;
        h = h_;
        x = x_;
        hc = h_c;
        beta = beta_;
```

```
    alpha = alpha_;
    rho = rho_;
    gamma = gamma_;
    tMin = t_min;
    tMax = t_max;
    tStep = t_step;
}

public Calculator(double I_pmin, double I_pmax, double I_pstep, double t_fMin, double t_fMax, double t_fStep, double t_min, double t_max, double t_step, double _td, double _coEfftd, double _powerTd, double x_, double alpha_, double rho_, double gamma_, double h_, double h_c, double beta_, double _BIL)
{
    Ipmin = I_pmin;
    Ipmax = I_pmax;
    Ipstep = I_pstep;
    tfMin = t_fMin;
    tfMax = t_fMax;
    tfstep = t_fStep;
    tD = _td;
    coEffOfTd = _coEfftd;
    poWerOfTd = _powerTd;
    bIL = _BIL;
    h = h_;
    x = x_;
    hc = h_c;
    beta = beta_;
    alpha = alpha_;
    rho = rho_;
    gamma = gamma_;
    tMin = t_min;
```

```
            tMax = t_max;
            tStep = t_step;
        }

        private Coordinate Calculate(double __Ip, double __tf, double __yo)
        {
            Ip = __Ip;
            tf = __tf;
            yo1 = __yo;

            fo = (30 * Ip * h) / (tf * beta * c);
            m1 = Math.Sqrt(Math.Pow((Math.Pow(((c * t) - x), 2) + Math.Pow(yo1, 2)), 2) + (4 *
Math.Pow(hc, 2)) * Math.Pow(((c * t) - x), 2));
            t0 = (Math.Pow((Math.Pow(x, 2) + Math.Pow(yo1, 2)), 0.5)) / c;
            f1 = m1 + Math.Pow((c * t - x), 2) - Math.Pow(yo1, 2);
            f2 = m1 - Math.Pow((c * t - x), 2) - Math.Pow(yo1, 2);
            mo = Math.Sqrt(Math.Pow((Math.Pow((c * t0 - x), 2) + Math.Pow(yo1, 2)), 2) + ((4 *
Math.Pow(hc, 2)) * (Math.Pow((c * t0 - x), 2))));
            no = Math.Sqrt(Math.Pow((Math.Pow((c * t0 + x), 2) + Math.Pow(yo1, 2)), 2) + (4 *
Math.Pow(hc, 2)) * (Math.Pow(((c * t0) + x), 2)));
            n1 = Math.Sqrt(Math.Pow((Math.Pow((c * t + x), 2) + Math.Pow(yo1, 2)), 2) + (4 *
Math.Pow(hc, 2)) * (Math.Pow(((c * t) + x), 2)));
            ttf = t - tf;

            m1a = Math.Sqrt(Math.Pow((Math.Pow((c * ttf - x), 2) + Math.Pow(yo1, 2)), 2) + (4 *
Math.Pow(hc, 2)) * Math.Pow(((c * ttf) - x), 2));
            n1a = Math.Sqrt(Math.Pow((Math.Pow((c * ttf + x), 2) + Math.Pow(yo1, 2)), 2) + (4 *
Math.Pow(hc, 2)) * Math.Pow(((c * ttf) + x), 2));
            f3 = mo + Math.Pow(yo1, 2) - Math.Pow(((c * t0) - x), 2);
            f4 = mo - Math.Pow(yo1, 2) + Math.Pow(((c * t0) - x), 2);
            f5 = n1 + Math.Pow(((c * t) + x), 2) - Math.Pow(yo1, 2);
```

```
f6 = n1 - Math.Pow(((c * t) + x), 2) + Math.Pow(yo1, 2);
f7 = no + Math.Pow(yo1, 2) - Math.Pow(((c * t0) + x), 2);
f8 = no - Math.Pow(yo1, 2) + Math.Pow(((c * t0) + x), 2);
bo = 1 - Math.Pow(beta, 2);
tof = t0 + tf;

f9 = bo * (Math.Pow((beta * x), 2) + Math.Pow(yo1, 2)) + Math.Pow((beta * c * t), 2)
* (1 + Math.Pow(beta, 2));
f10 = (2 * Math.Pow(beta, 2) * c * t) * Math.Pow(((Math.Pow(beta, 2) * Math.Pow(c,
2) * Math.Pow(t, 2)) + (bo * (Math.Pow(x, 2) + Math.Pow(yo1, 2)))), 0.5);
f11 = ((Math.Pow(c, 2) * Math.Pow(t, 2)) - Math.Pow(x, 2)) / Math.Pow(yo1, 2);

f12 = (f9 - f10) / (Math.Pow(bo, 2) * Math.Pow(yo1, 2));
f13 = (f1 * f3 * f5 * f7) / (f2 * f4 * f6 * f8);
f14 = (bo * (Math.Pow(x, 2) + Math.Pow(yo1, 2))) / (Math.Pow(beta, 2) *
Math.Pow(c, 2));
f15 = (t + Math.Pow((Math.Pow(t, 2) + f14), 0.5)) / (t0 + Math.Pow((Math.Pow(t0, 2)
+ f14), 0.5));
f15a = (ttf + Math.Pow((Math.Pow(ttf, 2) + f14), 0.5)) / (t0 +
Math.Pow((Math.Pow(t0, 2) + f14), 0.5));

V1 = fo * ((bo * Math.Log(f12)) - (bo * Math.Log(f11)) + (0.5 * Math.Log(f13)));

f1a = m1a + Math.Pow((c * ttf - x), 2) - Math.Pow(yo1, 2);
f2a = m1a - Math.Pow((c * ttf - x), 2) + Math.Pow(yo1, 2);
f3a = f3;
f4a = f4;
f5a = n1a + Math.Pow((c * ttf + x), 2) - Math.Pow(yo1, 2);
f6a = n1a - Math.Pow((c * ttf + x), 2) + Math.Pow(yo1, 2);
f7a = f7;
f8a = f8;
```

```
            f9a = (bo * (Math.Pow((beta * x), 2) + Math.Pow(yo1, 2))) + (1 + Math.Pow(beta, 2))
* Math.Pow(beta, 2) * Math.Pow(c, 2) * Math.Pow(ttf, 2);
            f10a = (2 * Math.Pow(beta, 2) * c * ttf) * Math.Pow((Math.Pow((beta * c * ttf), 2) +
bo * (Math.Pow(x, 2) + Math.Pow(yo1, 2))), 0.5);
            f11a = (Math.Pow(c, 2) * Math.Pow(ttf, 2) - Math.Pow(x, 2)) / Math.Pow(yo1, 2);
            f12a = (f9a - f10a) / (Math.Pow(bo, 2) * Math.Pow(yo1, 2));
            f13a = (f1a * f3a * f5a * f7a) / (f2a * f4a * f6a * f8a);

            V2 = -fo * ((bo * Math.Log(f12a)) - (bo * Math.Log(f11a)) + (0.5 * Math.Log(f13a)));

            if (t >= t0)
            {
              U_t_to = 1;
            }
            else
            {
              U_t_to = 0;
            }

            if (t >= tof)
            {
              U_t_tof = 1;
            }
            else
            {
              U_t_tof = 0;
            }

            v = ((V1 * U_t_to) + (V2 * U_t_tof));

            return new Coordinate(Ip, rs, tf, yo1, t, v, v1, v2);
```

```
}

public GraphPointList CalculateUsingIp(double _Ip)
{
   GraphPointList justGo = new GraphPointList();
   c = 300000000;
   Ip = _Ip;
   t = tMin;

   if (rs != 0.0 && yo1 == 0.0)
   {
      yo1 = Calculate_Y0(rs, h);
   }
   else
   {
      if (rs == 0.0 && yo1 == 0.0)
      {
         rs = Calculate_Rs(Ip);
         yo1 = Calculate_Y0(rs, h);
      }
   }

   while (t <= tMax)
   {
      justGo.Add(Calculate(Ip, tf, yo1));
      t = t + tStep;
   }
   return justGo;
}
```

```
public GraphPointList CalculateUsingIpStep(double _IpMin, double _IpMax, double
_IpStep)
{
    GraphPointList justGo = new GraphPointList();
    MultiLevelGraphPointList jest = new MultiLevelGraphPointList();
    List<MultiLevelGraphPointList> ours = new List<MultiLevelGraphPointList>();
    ProbabilityList emi = new ProbabilityList();
    MultiLevelProbabilityList you = new MultiLevelProbabilityList();
    Coordinate temi = new Coordinate();
    Probability jojo = new Probability();
    c = 300000000;
    Ipmin = _IpMin;
    Ipmax = _IpMax;
    Ipstep = _IpStep;
    z = Ipmin;
    t = tMin;
    tfCounter = tfMin;

    if (ng == 0.0 && coEffOfTd != 0.0 && poWerOfTd != 0.0 && tD != 0.0)
    {
        ng = CalculateNg(coEffOfTd, poWerOfTd, tD);
    }

    while (z <= Ipmax)
    {

        if (rs != 0.0 && yo1 == 0.0)
        {
            yo1 = Calculate_Y0(rs, h);
        }
        else
```

```
{
    if (rs == 0.0 && yo1 == 0.0)
    {
        rs = Calculate_Rs(z);
        yo1 = Calculate_Y0(rs, h);
    }
}

while (tfCounter <= tfMax)
{
    jojo = CalculateJointProbabilityDensityFunction(z, tfCounter);
    emi.Add(jojo);
    while (t <= tMax)
    {
        temi = Calculate(z, tfCounter, yo1);
        temi.Ng = ng;
        double substitute = temi.V;
        Coordinate subReturn = new Coordinate();
        if (substitute.ToString().Contains('.') == true)
        {
            if (substitute.GetType() == typeof(double))
            {
                while (TestV_Value(substitute, bIL) == false)
                {
                    subReturn = GetIdealV(substitute, bIL, temi.Y0);
                    temi.Y02 = subReturn.Y02;
                    temi.A = CalculateAreaToCauseLineFlashOver(temi.Y02, temi.Y0);
                    temi.Nfo =
CalculateExpectedNumberOfLineFlashOversPer100kmPerYear(jojo.P, Ipstep, tfstep, temi.Ng,
temi.A);
                    substitute = subReturn.V;
```

```
                    }
                }
            }
            justGo.Add(temi);
            t = t + tStep;
        }
        jest.Add(justGo);
        tfCounter = tfCounter + tfstep;
        t = tMin;
    }
    ours.Add(jest);
    you.Add(emi);
    z = z + Ipstep;
    tfCounter = tfMin;
}
output.Coordinates1 = ours;
output.Probs = you;
Sort(output);
return megaCoordinateList;
}

public double Calculate_Rs(double __Ip)
{
    double ____Ip = __Ip;
    double ___Rs = alpha * Math.Pow((____Ip / 1000), gamma); ;
    return ___Rs;
}

public double Calculate_Y0(double __rs, double __h)
{
    double ____Rs = __rs;
```

```
        double ____h = __h;
        double ____Y0 = 0.0;

        if (____Y0 == 0.0 && ((rho * ____Rs) <= ____h))
        {
            ____Y0 = ____Rs;
        }
        else
        {
            if (____Y0 == 0.0)
            {
                ____Y0 = Math.Sqrt((Math.Pow(____Rs, 2.0)) - Math.Pow((rho * ____Rs -
____h), 2.0));
            }
        }
        return ____Y0;
    }

    public static double CalculateTotalNfo(Calculator toUse)
    {
        double sum = 0;
        GraphPointList aid = new GraphPointList();
        aid = toUse.megaCoordinateList;
        if (aid != null)
        {
            foreach (Coordinate it in aid)
            {
                sum = sum + it.Nfo;
            }
        }
        return sum;
```

```
}

void Sort(ResponseOfCalculateMethod _resultOutput)
{
   resultOutput = _resultOutput;
   megaCoordinateList = new GraphPointList();
   megaProbabilityList = new ProbabilityList();
   foreach (MultiLevelGraphPointList result in resultOutput.Coordinates1)
   {
      foreach (GraphPointList item in result)
      {
         foreach (Coordinate it in item)
         {
            if (megaCoordinateList.Contains(it) == false)
            {
               megaCoordinateList.Add(it);
            }
         }
      }
   }
   foreach (ProbabilityList item in resultOutput.Probs)
   {
      foreach (Probability it in item)
      {
         if (megaProbabilityList.Contains(it) == false)
         {
            megaProbabilityList.Add(it);
         }
      }
   }
```

```
}

public double CalculateNg(double coeffOfTd, double powerOfTd, double Td)
{
   double _Td;
   double _coEffOfTd;
   double _powerOfTd;
   double _Ng;

   _Td = Td;
   _coEffOfTd = coeffOfTd;
   _powerOfTd = powerOfTd;

   _Ng = _coEffOfTd * Math.Pow(_Td, _powerOfTd);

   return _Ng;
}

//methods called at a given (Ip, tf) starts here.
public Probability CalculateJointProbabilityDensityFunction(double _ip, double _tf)
{
   double __Ip = _ip;
   double __tf = _tf;

   if (__Ip <= 20000)
   {
      p1 = 1 / (2 * (22 / 7) * (__Ip / 1000) * (__tf * 1000000) * 1.33 * 0.553 *
Math.Sqrt(1 - Math.Pow(0.47, 2)));
      p2 = (-0.5 / (1 - Math.Pow(0.47, 2)));
      p3 = Math.Pow(((Math.Log((__Ip / 1000)) - Math.Log(61.1)) / 1.33), 2);
```

```
                p4 = (2 * 0.47 * (Math.Log((__Ip / 1000)) - Math.Log(61.1)) * (Math.Log(__tf *
1000000) - Math.Log(3.83))) / (1.33 * 0.553);
                p5 = Math.Pow(((Math.Log(__tf * 1000000) - Math.Log(3.83)) / 0.553), 2);
                p = p1 * Math.Exp(p2 * (p3 - p4 + p5));
            }
            else
            {
                if (__Ip > 20000)
                {
                    p1 = 1 / (2 * (22 / 7) * (__Ip / 1000) * (__tf * 1000000) * 0.605 * 0.553 *
Math.Sqrt(1 - Math.Pow(0.47, 2)));
                    p2 = (-0.5 / (1 - Math.Pow(0.47, 2)));
                    p3 = Math.Pow(((Math.Log((__Ip / 1000)) - Math.Log(61.1)) / 1.33), 2);
                    p4 = (2 * 0.47 * (Math.Log((__Ip / 1000)) - Math.Log(61.1)) * (Math.Log(__tf *
1000000) - Math.Log(3.83))) / (1.33 * 0.553);
                    p5 = Math.Pow(((Math.Log(__tf * 1000000) - Math.Log(3.83)) / 0.553), 2);
                    p = p1 * Math.Exp(p2 * (p3 - p4 + p5));
                }
            }
            moi = new Probability(__Ip, __tf, p);
            return moi;
        }
        //methods called at a given (Ip, tf) ends here.


        //methods that are called for every t btw tmin and tmax at a given (Ip, tf) starts here.
        public double CalculateV_UsingIpStep(double __Ip, double __tf)
        {
            Ip = __Ip;
            tf = __tf;
            double answer;
```

```
fo = (30 * Ip * h) / (tf * beta * c);
m1 = Math.Sqrt(Math.Pow((Math.Pow(((c * t) - x), 2) + Math.Pow(yo1, 2)), 2) + (4 * Math.Pow(hc, 2)) * Math.Pow(((c * t) - x), 2));
t0 = (Math.Pow((Math.Pow(x, 2) + Math.Pow(yo1, 2)), 0.5)) / c;
f1 = m1 + Math.Pow((c * t - x), 2) - Math.Pow(yo1, 2);
f2 = m1 - Math.Pow((c * t - x), 2) - Math.Pow(yo1, 2);
mo = Math.Sqrt(Math.Pow((Math.Pow((c * t0 - x), 2) + Math.Pow(yo1, 2)), 2) + ((4 * Math.Pow(hc, 2)) * (Math.Pow((c * t0 - x), 2))));
no = Math.Sqrt(Math.Pow((Math.Pow((c * t0 + x), 2) + Math.Pow(yo1, 2)), 2) + (4 * Math.Pow(hc, 2)) * (Math.Pow(((c * t0) + x), 2)));
n1 = Math.Sqrt(Math.Pow((Math.Pow((c * t0 + x), 2) + Math.Pow(yo1, 2)), 2) + (4 * Math.Pow(hc, 2)) * (Math.Pow(((c * t) + x), 2)));
ttf = t - tf;

m1a = Math.Sqrt(Math.Pow((Math.Pow((c * ttf - x), 2) + Math.Pow(yo1, 2)), 2) + (4 * Math.Pow(hc, 2)) * Math.Pow(((c * ttf) - x), 2));
n1a = Math.Sqrt(Math.Pow((Math.Pow((c * ttf + x), 2) + Math.Pow(yo1, 2)), 2) + (4 * Math.Pow(hc, 2)) * Math.Pow(((c * ttf) + x), 2));
f3 = mo + Math.Pow(yo1, 2) - Math.Pow(((c * t0) - x), 2);
f4 = mo - Math.Pow(yo1, 2) + Math.Pow(((c * t0) - x), 2);
f5 = n1 + Math.Pow(((c * t) + x), 2) - Math.Pow(yo1, 2);
f6 = n1 - Math.Pow(((c * t) + x), 2) + Math.Pow(yo1, 2);
f7 = no + Math.Pow(yo1, 2) - Math.Pow(((c * t0) + x), 2);
f8 = no - Math.Pow(yo1, 2) + Math.Pow(((c * t0) + x), 2);
bo = 1 - Math.Pow(beta, 2);
tof = t0 + tf;

f9 = bo * (Math.Pow((beta * x), 2) + Math.Pow(yo1, 2)) + Math.Pow((beta * c * t), 2) * (1 + Math.Pow(beta, 2));
f10 = (2 * Math.Pow(beta, 2) * c * t) * Math.Pow(((Math.Pow(beta, 2) * Math.Pow(c, 2) * Math.Pow(t, 2)) + (bo * (Math.Pow(x, 2) + Math.Pow(yo1, 2)))), 0.5);
```

```
f11 = ((Math.Pow(c, 2) * Math.Pow(t, 2)) - Math.Pow(x, 2)) / Math.Pow(yo1, 2);

f12 = (f9 - f10) / (Math.Pow(bo, 2) * Math.Pow(yo1, 2));
f13 = (f1 * f3 * f5 * f7) / (f2 * f4 * f6 * f8);
f14 = (bo * (Math.Pow(x, 2) + Math.Pow(yo1, 2))) / (Math.Pow(beta, 2) *
Math.Pow(c, 2));
f15 = (t + Math.Pow((Math.Pow(t, 2) + f14), 0.5)) / (t0 + Math.Pow((Math.Pow(t0, 2)
+ f14), 0.5));
f15a = (ttf + Math.Pow((Math.Pow(ttf, 2) + f14), 0.5)) / (t0 +
Math.Pow((Math.Pow(t0, 2) + f14), 0.5));

V1 = fo * ((bo * Math.Log(f12)) - (bo * Math.Log(f11)) + (0.5 * Math.Log(f13)));

f1a = m1a + Math.Pow((c * ttf - x), 2) - Math.Pow(yo1, 2);
f2a = m1a - Math.Pow((c * ttf - x), 2) + Math.Pow(yo1, 2);
f3a = f3;
f4a = f4;
f5a = n1a + Math.Pow((c * ttf + x), 2) - Math.Pow(yo1, 2);
f6a = n1a - Math.Pow((c * ttf + x), 2) + Math.Pow(yo1, 2);
f7a = f7;
f8a = f8;
f9a = (bo * (Math.Pow((beta * x), 2) + Math.Pow(yo1, 2))) + (1 + Math.Pow(beta, 2))
* Math.Pow(beta, 2) * Math.Pow(c, 2) * Math.Pow(ttf, 2);
f10a = (2 * Math.Pow(beta, 2) * c * ttf) * Math.Pow((Math.Pow((beta * c * ttf), 2) +
bo * (Math.Pow(x, 2) + Math.Pow(yo1, 2))), 0.5);
f11a = (Math.Pow(c, 2) * Math.Pow(ttf, 2) - Math.Pow(x, 2)) / Math.Pow(yo1, 2);
f12a = (f9a - f10a) / (Math.Pow(bo, 2) * Math.Pow(yo1, 2));
f13a = (f1a * f3a * f5a * f7a) / (f2a * f4a * f6a * f8a);

V2 = -fo * ((bo * Math.Log(f12a)) - (bo * Math.Log(f11a)) + (0.5 * Math.Log(f13a)));
```

```
    if (t >= t0)
    {
        U_t_to = 1;
    }
    else
    {
        U_t_to = 0;
    }

    if (t >= tof)
    {
        U_t_tof = 1;
    }
    else
    {
        U_t_tof = 0;
    }

    v = ((V1 * U_t_to) + (V2 * U_t_tof));
    answer = v;
    return answer;
}

public bool TestV_Value(double _v, double _BIL)
{

    double ans = _v;
    double __bIL = _BIL;
    bool returnVal = false;
    if (ans > __bIL)
    {
```

```
            returnVal = false;
        }
        else
        {
            if (ans < __bIL)
            {
                returnVal = true;
            }
        }
        return returnVal;
    }

    public Coordinate GetIdealV(double _v, double _BIL, double _yo)
    {
        double __bIL = _BIL;
        double __v = _v;
        double idealV;
        Coordinate superSub = new Coordinate();
        double yoSearch = _yo;

        if (__v.GetType() == typeof(double))
        {
            while (__v >= __bIL)
            {
                yoSearch = yoSearch + 0.001;
                fo = (30 * Ip * h) / (tf * beta * c);
                m1 = Math.Sqrt(Math.Pow((Math.Pow(((c * t) - x), 2) + Math.Pow(yoSearch, 2)),
2) + (4 * Math.Pow(hc, 2)) * Math.Pow(((c * t) - x), 2));
                t0 = (Math.Pow((Math.Pow(x, 2) + Math.Pow(yoSearch, 2)), 0.5)) / c;
                f1 = m1 + Math.Pow((c * t - x), 2) - Math.Pow(yoSearch, 2);
                f2 = m1 - Math.Pow((c * t - x), 2) - Math.Pow(yoSearch, 2);
```

```
mo = Math.Sqrt(Math.Pow((Math.Pow((c * t0 - x), 2) + Math.Pow(yoSearch, 2)), 2) + ((4 * Math.Pow(hc, 2)) * (Math.Pow((c * t0 - x), 2))));
no = Math.Sqrt(Math.Pow((Math.Pow((c * t0 + x), 2) + Math.Pow(yoSearch, 2)), 2) + (4 * Math.Pow(hc, 2)) * (Math.Pow(((c * t0) + x), 2)));
n1 = Math.Sqrt(Math.Pow((Math.Pow((c * t0 + x), 2) + Math.Pow(yoSearch, 2)), 2) + (4 * Math.Pow(hc, 2)) * (Math.Pow(((c * t) + x), 2)));
ttf = t - tf;

m1a = Math.Sqrt(Math.Pow((Math.Pow((c * ttf - x), 2) + Math.Pow(yoSearch, 2)), 2) + (4 * Math.Pow(hc, 2)) * Math.Pow(((c * ttf) - x), 2));
n1a = Math.Sqrt(Math.Pow((Math.Pow((c * ttf + x), 2) + Math.Pow(yoSearch, 2)), 2) + (4 * Math.Pow(hc, 2)) * Math.Pow(((c * ttf) + x), 2));
f3 = mo + Math.Pow(yoSearch, 2) - Math.Pow(((c * t0) - x), 2);
f4 = mo - Math.Pow(yoSearch, 2) + Math.Pow(((c * t0) - x), 2);
f5 = n1 + Math.Pow(((c * t) + x), 2) - Math.Pow(yoSearch, 2);
f6 = n1 - Math.Pow(((c * t) + x), 2) + Math.Pow(yoSearch, 2);
f7 = no + Math.Pow(yoSearch, 2) - Math.Pow(((c * t0) + x), 2);
f8 = no - Math.Pow(yoSearch, 2) + Math.Pow(((c * t0) + x), 2);
bo = 1 - Math.Pow(beta, 2);
tof = t0 + tf;

f9 = bo * (Math.Pow((beta * x), 2) + Math.Pow(yoSearch, 2)) + Math.Pow((beta * c * t), 2) * (1 + Math.Pow(beta, 2));
f10 = (2 * Math.Pow(beta, 2) * c * t) * Math.Pow(((Math.Pow(beta, 2) * Math.Pow(c, 2) * Math.Pow(t, 2)) + (bo * (Math.Pow(x, 2) + Math.Pow(yoSearch, 2)))), 0.5);
f11 = ((Math.Pow(c, 2) * Math.Pow(t, 2)) - Math.Pow(x, 2)) / Math.Pow(yoSearch, 2);

f12 = (f9 - f10) / (Math.Pow(bo, 2) * Math.Pow(yoSearch, 2));
f13 = (f1 * f3 * f5 * f7) / (f2 * f4 * f6 * f8);
```

```
            f14 = (bo * (Math.Pow(x, 2) + Math.Pow(yoSearch, 2))) / (Math.Pow(beta, 2) *
Math.Pow(c, 2));
            f15 = (t + Math.Pow((Math.Pow(t, 2) + f14), 0.5)) / (t0 +
Math.Pow((Math.Pow(t0, 2) + f14), 0.5));
            f15a = (ttf + Math.Pow((Math.Pow(ttf, 2) + f14), 0.5)) / (t0 +
Math.Pow((Math.Pow(t0, 2) + f14), 0.5));

            V1 = fo * ((bo * Math.Log(f12)) - (bo * Math.Log(f11)) + (0.5 *
Math.Log(f13)));


            f1a = m1a + Math.Pow((c * ttf - x), 2) - Math.Pow(yoSearch, 2);
            f2a = m1a - Math.Pow((c * ttf - x), 2) + Math.Pow(yoSearch, 2);
            f3a = f3;
            f4a = f4;
            f5a = n1a + Math.Pow((c * ttf + x), 2) - Math.Pow(yoSearch, 2);
            f6a = n1a - Math.Pow((c * ttf + x), 2) + Math.Pow(yoSearch, 2);
            f7a = f7;
            f8a = f8;
            f9a = (bo * (Math.Pow((beta * x), 2) + Math.Pow(yoSearch, 2))) + (1 +
Math.Pow(beta, 2)) * Math.Pow(beta, 2) * Math.Pow(c, 2) * Math.Pow(ttf, 2);
            f10a = (2 * Math.Pow(beta, 2) * c * ttf) * Math.Pow((Math.Pow((beta * c * ttf),
2) + bo * (Math.Pow(x, 2) + Math.Pow(yoSearch, 2))), 0.5);
            f11a = (Math.Pow(c, 2) * Math.Pow(ttf, 2) - Math.Pow(x, 2)) /
Math.Pow(yoSearch, 2);
            f12a = (f9a - f10a) / (Math.Pow(bo, 2) * Math.Pow(yoSearch, 2));
            f13a = (f1a * f3a * f5a * f7a) / (f2a * f4a * f6a * f8a);

            V2 = -fo * ((bo * Math.Log(f12a)) - (bo * Math.Log(f11a)) + (0.5 *
Math.Log(f13a)));


            if (t >= t0)
```

```
            {
                U_t_to = 1;
            }
            else
            {
                U_t_to = 0;
            }

            if (t >= tof)
            {
                U_t_tof = 1;
            }
            else
            {
                U_t_tof = 0;
            }

            __v = ((V1 * U_t_to) + (V2 * U_t_tof));
        }
    }
    else
    {
        yoSearch = 0.0;
    }
    superSub.V = __v;
    superSub.Y0 = yo1;
    superSub.Y02 = yoSearch;
    idealV = __v;
    return superSub;
}
```

```
        public double CalculateAreaToCauseLineFlashOver(double _yo2, double _yo1)
        {
            double _A;
            double ___y02 = _yo2;
            double ___y01 = _yo1;
            _A = 0.2 * ((___y02 - ___y01) / 1000);
            return _A;
        }

        public double CalculateExpectedNumberOfLineFlashOversPer100kmPerYear(double
_jointProbability, double _IpStep, double _tfStep, double _groundFlashDensity_ng, double
_area_a)
        {
            double _NFO;
            double jProb = _jointProbability;
            double ____Ipstep = _IpStep;
            double ____Tfstep = _tfStep;
            double gFDensity = _groundFlashDensity_ng;
            double __area = _area_a;
            _NFO = jProb * (____Ipstep) * (____Tfstep) * gFDensity * _area_a;
            return _NFO;
        }
        //methods that are called for every t btw tmin and tmax at a given (Ip, tf) stops here.

        public void Clear()
        {

        }
    }
}
```

APPENDIX III

Research Journal of Environmental and Earth Sciences 4(5): 529-533, 2012
ISSN: 2041-0492

Submitted: February 18, 2012 Accepted: March 24, 2012 Published: May 15, 2012

Comparison of Return Stroke Current Profiles for Transmission-Line-Type and Traveling-Current-Source-Type Models

[1]J.O. Adepitan and [2]E.O. Oladiran
[1]Department of Physics and Telecommunication, Tai Solarin University of Education, Ijagun, Ijebu, Nigeria
[2]Department of Physics, University of Ibadan, Ibadan

Abstract: The study is aimed at determining the dependence of the current along a channel on the model used, assuming the same base current. We compared three transmission-line-type models, namely: Transmission Line (TL), Modified Transmission Line with Linear decay, Modified Transmission Line with Exponential decay and two traveling-current-source-type models: Bruce-Golde (BG) and Traveling Current Source (TCS) models. The current profiles along the channel at different heights predicted by these models are presented and discussed. Comparison is based on the assumption that all the models have the same base current. It was found that at low heights and within a time window frame of 15 μs, the currents of the transmission-line-type models predict a zero value at one time or the other with a maximum turning point following some 1μs after. A linear relationship is predicted between the current peak and the channel height. A discontinuity of current peak was observed at high heights. No zero value of current was recorded in case of TCS both at low and high channel heights.

Keywords: Channel base current, channel height, lightning channel, lightning models, return stroke current

INTRODUCTION

Lightning return stroke models are categorized into four classes:

- **The gas dynamic or "physical" models:** These are primarily concerned with the radial evolution of a short segment of the lightning channel and its associated shock wave.
- **Electromagnetic models:** These are usually based on the so-called lossy thinwire antenna approximation of the lightning channel. These models involve a numerical solution of Maxwell's equations to find the current distribution along the channel from which remote electric and magnetic field can be computed.
- **The distributed circuit models, also called RLC transmission line models:** They can be viewed as an approximation to the electromagnetic models and they represent the lightning discharge as a transient process on a transmission line characterized by resistance, inductance and capacitance, all per unit length. These models are used to determine the channel current versus time and height and can therefore also by used for the computation of remote electric and magnetic fields.
- **The last class is the engineering models:** In which a spatial and temporal distribution of the channel current (or the channel line charge density) is specified based on such observed lightning return stroke characteristics as current at the channel base, the speed of the upward propagating wave front and the channel luminosity profile.

Rakov and Uman (1998) classified a number of frequently used "engineering" return stroke models into two categories, transmission-line-type models and traveling-current-source-type models, with the implied location of the current source and the direction of the current wave as the distinguishing factors. The current source in the transmission-line-type models is often visualized to be at the lightning channel base where it injects an upward-traveling current wave that propagates behind and at the same speed as the upward-propagating return stroke front. The current source in the traveling-current-source-type models is often visualized as located at the front of the upward-moving return stroke from which point the current injected into the channel propagates downward to ground at the speed of light. Traveling-current-source-type models can also be viewed as involving current sources distributed along the lightning channel that are progressively activated by the upward-moving return stroke front, releasing the charge deposited by the preceding leader (Rachidi *et al*., 2002).

In the Transmission Line (TL) model the return stroke process is modeled as a current wave injected at the

Corresponding Author: J.O. Adepitan, Department of Physics and Telecommunication, Tai Solarin University of Education, Ijagun, Ijebu, Nigeria

Table 1: Transmission-line type models for $t \geq (z'/v_f)$

Models	$P(z')$	v	Current equation
Transmission Line(TL) Uman and McLain (1969)	1	v_f	$I(z', t) = I(0, t - z'/v)$ for $t \geq z'/v_f$ $I(z', t) = 0$ for $t < z'/v_f$
Modified Transmission Line with Linear current decay (MTLL) Rakov and Dulzon (1991)	$1 - z'/H$	v_f	$I(z', t) = [1 - z'/H]$ $I(0, 1 - z'/v)$ for $t \geq z'/v_f$ $I(z', t) = 0$ for $t < z'/v_f$
Modified Transmission Line with Exponential (MTLE) current decay *Nucci et al.* (1988)	$exp(-z'/\lambda)$	v_f	$I(z', t) = (0, 1 - z'/v)$ $exp(-z'/\lambda)$ for $t \geq z'/v_f$ $I(z', t) = 0$ for $t < z'/v_f$

H = total channel height = constant, $v = v_f$ = constant, λ = constant = current decay constant

Table 2: Traveling current source-type models for $t \geq z'/v_f$

Models	$P(z')$	v	Current equation
Bruce and Golde (BG) Bruce and Golde (1941)	1	∞	$I(z', t) = I(0, 1)$ f or $t \geq z'/v_f$
Traveling Current Source (TCS) Heidler(1985)	1	-c	$I(z', t) = I(0, 1 + z'/v)$ for $t \geq z'/v_f$ $I(z', t) = 0$ for $t \geq z'/v_f$

P(z') is model-dependent attenuation function

base of the lightning channel and propagating upward along the channel with neither attenuation nor dispersion and at an assumed constant speed. In the Traveling Current Source (TCS) model the return stroke process is modeled as a current source traveling upward at an assumed constant speed and injecting a current wave into the channel, which then propagates downward at the speed of light and is absorbed at ground without reflection.

For the calculation of the lightning return-stroke electromagnetic field, a spatial-temporal distribution of the current along the channel $i(z', t)$ must be assumed. To this purpose several models have been proposed. It is to be observed that only models in which the return-stroke current $i(z', t)$ can be simply related to a specified channel base (ground-level) current $i(0, t)$ are suitable, since only the channel-base current can be measured directly and only for it experimental results are available.

The most commonly adopted engineering return-stroke models used to calculate lightning-induced voltages are summarized in Table 1 and 2:

The Transmission Line (TL) model is the most widely used model of the lightning return stroke and is the simplest of the models in the transmission-line-type category. The TL model has been primarily employed to estimate return stroke peak currents and peak current derivatives from measurements of the peak electric field and peak electric field derivative, respectively, with an assumed return stroke speed. In the TL model the current specified at the base of the channel I(0, t) is assumed to propagate upward along the channel with a constant speed v, the speed of the return stroke front. The current at a given height z' is equal to the current at ground at time z'/v earlier.

The Traveling Current Source (TCS) model, proposed by Heidler (1985), is the simplest member of the category of traveling-current-source-type models. In the TCS model, the current source is implied to be at the upward propagating (at constant speed v) return stroke front and the current wave propagates downward with the speed of light c to the Earth where it vanishes (which implies that the channel is terminated in its characteristic impedance). The current at a given height z' is equal to the current at ground at time z'/c later.

We will identify and discuss significant features of the current profiles of engineering return stroke models.

METHODOLOGY

For the current at the channel base $i(0, t)$ of ground-initiated lightning return stroke, analytical expression (Heidler, 1985) is adopted:

$$i(0,t) = \frac{I_0}{\eta} \frac{\left(t/\tau_1\right)^n}{1 + \left(t/\tau_1\right)^n} \exp\left(-t/\tau_2\right) \qquad (1)$$

where,

$$\eta = \exp\left[-\left(\frac{\tau_1}{\tau_2}\right)\left(\frac{n\,\tau_2}{\tau_1}\right)^{(1/n)}\right] \qquad (2)$$

I_0 = Amplitude of the channel-base current
τ_1 = Front time constant
τ_2 = Decay time constant
η = Amplitude correction factor

n = Exponent (2 ... 10)

The function allows for the adjustment of the current amplitude by varying I_0

Sum of two functions given in Eq. (1) was chosen so as to obtain the overall waveshape of the current as observed in typical experimental results. The parameters listed in Table 1 were chosen. These values were adapted from Berger *et al.* (1975). The same undisturbed base current was employed in the comparison of the transmission-line type and traveling-current-source-type models.

Adapting MTLE, TL, MTLL, BG and TCS models, the current at various heights (z' = 200, 300 m, 1, 2, 3 and 4 km) and a time window frame of between 0 and 15 μs were calculated. Most literature relating to propagation of lightning over the ground adopted the value of n = 2. The same value is also adopted in this work. Wave speed of 0.5 c is assumed. The cloud height, H = 5 km for tropic was adopted (Aina, 1971).

Table 3: Typical values of parameters applied to base current. (Berger *et al*., 1975)

I_1(kA)	τ_{11}(μs)	τ_{12}(μs)	n_1	I_2(kA)	τ_{21}(μs)	τ_{22}(μs)	n_2
10.7	0.25	2.5	2	6.5	2.1	230	2

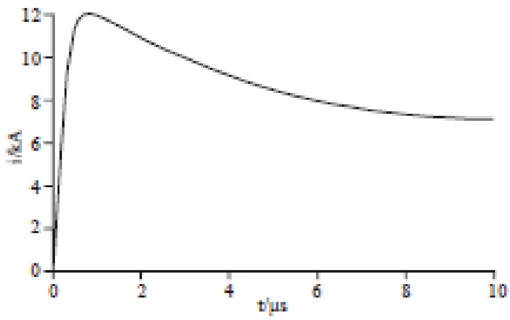

Fig. 1: Profile of undisturbed base-current, i(0, t), same for all models, using the above typical parameters. The total channel height, H = 5 km, Return stroke speed, v = 0.5c (m/μs)

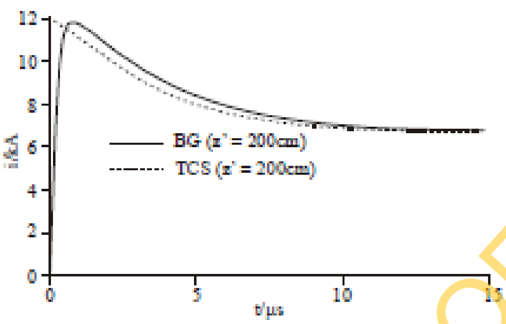

Fig. 2: Current as a function of time at height, z' = 200 m (BG and TCS models) μs

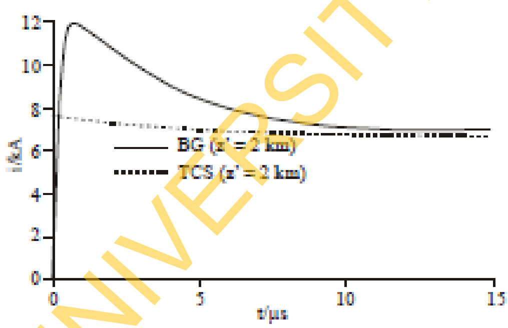

Fig. 3: Current as a function of time at height, z' = 2 km, cloud height, H = 5 km (BG and TCS models)

RESULTS AND DISCUSSION

The profile of the common undisturbed base current is shown in Fig. 1 using the parameters in Table 3. Figure 2 and 3 show the profiles of TCS type models at channel heights 200 m and 2 km, respectively. For channel height z' = 200 m, a time lag of 0.65 μs occurred between the peaks of the current of BG model compare and that of TCS. It was observed that the current almost coincided in both case beyond the time for the peak values of the currents. Figure 3 revealed that at high channel height, say z' = 2 km, the current of TCS model is almost constant with time., with no peak value.

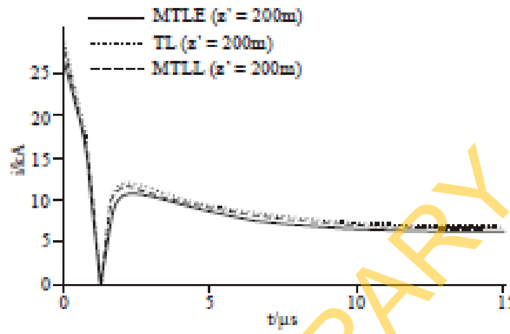

Fig. 4: Current as a function of time at height, z' = 200 m, cloud height, H = 5 km (MTLE, TL and MTLL models)

Table 4: Peak values of the currents with different return stroke models at different heights (v = 0.5c)

Model	Z' = 200 m	Z' = 300 m	Z' = 500 m	Z' = 1 km
MTLE	10.9 kA	10.9 kA	9.7 kA	7.6 kA
MTLL	11.6 kA	10.9 kA	10.9 kA	9.9 kA
TL	12.1 kA	12.1 kA	12.1 kA	12.1 kA

Case A-low heights: Figure 4 presents return stroke current profile as a function of time, t, within a window frame of 15 μs and channel height, z' = 200 m for MTLE, TL and MTLL models. In case of MTLE model, at this height, the current dropped rapidly from 27.1 kA at time t = 0 to a minimum turning point with current, i = 0 within 1.3 μs. The current picked up to a maximum turning point with peak current, I_p = 10.9 kA within the next 0.9 μs. Thereafter the current decreased gradually with time.

TL and MTLL models followed the same wave form as that of MTLE. It is observed that the minimum turning point of the three transmission-line-type models coincide at time t = 1.3 μs. Also the maximum turning point occurred at the same time, t = 2.2 μs with slight variation in the current peak as shown in Table 4.

Figure 5 presents return stroke current profile as a function of time, t, within a window frame of 15 μs and channel height, z' = 500 m for MTLE, TL and MTLL models. In case of MTLE model, at this height, the current dropped rapidly from 67.3 kA at time t = 0 to a minimum turning point with current, i = 0 within 3.4 μs. The current picked up to a maximum turning point with peak current, I_p = 13.2 kA within the next 0.9 μs. Thereafter the current decreased gradually with time.

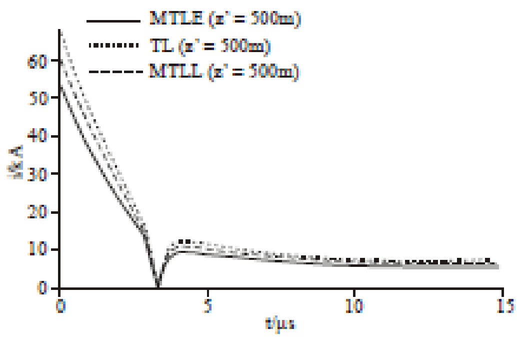

Fig. 5: Current as a function of time at height, z' = 500 m, cloud height, H = 5 km (MTLE, TL and MTLL models)

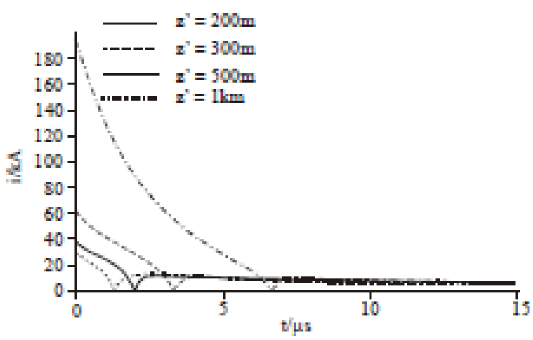

Fig. 6: Current as a function of time for MTLL model

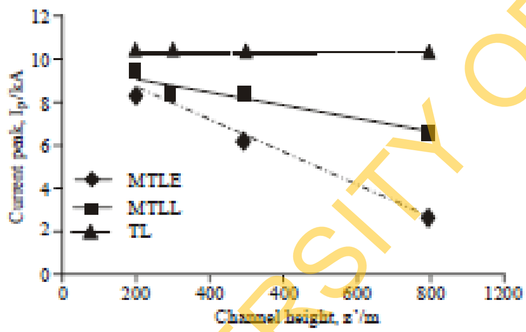

Fig. 7: Relationship between current peak, I_p and channel height, z'

TL and MTLL models followed the same wave form as that of MTLE.

Figure 6 revealed that in case of MTLL, a time delay of 2 µs was observed in the wave form at z' = 500 m relative to that at z' = 200 m. The delay time of waveform was 5.3 µs in case of channel height, z' = 1 km relative to that of z' = 200 m. It is also observed that peak current attenuates with increase in channel height (Table 4 and Fig. 6). The same pattern of time delay in wave form was observed for both MTLE and TL. A linear relationship is established between the peak current, I_p and the channel height, z' (Fig. 7)

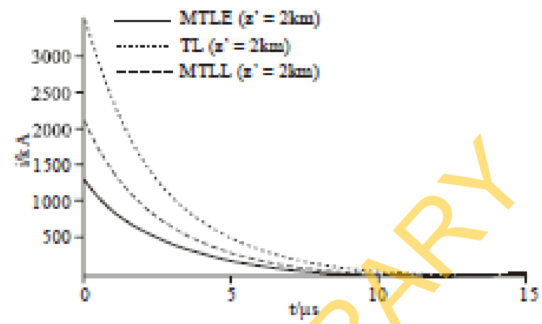

Fig. 8: Current as a function of time at height, z' = 2 km, cloud height, H = 5 km (MTLE, TL and TLL models)

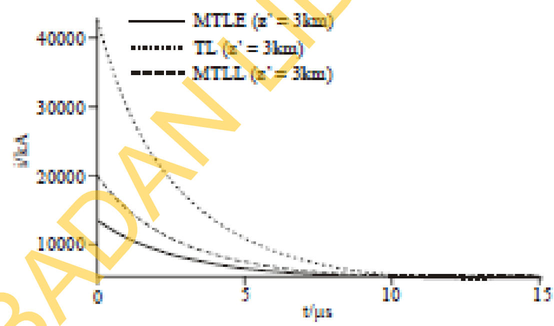

Fig. 9: Current as a function of time at height, z' = 3 km, cloud height, H = 5 km. (MTLE, TL and MTLL models)

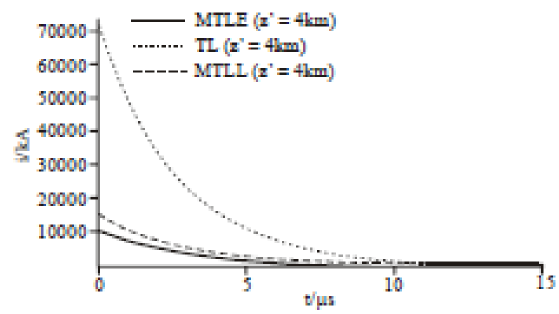

Fig. 10: Current as a function of time at height, z' = 4000 m, cloud height, H = 5 km. (MTLE, TL and MTLL models)

Case B-high heights: Figure 8 to10 represent return stroke current profiles as a function of time, t, within a window frame of 15 µs and channel height, z' = 2, 3 and 4 km for MTLE, TL and MTLL models, respectively. The wave forms are the same for transmission-line-type models. The minimum and maximum turning points observed in current profiles at low heights are discontinuous at heights z' = 2 km and above. A rapid increase in the values of the current with height is observed.

CONCLUSION

We compared three transmission-line-type models, namely: Transmission Line (TL), Modified Transmission Line with Linear decay, Modified Transmission Line with Exponential decay and two traveling-current-source-type models: Bruce-Golde (BG) and Traveling Current Source (TCS) models. The current profiles along the channel at different heights predicted by these models are presented and discussed. Comparison is based on the assumption that all the models have the same "undisturbed base current". At low heights and within a time window frame of 15μs, the currents of the transmission-line-type models predict a zero value at one time or the other with a maximum turning point following some 1 μs after. A linear relationship is predicted between the current peak and the channel height. There is discontinuity of current peak at high heights. No zero value of current was recorded in case of TCS both at low and high channel heights.

REFERENCES

Aina, J.I., 1971. Lightning discharge studies in a tropical area. J. Geomagn. Geoelectr. 23(3): 347-358.

Berger, K., R.B. Anderson and H. Kroninger, 1975. Parameters of lightning flashes. Electra, No. 41.

Bruce, C.E.R. and R.F. Gold, 1941. The lightning Discharge. J. Int. Electr. Eng., 88: 487-520.

Heidler, F., 1985. Traveling Current Source Model for LEMP Calculation. Paper Presented at the 6th International Symposium on Electromagnetic Compatibility, Swiss Fed. Inst. of Technol., Zurich, Switzerland.

Nucci, C.A., C. Mazzetti, F. Rachidi and M, Ianoz, 1988. On lightning Return Stroke Models for LEMP Calculations, Paper Presented at the 19th International Conference on Lightning Protection, O¨VE, Graz, Austria.

Rakov, V.A. and A.A. Dulzon, 1991. A modified transmission line model for lightning return stroke field calculation. In Proceeding of 9th International Symposium on EMC, Zurich, Switzerland, 44H1, pp: 229-235.

Rakov, V.A. and M.A. Uman, 1998. Review and evaluation of lightning return stroke models including some aspects of their application. IEEE T. Electromagn. Compat., 40: 403-426.

Rachidi, F., V.A. Rakov, C.A. Nucci and J.L. Bermudez, 2002. The effect of vertically extended strike object on the distribution of current along the lightning channel. J. Geophys. Res., 107(23): 4699, Doi: 10.1029/2002JD002119.

Uman, M.A. and D.K. McLain, 1969. Magnetic field of lightning return stroke. J. Geophys. Res., 74: 6899-6910.

Research Journal of Environmental and Earth Sciences 4(9): 850-856, 2012
ISSN: 2041-0492

Submitted: July 21, 2012 Accepted: August 17, 2012 Published: September 20, 2012

Analysis of the Dependence of Power Outages on Lightning Events within the Ijebu Province, Nigeria

[1]J.O. Adepitan and [2]E.O. Oladiran
[1]Department of Physics and Telecommunication, Tai Solarin University of Education, Ijagun, Ijebu, Nigeria
[2]Department of Physics, University of Ibadan, Ibadan, Nigeria

Abstract: The study aimed at developing a model for lightning-induced outages in Nigeria from results obtained on determining the proportion and rate of lightning-induced outages out of the total power outages experienced in Ijebu province of Nigeria. Power outage records for Ijebu province, comprising Ijebu-Ode and Sagamu areas, Ogun state, Nigeria for the years 2002-2006 were collected from Power Holding Company of Nigeria (PHCN). Unintentional stochastic outages were separated from those due to deliberate load shedding. Lightning events records were collected from Nigeria Meteorological Agency for the same period. The two sets of time series were superimposed. Outages with time, $t<1$ min after lightning events were classified as 'Lightning-Induced' (LI). Those with $1\leq t\leq 6$ min were classified as 'Possibly Lightning-Induced' (PLI) while those with $t>6$ min were classified as 'Others' (OT). The two sets of data were analyzed in order to determine percentage of lightning-induced outagfes. Also, thunderstorm days and power line parameters were used as input data for modified FLASH 1.7 software (considering tropical region) to estimate the rate of lightning induced outages. The five-year period, 2002 to 2006, experienced no significant difference ($p<0.05$) in the mean of percentage of LI outages for both areas, calculated as 8.6 for Ijebu-Ode and 9.5 for Sagamu. The corresponding values for PLI being 1 and 2%; whereas OT had values 90.4 and 88.5%. Where earth wires were available on the transmission lines, the mafn lightning-induced outage rate was 1/100 km-year. The mean flashover rate for unshielded lines was 22/100 km-year. A linear relationship was established between the annual lightning-induced outages and the annual lightning days for the province. Lightning accounted for approximately 10% of the random outages experienced in Ijebu province. Lightning-induced outages are linearly related to lightning days. Lightning-induced outage rate is much higher over unshielded than shielded transmission lines.

Keywords: Lightning-induced outage distribution, power outages, thunderstorm days

INTRODUCTION

An electrical outage is defined as the unplanned loss of power to a load. This condition is also commonly referred to as a 'forced outage' or a 'failure' of power system component under study; in this case, the overhead transmission and distribution lines. (IEEE Standard, 493-1990).

A number of factors are responsible for power outages, resulting into power interruption; thus affecting the reliability of a power distribution system. Some of the causes of power outages are:

Wind: Wind may cause power lines to touch, resulting into a fault or a short-circuit may occur, which can interrupt electrical service.

Snow: Winter storms can create a buildup of snow and ice on power lines and trees. The weight of the snow and ice can cause tree limbs and trees to fall onto power lines, either knocking the lines and poles down and breaking them, or causing a short-circuit by knocking the lines into each other.

Vehicle accidents: Another common cause of electrical outages is collision of vehicles with power poles. At times a collision will cause a pole to break or make the lines sway enough that they touch and cause a short-circuit.

Birds and small animals: Birds often climb or nest on certain pieces of equipment such as transformers and fuses. Sometimes the birds or small animals, as the case may be will touch two wires at one time and cause a short-circuit.

Trees: Trees often fall on power lines as a result of storm or rain or flood uprooting a tree. At times the

Corresponding Author: J.O. Adepitan, Department of Physics and Telecommunication, Tai Solarin University of Education, Ijagun, Ijebu, Nigeria

branches of a tree may come in contact with power lines.

Bush burning: This is common during the dry season and base of wooden poles are often burnt thus resulting into power lines coming in contact with one another.

Erosion: Erosion often washes off the base of electric poles, causing poles to collapse resulting in short circuit.

Vandalization: of power lines: Sometimes cases of vandalization of power lines by disgruntled elements result in outages lasting weeks or months.

Outages caused by lightning: Electrical power interruptions are one of the most readily apparent effects of lightning on human activity. Lightning strokes to nearby ground and overhead power lines have been reported as a major cause of power outages worldwide. Most of the twenty first century electronics equipments are highly sensitive with low damage threshold level. Thus they are easily damaged by either transient voltage or current. Lightning has always been suspected as one of the reasons of power line outages and damage to equipments in distribution network. For instance, in 2003 United States, Canada and Europe suffered a series of blackouts leaving more than 60 million people without electricity. Some of the reason adduced to the outage was believed to be due to lightning strike (Andersson *et al.* 2005). Lightning damage to power lines in the U.S. costs almost $ 1 billion annually and 30% of all power outages are lightning related, according to studies by the Electric Power Research Institute (Kithil, 1998). Assessment of the 32 year reliability of 13.8 kV electrical distribution systems at Oak Ridge National Laboratory (ORNL) in Tennessee revealed that weather-related events accounted for 56% of the feeder outages recorded. Fifty seven out of 76 weather-related outages were attributed to lightning (Tolbert *et al.*, 1995). According to Power Holding Company of Nigeria (PHCN), a total of 13,324 faults at 33 KV and 22,255 faults at 11 KV levels were recorded in year 2002 and a bulk of these faults were caused by thunder storms and lightning (NEPA 2002 Annual Report and Accounts).

The reliability of the supply provided by an electric power system is judged by the frequency and duration of supply interruptions to consumers.

Load shedding and outages are regular occurrences with PHCN. However, PHCN had always adduced the reason for frequent outages to lightning strikes. The PHCN report raised question such as: "What percentage of these faults was caused by lightning and what fraction of the faults resulted into full outage? The dearth of information on the contribution of lightning strokes to the perennial power outages in Nigeria has rendered any preventive action unfeasible. This study aimed at analyzing data on lightning events and power outages in Ijebu-Ode and Sagamu areas of Ijebu province, Nigeria for five years (2002-2006) in order to determine the association between the two variables; and to develop a model for lightning-induced outages in Nigeria.

Modified IEEE FLASH 1.7: The soft ware is used to determine the backflash and shielding failure rate of power lines. The calculation is based among other input parameters on:

- Ground flash density of the terrain over which the line passed
- Tower geometry and line configuration

IEEE Flash 1.7 is designed with relationship between ground flash density, N_g and thunderstorm days, T_d, as $N_g = 0,\ 04T_d^{1.25}$. This is suitable for temperate regions only. The errors found in applying equation $N_g = 0,\ 04T_d^{1.25}$ in determination of ground flash density in Colombia have reached values up to 1568% (Torres, 2003). Hence, it was necessary to modify the software by replacing $N_g = 0,\ 04T_d^{1.25}$ with $N_g = 0,\ 0017.T_d^{1.56}$; which is suitable for tropical regions between 2-10° North (Torres, 2003). This is region within which Ijebu-Ode, situated (6°48′N, 3°52′E) and Sagamu (6°0′N, 3°38′E) fall.

METHODOLOGY

Power outage records for Ijebu province, comprising Ijebu-Ode (6°48′N, 3°52′E) and Sagamu (6°50′N, 3°38′E) areas, Ogun state, Nigeria for the years 2002-2006 were collected from Power Holding Company of Nigeria. Unintentional stochastic outages were separated from those due to deliberate load shedding. Lightning events records were collected from Nigeria Meteorological Agency for the same period for Ijebu-Ode station. Sagamu has no meteorological station. Hence same lightning data were used for Sagamu due to proximity to Ijebu-Ode. The two sets of time series were superimposed. Outages with time, t<1 minute after lightning events were classified as 'Lightning-Induced'(LI). Those with 1≤t≤6 min were classified as 'Possibly Lightning-Induced' (PLI) while those with t>6 min were classified as 'Others'(OT). The two sets of data were analyzed in order to determine statistical parameters and estimate lightning induced outages. Also, thunderstorm days and power

Table 1: Dimensions of vertically configured transmission and distribution lines in Ijebu province

Line type	Tower height (m)	Cross-arm height (m)	Phase conductor distance from center (m)	Phase conductor Height (m)	Sag (m)	Radius (mm)	Shield wire Sag (m)	Radius (mm)	Span (m)
132 kV	26.296	17.2	(+)2.743	15.02	4.00	6.90	2.00	3.30	365.00
		17.2	(-)2.743	15.02					
		21.8	(+)2.743	19.55					
33 kV	10.363		(+)0.762	10.36		5.64			250.00
			0						
			(-)0.762						
11 kV	8.534		(+)0.762	8.53	2.00	5.64			250.00
			0						
			(-)0.762						

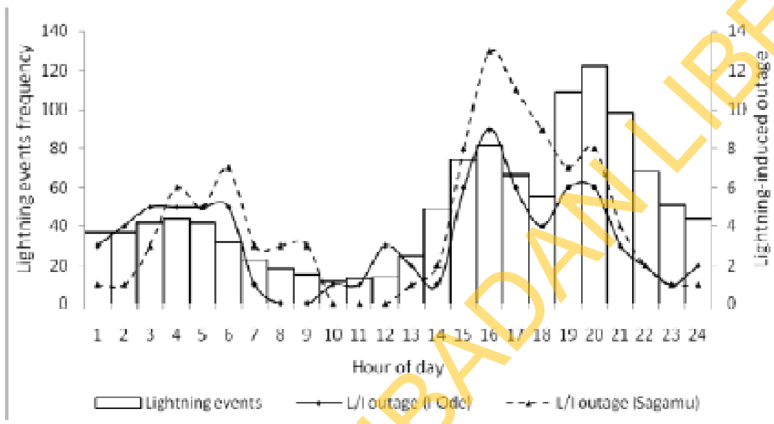

Fig. 1: Correlate of lightning-induced outages with lightning events (hourly basis)

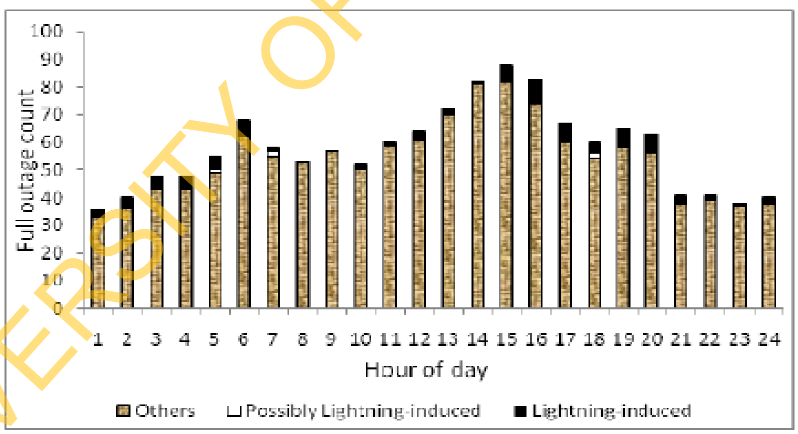

Fig. 2: Time of day trend of causes of full outages at Ijebh-Ode area (2002-2006)

line parameters (Table 1) were used as input data for modified FLASH 1.7 software (considering tropical region) to estimate the rate of lightning induced outages.

RESULTS AND DISCUSSION

Lightning-induced outages peaks were recorded at 15:00 and 20:00 h LT. This was due to the fact that lightning activities equally reached peaks at these periods (Fig. 1). The observation is corroborated by Oladiran *et al.* (1988); while carrying out a research on the lightning flash rate at Ibadan (Lat. 7°21′N, Long. 3°51′E) -a meteorological environment of Ijebu-Ode- discovered that lightning activities are high around 15:00 and 20:00 h LT with peak coming up around 18:00 h LT. No lightning-induced outage was recorded during 10:00 to 12:00 h LT in Sagamu and 08:00 and

09:00 h LT in Ijebu-Ode. This was due to the fact that 08:00 to 12:00 h LT recorded period of low lightning activities (Fig. 1). The observation was corroborated by Oladiran *et al.* (1988), which revealed 0600 to 1300 h LT as period of low lightning activities.

Figure 2 and 3 revealed that for the five years under consideration, there was no hour of the day that one type of outage or the other was not recorded at Ijebu-Ode and Sagamu areas.

The highest number of lightning-induced power outages was recorded during the month of June, for type of outage or the other was not recorded at Ijebu-Ode and Sagamu areas.

The highest number of lightning-induced power outages was recorded during the month of June, for the raining season, when lightning activities is on the increase.

There was no lightning-induced power outage recorded during the months of August and December in both areas; due to the fact that there is usually a break of raining activities in August and most Decembers are free of rain with little or no thunder and lightning activities (Fig. 4 and 5).

The Mean random power outage frequencies for Ijebu-Ode and Sagamu areas for the period under consideration were 94 and 104 outages outages/year, respectively. The five-year period, 2002 to 2006, experienced no significant difference ($p<0.05$) in the mean of percentage of lightning-induced outages for both areas, calculated as 8.6% for Ijebu-Ode and 9.5% for Sagamu. The mean Percentage Of Possibly Lightning-Induced (PLI) outage for Ijebu-Ode and Sagamu areas were 1 and 2%, respectively; while OT had values 90.4 and 88.5% (Table 2). The mean duration of lightning-induced outage was 2 h for Ijebu-Ode area and 2.5 h for Sagamu area (Table 2).

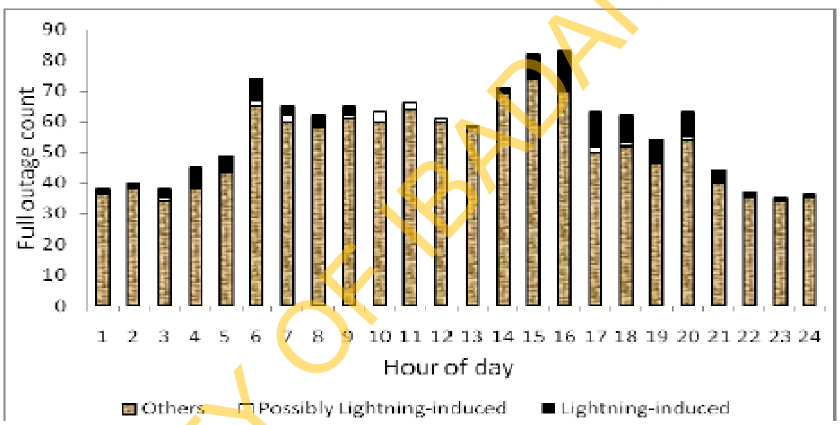

Fig. 3: Time of day trend of causes of full outages at Sagamu area (2002-2006)

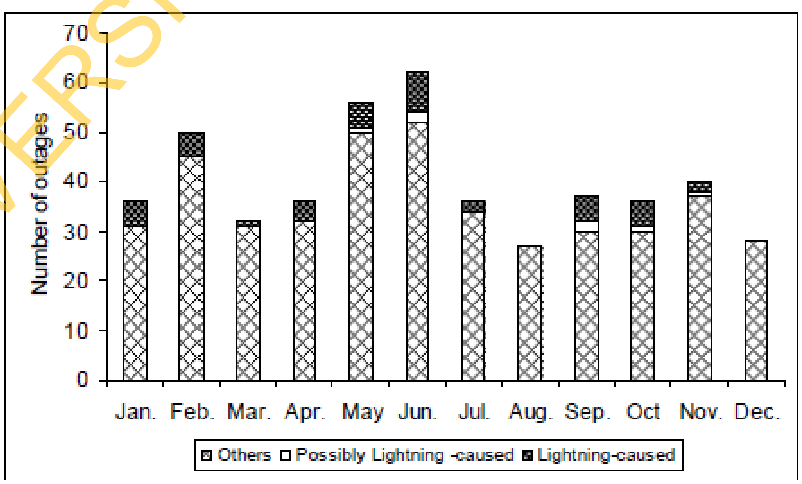

Fig. 4: Time of year trend in full outages at Ijebu-Ode area (2002-2006)

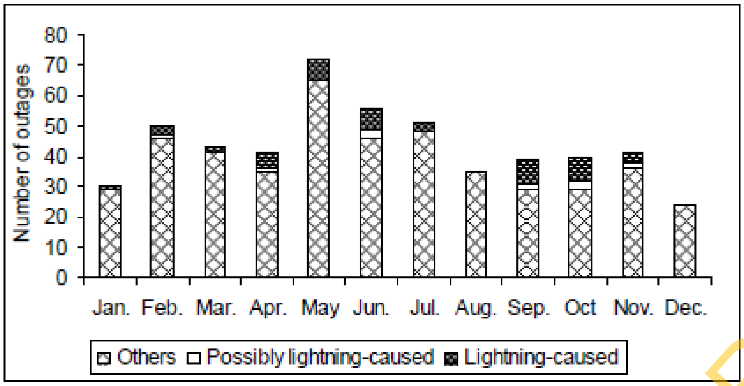

Fig. 5: Time of year trend in full outages at Sagamu area (2002-2006)

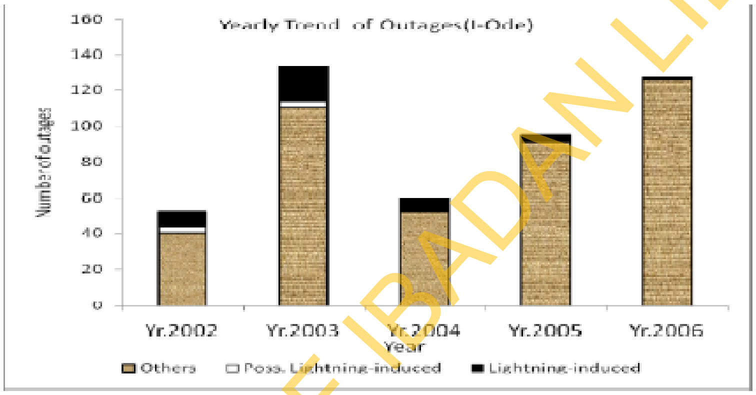

Fig. 6: Yearly trend of lightning-induced outages in Ijebu-Ode area

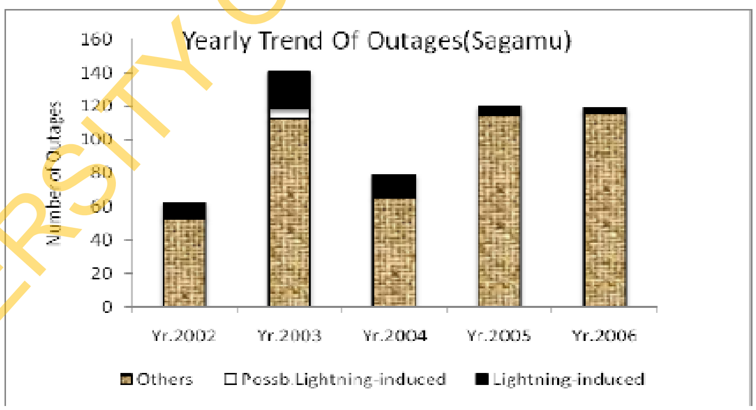

Fig. 7: Yearly trend of lightning-induced outages in Sagamu area

Generally, an annual increase in total power outages were recorded over the years (Fig. 6 and 7) at Ijebu-Ode and Sagamu areas, though lightning-induced outages declined over the years (Fig. 8). A linear relationship was developed between the annual lightning- induced outages, F and the annual lightning days, T. For Ijebu-Ode, $F = -19.1 + 0.38T$. And for Sagamu; $F = -19.5 + 0.40\ T$ (Fig. 9).

Using the modified IEEE Flash 1.7, Table 3 showed the Flashover rates (outages per 100 km-year) of overhead power lines in the province. Where earth wires were available on the transmission lines, the

Table 2: Annual outage frequency (number/year) and duration (h) in Ijebu province

		Ijebu-ode outages						Sagamu outages					
		Total		Lightning-induced			P LI	Total		Lightning-induced			PLI
Year	Thunder storm days	Count	Hour	Count	Hour	Hour/Count	Count	Count	Hour	Count	Hour	Hour/Count	Count
2002	90	52	119	9	19	2.1	3	64	144	8	16	2.0	2
2003	92	134	403	20	47	1.9	3	147	332	22	53	2.4	7
2004	95	60	298	8	22	2.8	0	71	268	14	34	2.4	0
2005	97	95	210	4	5	1.3	0	120	276	5	11	2.2	0
2006	93	127	343	1	1	2.0	0	119	309	2	7	3.5	1
Mean	93	94	274.6	8	18.8	2.0	1	104	265.8	10	24.2	2.5	2

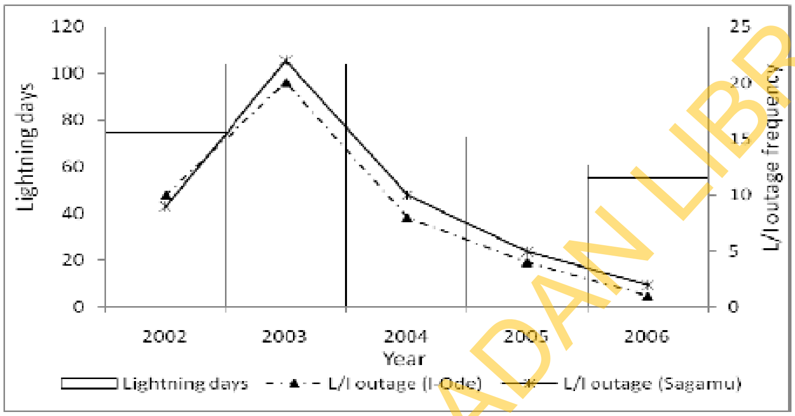

Fig. 8: Correlate of lightning-induced outages with lightning events (annual basis)

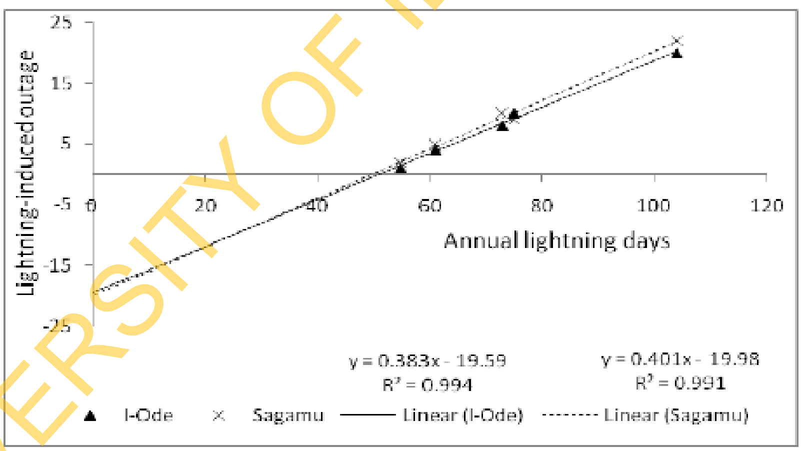

Fig. 9: Graph of lightning-induced outages against lightning days

Table 3: Flashover rates (outages per 100 km/year) of overhead power lines in Ijebu province

Year	Thunder storm days	132 kV shielded transmission line	132 kV unshielded transmission line	33 kV distribution line	11 kV distribution line
2002	90	1	21	21	19
2003	92	1	22	22	19
2004	95	1	23	23	20
2005	97	1	24	24	21
2006	93	1	22	22	20
Mean	93	1	22	22	20

mean lightning-induced outage rate was 1/100 km-year. The mean flashover rate for unshielded lines was 22/100 km-year.

CONCLUSION

Lightning accounted for approximately 10% of the random outages experienced in Ijebu province. Lightning-induced outages are linearly related to lightning days. Lightning-induced outage rate is much higher over unshielded than shielded transmission lines.

REFERENCES

Andersson, G., P. Donalek, R. Farmer, N. Hatziargyriou, I. Kamwa, P. Kundur, N. Martins, J. Paserba, P. Pourbeik, J. Sanchez-Gasca, R. Schulz, A. Stankovic, C. Taylor and V. Vittal, 2005. Causes of the 2003 major grid blackout in North America and Europe and recommended means to improve system dynamic performance. IEEE Tran. Over Power Sys., 20(4): 1922-1928.

IEEE Standard, 493-1990. IEEE Recommended Practice for Design of Reliable Industrial and Commercial Power System. 54: 75-204.

Kithil, R., 1998. Lightning protection codes: Confusion and costs in the USA. Proceeding of the 24th Int'l Lightning Protection Conference, Birmingham, U.K.

National Electric Power Authority (NEPA), 2002. Annual Report and Accounts.

Oladiran, E.O., Aina, J.I. and S. Israelsson, 1988. Lightning flash-rate characteristics of the tropical thunder cloud. Proceedings of 8th International Conference of Atmospheric Electricity, pp: 757-765.

Tolbert, L.M., J.T. Cleveland and L.J. Degenhardt, 1995. Relaibility of lightning resistant overhead distribution lines. IEEE Industrial and Commercial Power Systems Technical Conference, Conference Record, Papers Presented at the 1995 Annual Meeting, 7-12 May.

Torres, H., 2003. Ground Flash Density: Definition of the appropriate grid size and a proposal of relationship Ng vs. Td for Tropical zones. Activity Report of TF C4.01.02-B, Working Group C4.01 Lightning, CIGRE Dallas, Tx., USA, September 2003, In Comments to IEEE STD 1410-2004 Guide for Improving the Lightning Performance of Electric Power Overhead Distribution Lines July 2005.